Effects of Active Vision and Internal State on *Drosophila* Visual Behaviour

James McManus

July 18, 2023

A thesis presented for the degree of

Doctor of Philosophy

Contents

Abstract

For many people, fruit flies are simply an annoyance. However, as they perform their persistent straight-line flights, followed by quick switches in direction, they display a remarkable ability in both vision and agility. A Key part of the fruit fly visual system that ensures that this behaviour occurs is the ability to stabilise locomotion within the world given perturbation, this is the optomotor response. Recent studies have introduced the existence of anti-optomotor behaviour in *Drosophila*. Under certain conditions, flies show a consistent, large, and sustained response in the opposite direction to rotational optic flow. However, the underlying reasons for this behaviour remain unclear.

We aimed to investigate the features and reasons for the anti-optomotor response. In addition we aimed to investigate the ability of flies to use active sensing mechanisms to allow for greater visual motion perception.

Our findings reveal that flies perceive rotational optic flow normally during anti-optomotor behaviour. However, they exhibit significant visual nystagmus of the head, which coincides with the occurrence of anti-optomotor behaviour. Moreover, this behavior is linked to high-frequency locomotory activity, and looming stimuli that increase the likelihood of directional changes also amplify the occurrence of anti-optomotor behaviour. Interestingly, restraining head movements does not eliminate the anti-optomotor response, although it does impair overall turning ability at lower stimulus wavelengths. Furthermore, our study reveals that fruit flies possess better visual acuity than previously believed, as they respond to 2° wavelength gratings, well below the 4-5° Nyquist limit. Notably, this behaviour is observable exclusively through head-optomotor responses, emphasizing the significance of active sensing mechanisms in fly vision.

The characteristics of anti-optomotor behaviour suggest that a saccadic-like behavioural

pattern resembling course-changing movements is the fundamental cause of this phenomenon, although the exact neural circuitry involved is still unknown. Additionally, the presence of hyperacute behavioural responses lends support to the microsaccadic sampling hypothesis of animal vision, and furthermore explains previous contradictory findings in regards to this phenomenon.

Acknowledgements

There are many people, both inside and outside of Sheffield who have made this thesis possible. I would firstly like to thank the organisation that has financially supported my research, EPSRC, as well as the entire Brains on Board Organisation for allowing such a welcoming and exciting research collective.

I would like to thank my supervisor Mikko, for the opportunity to undertake this PhD, for giving me the freedom to explore my own ideas, and for the frequent trips to Crookes Valley Park Lake, which have given a new meaning to phrase 'wet lab'. I would like to thank my advisors, Walter and Andrew, who provided important feedback and positive encouragement. I would also like to thank Andrew for providing our weekly lab meetings, as well as his advice on genetics, and my ideas. I would like to thank my examiners Tom Clandinin and Anton Nikolaev for suggestions and corrections to this thesis.

I would like to thank the members of our lab, Keivan, Neveen, Jouni, Joni, and Ben, as well as the members of our office, Katie, Tom, Gregor, Anthi, Chun, Alice, and Hoger, who provided the infrequent free croissant, the frequent attack with nerf bullets, and the permanent good times. Lily the cat is also deserving of a certain form of thanks, for introducing the occasional typo during the final few weeks of writing this thesis.

Finally, this thesis genuinely would not have existed without Hannah, who picked me up during the low points more times than I would care to admit. She listened to me babble on when I was excited about an idea, and she listened to me drone on about the inevitable failures. She has been a constant force of encouragement and brightness from the beginning to the end.

1 Anti-Optomotor Behaviour in *Drosophila*

1.1 Introduction

1.1.1 Preface

How does a brain see the world? One way to imagine a brain working is like a river of information coursing through the brain. Light hits the photoreceptors and begins the process of sifting, modifying, and sorting of information as it makes its uncountably many journeys through the tributaries of every dendrite and axon, before reaching the all-consuming mouth of the river: behaviour. In another way though, the brain is not a river, it is a living thing. It has its own rhythms, feedback, and internal force. These two ways of seeing represent two paradigms of brain function, as a passive, or an active process.

Metaphors for how the brain works have always been strongly grounded in the historical-technological context in which they have been conceived. Clock-driven mechanisms dominated scientific metaphors in which clocks were the most advanced technologies that could be reduced to pure mechanism (Popper, 1966), from then, the telegraph metaphor of Helmholtz followed the discovery of action potentials in squid (De Palma & Pareti, 2007). More recently the brain-as-a-computer paradigm (Maccormac, 1986) has been displaced by a artificial neural network hypothesis (Gidon et al., 2020; Whittington & Bogacz, 2019). It seems that despite all the degrees of freedom of human imagination, our minds predominantly end up favouring the near, the understandable, and reducible. Vision research has developed along the same lines. Most conceptions of the eye of both vertebrates and invertebrates consider the eye to act like a static camera. The need to apply these technologies to agents acting in the real world (self-driving cars, robots, drones), has shown that the problem of computer vision requires a different conception of the visual system, that of an active, moving, integrated

part of the environment in which it is situated. In the following thesis I hope to demonstrate that the behaviour of fruit flies cannot be easily modelled as a simple input-output system, and that both their internal state, and active mechanisms contribute to the behaviours we observe. I investigate the optomotor response in flies, showing that via active mechanisms, they can extract more information from the world than would be expected if we were to view their visual system statically. I investigate how flies move about the world, in a way that depends on their internal state. Moreover, I show how active vision interacts with the optomotor response, and leads flies to behave in unexpected ways. Finally, I investigate the neural architecture that might allow flies to use active mechanisms to extract depth information from their environment.

1.1.2 Early Visual Pathway

The fruit fly has 750 repeating structures that make up its compound eye; these are the ommatidia. Each ommatidium's lens focusses light on the rhabdomere, which is made up of the eight photoreceptors: R1-R8 (Katz & Minke, 2009). Because of the anatomical arrangement of the photoreceptors and the lenses, many of these photoreceptors sample very similar regions of space, and are neurally superimposed at the lamina (Agi et al., 2014), where the R1-R6 photoreceptors terminate (Shaw, 1984). In contrast, R7-8, apart from forming gap-junctions with R1 and R6 terminals (Shaw et al., 1989) to exchange information that broadens the spectral range of motion vision (Wardill et al., 2012), do not have chemical synapses in the lamina but terminate directly in the medulla (Morante & Desplan, 2005).

The lamina is the first optic neuropil, is made up of 700-800 repeating cartridges with a stereotyped structure (Tuthill et al., 2013) containing monopolar, amacrine, transmedullary, centrifugal, and wide-field cells (Rivera-Alba et al., 2011). Each medullary cartridge receives input from the 6 different R1-R6 photoreceptors that have broadly similar receptive fields,

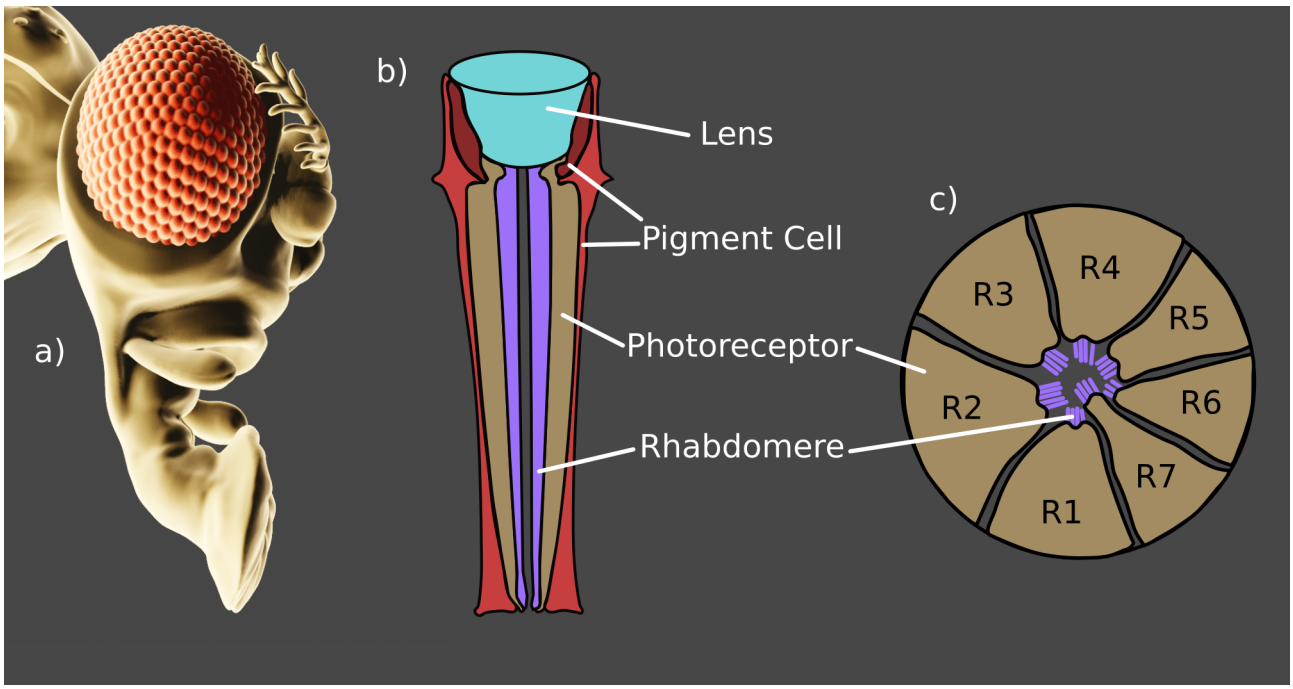

Figure 1: The Structure of the Fruit Fly Ommatidium.
(a) 3D model of the fly, showing the 750 lenses in each ommatidium
(b) Distal-proximal section of the ommatidium. The lens sits on top of and is supported by primary and secondary pigment cells. The photoreceptor cell bodies line the outside of the ommatidium, while the rhabdomeres lie in the centre.
(c) Cross section of the ommatidium. R1-R6 point their rhabdomere inwards but not exactly in the centre, R7 sits on top of R8 (not shown) and its microvilli lie in the centre of the ommatidium.

and thus each cartridge processes information from the photoreceptors within that region (Agi et al., 2014). Cells in the lamina are thought to co-ordinate a massively parallelised effort to perform preprocessing and extract simple properties from the photoreceptor signals, including gain-control (Tuthill et al., 2013), on- and off- detection (Clark et al., 2011; Joesch et al., 2010), and luminance invariant processing (Ketkar et al., 2022). At the lamina, R1-6 directly connect to the monopolar L1-L3 cells, as well as the multipolar amacrine cells (Am), with smaller subsets of R1-6 connecting to L4, T1, C2, C3, and Lawf (Rivera-Alba et al., 2011).

At the level of the lamina, visual processing in flies is divided into two distinct pathways. The on-pathway is specifically sensitive to increases in light intensity over time, whereas the off-pathway is responsive to decreases.

Initially, it was widely believed that this parallel arrangement was a result of separate in-

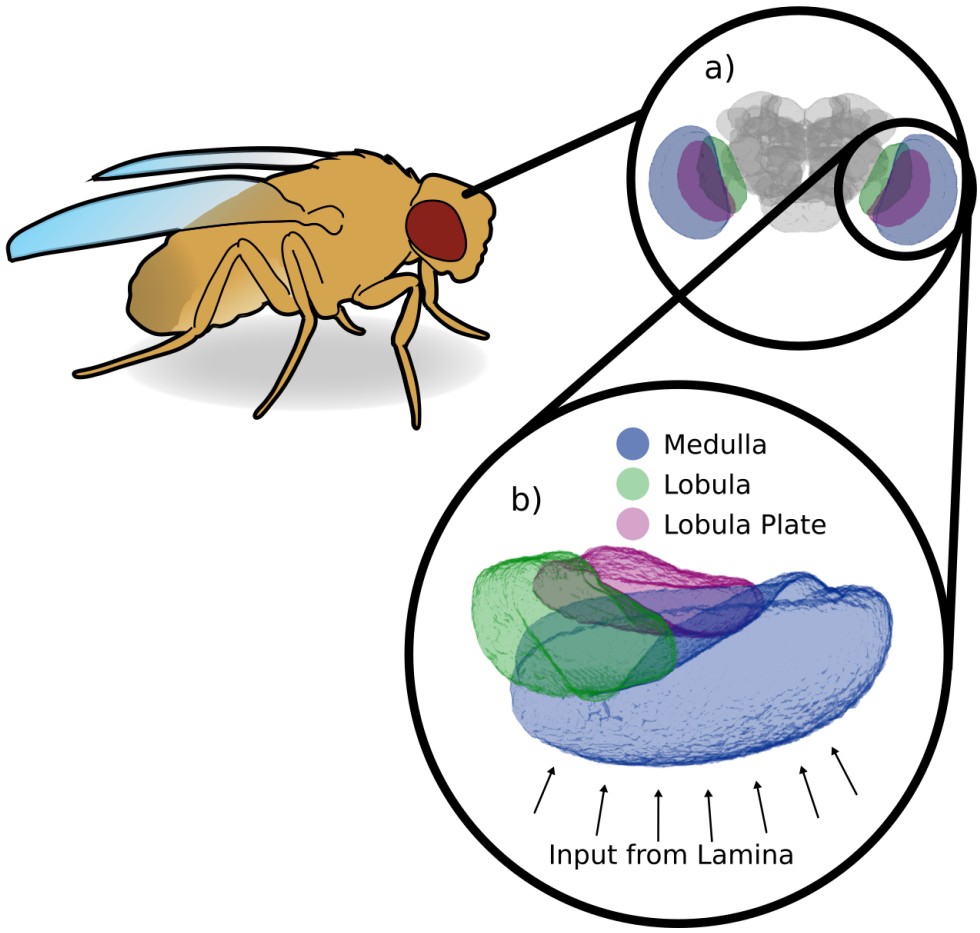

Figure 2: The fruit fly's visual anatomy.
(a & b) The fly's early visual system consists of the retina (not shown), lamina (not shown), medulla (blue), lobula (green) and lobula plate (pink).

puts from L1, leading to ON responses, and L2, leading to OFF responses (Joesch et al., 2010, Rister et al., 2007). However, there is a growing consensus that the monopolar cells in the lamina represent a diverse range of initial convolutions of photoreceptor responses, which are shared between the pathways depending on the specific conditions in which flies operate. Combinatorial genetic interventions have revealed that off-responses to rotating stimuli necessitate input from L1-L3 (Silies et al., 2013). To add nuance to our understanding, it has been observed that slowdown responses to translational stimuli are significantly diminished when L2 and L3 are simultaneously blocked (Silies et al., 2013). Furthermore, the contributions of L1-L3 have been found to provide luminance information to both pathways, particularly under changes in the background luminance level (Ketkar et al., 2020, 2022). The role of L4 in motion selectivity has yielded inconsistent findings, as some studies

demonstrate that complete inhibition of L4 blocks the motion sensitivity of downstream cells to off-edges (Meier et al., 2013), accompanied by corresponding behavioural effects (Bahl et al., 2015; Tuthill et al., 2013), while others report only minimal behavioural effects (Silies et al., 2013).

These genetic dissections collectively reveal that the visual system is not characterized by simple, independent, and segregated pathways; instead, they suggest the existence of multiple routes through which information is extracted from the environment. Moreover, it should be noted that while certain studies have attempted to inhibit specific neurons and concluded that they are not essential for a particular behaviour, subsequent research has revealed that under different conditions, these neurons may indeed play a critical role, indicating the context-dependent nature of the neuronal requirements for specific behaviours.

1.1.3 Mid-Late Visual Pathway

Cells in the lamina project to the medulla. Of the laminar cells that appear to contribute to motion vision; Am connects strongly to T1, L1 to Mi1 and Tm3, and L2 to Tm1, Tm2, and Tm4 in the medulla, whilst L3 connects to Tm9 and Mi9 (Arenz et al., 2017; Rivera-Alba et al., 2011). L4 cells, which also form cross-cartridge connections (Rivera-Alba et al., 2011), innervate Tm2 cells along with L2 (Takemura et al., 2011). L5 cells, which share connections with L1, connect to Mi4 neurons (Takemura et al., 2017).

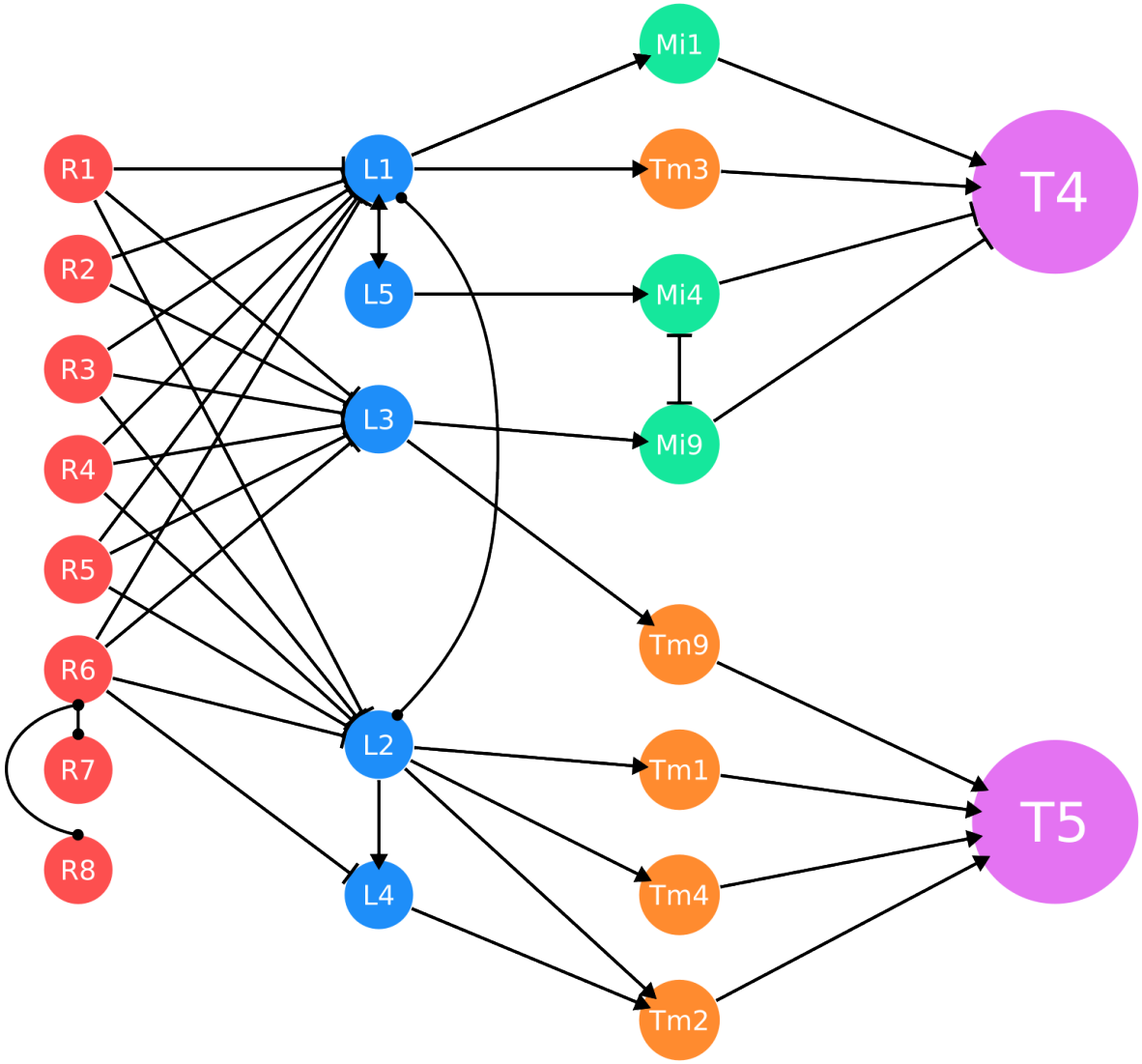

Figure 3: The Early Motion Visual Pathway in Drosophila
Photoreceptors (red) connect via sign-inverting synapses with laminar cells (blue), These connect to transmedullary (orange) and medulla intrinsic (green) cells. These go on to form inputs with either the T4 cells directly in the medulla, or to T5 cells in the lobula. Electrical connections exist between R7/8 and R6, as well as between L1 and L2.

The primarily transmedullary cells of the off-pathway connect to T5 cells whose somata lie in the lobula, whilst the on-pathway cells connect to T4 directly within the medulla itself. (Arenz et al., Shinomiya et al., 2022). The T4 and T5 cells are the first direction-selecive cells of the on- and off- pathways and have receptive fields covering only a small region of space. The direction selectivity in T4 emerges from excitatory input from Mi1 and Tm3, and inhibitory input from Mi4 and Mi9. This antagonism results in direction selectivity that arises in the medullary dendrites of T4 (Strother et al. 2017). T5 cells receive transmedullary input from

Tm1, Tm4, Tm9 and Tm2 (Shinomiya et al., 2014).

Individual T4/T5 cells appear to respond most strongly to one of the four cardinal directions (Maisak et al., 2013), although at the population level, it appears there are six directional clusters that are maximally encoded by the T4/T5 Cells (Henning et al., 2022). The four subtypes of T4/T5 innervate corresponding specific layers of the lobula plate. Here, connections to the lobula plate tangential cells (Fischbach & Dittrich, 1989), as well as other neurons of the lobula plate such as lobula plate intrinsic cells, which also innervate the LPTCs (Mauss et al., 2015) occurs. Most cells in the lobula plate that receive inputs from T4 and T5 receive from both subtypes (Shinomiya et al., 2022), combining the on- and off- pathways.

From the lobula and lobula plate, visual projection neurons carry information to central (Wu et al., 2016) and descending areas (Sen et al., 2017). These areas additionally receive centrifugally projecting neurons from the central brain. Visual projection neurons, such as the lobula plate lobula columnar (LPLC) or the lobula columnar (LC) neurons, have distinct visuospatial features, such as responding to the motion of small moving objects (LC18), or to looming stimuli (LPLC1) (Klapoetke et al., 2022).

1.1.4 Lobula Plate Tangential Cells

Lobula plate tangential neurons are large, graded neurons that integrate retinotopic motion information from a large portion of the visual field (Borst & Egelhaaf, 1992). Vertical system cells are a subtype of LPTC that responds to vertical motion, while horizontal system cells respond to horizontal motion (Borst et al., 2020). Each cell has a preferred direction, which they depolarise to, as well as a null direction, which they hyperpolarise to (Schnell et al., 2010).

The LPTCs are thought to compute the global motion signal via motion opponency, driven fundamentally by the T4/T5 input. A direct connection between T4/T5 cells provides an

excitatory, cholinergic component in the preferred direction (Schnell et al., 2012), whilst an indirect connection, via bi-stratified (Mauss et al., 2015) LPi cells provides the inhibitory, glutamatergic component of the waveform (Mauss et al., 2015). The LPTCs are required for the optomotor response. The optomotor blind mutant, omb, was found to lack both LPTCs and an optomotor response, despite having normal retinal responses to light (Heisenberg et al., 1978). LPTCs carry motion information computed in the lobula plate to the rest of the brain, including directly onto head motorneurons (Wertz et al., 2008, 2012).

1.1.5 Classical Models of Motion Detection

Elementary Motion Detectors, or Hassenstein-Reichardt Correlators, are models of motion detection circuits. The general principle is that motion can be detected via cross-correlating two distinct signals that are separated in time and space (Fitzgerald & Clark, 2015). In the classical model, this occurs by temporally filtering the visual signal from one receptive field, and correlating this, along with a multiplicative or non-linear step, with the signal from a different receptive field (Vogt & Desplan, 2007), with the full correlator also containing a mirror-symmetric preferred-direction excitation and null-direction inhibition (Arenz et al., 2017). Other motion detection models have been proposed by looking at non-insect systems, these include Barlow-Levick model and the Motion Energy model (Currier 2023).

This simple system predicts many features of both insect and vertebrate vision, including the phi and reversed phi illusion (Gruntman et al., 2021; Tuthill et al., 2011). Simple EMDs cannot predict fly behaviour in response to second order motion however (Theobald et al., 2008), which is motion containing higher-order statistical correlations, such as a target moving against a moving background. However, no single model of the EMD appears to completely describes *Drosophila* motion vision, with some pointing out that there may not be a single unified EMD model that is used ubiquitously in the fly brain, particularly for all features

and contexts under which motion is detected (Yang & Clandinin 2018).

1.1.6 Biological Implementations of EMDs

The reichardt-correlator model necessitates that visual signals from adjacent regions in space are integrated with some modulation of the time at which the signals are transmitted. This is implemented early on, with the monopolar cells having a range of spatiotemporal characteristics. L1 and L2 responses are rapid and transient, whilst L3 is more sustained (Silies et al., 2013), with all possessing centre-surround inhibition, unlike photoreceptors. This diversity in the response properties of laminar cells is further amplified in lobula and medullary neurons, which exhibit a wide range of spatiotemporal properties (Arenz et al., 2017; Currier et al., 2023). In particular, the inputs to T4 and T5 cells are highly diverse in their temporal characteristics. With T4 inputs Mi1 and Tm3 having fast and biphasic responses, and Mi4 and Mi0 having slower monophasic responses (Behnia et al., 2014). T5 receives fast Tm2, intermediary Tm4 and Tm1, and slower Tm9 inputs, all monophasically (Arenz et al., 2017). The nonlinearity required for the Hassenstein-Reichardt detector has been found to come about in T4 neurons via excitatory cholinergic inhibitory glutamatergic input (Groschner et al., 2022).

1.1.7 The Optomotor Response

One of the key ways in which motion detection can be studied behaviourally is via the optomotor response. The optomotor response is a course-correction and gaze-stabilization mechanism that is well-studied in insects (Götz & Wenking, 1973; Reichardt & Wenking, 1969), but also exists in rodents (Mitchiner et al., 1976), fish (Neuhauss et al., 1999), birds (Fite, 1968), and humans (Warren et al., 2001). For flies, every step or wingbeat produces an output as well as an error. The error is the difference between the expected output and

the actual output, as detected by the sensory organs. Errors can arise intrinsically (e.g. imperfect co-ordination or transmission of the motorneurons) or extrinsically (e.g. the wind).

The optomotor response is the error, calculated from the rotational optic flow by the visual system. The response means that if the fly intends to walk directly forwards, and it observes clockwise optic flow, this indicates that the fly has moved to the left. The response would be to course correct and move to the right. If we apply an external rotation to observe the optomotor response ourselves, it appears as if the fly is following the rotation. The optomotor response was first reported for flies in a flight simulator (Reichardt & Wenking, 1969) , but is also present during walking (Götz & Wenking, 1973). It can be detected either from the torque produced via flying motion (Blondeau & Heisenberg, 1982), changes in the wing-beat amplitude (Götz, 1987), from free-walking behaviour (Geurten et al., 2014), fixed-thorax trackball behaviour (Kain et al., 2013).

For gratings and other periodic stimuli, the optomotor response size is modulated primarily by the temporal frequency (TF) of the moving environment (Creamer et al., 2018); this is the velocity divided by the wavelength of the grating. The strength of the optomotor response follows a bell-shaped curve with respect to temporal frequency, producing low-strength responses at very low TFs, strong responses at medium TFs, and weak responses again at very high TFs (Duistermars et al., 2007). If the system was instantaneous and errorless, the strength of its optomotor response could follow a linear relationship with respect to velocity. However, this bell-shaped tuning has been proposed as a mechanism to avoid positive-feedback cycles at high-gains, where a high gain optomotor correction introduces a high error that then needs to be corrected in the opposite direction (Warzecha & Egelhaaf, 1996).

Since the optomotor responses is dependent on the wavelength of gratings, it is pattern-dependent. It is not clear why the fly's optomotor behaviour is dependent on a pattern-dependent tuning curve, rather than a velocity-dependent tuning curve, which would be

pattern-independent. Some have suggested that these two systems are functionally equivalent under naturalistic conditions (Dror et al., 2001). Still, it seems possible that under some circumstances the pattern specificity might be be disadvantageous since some patterns in the wild resemble laboratory-style stimuli (How & Zanker, 2014). One suggestion is that the fly simply does not possess the circuitry to carry out this velocity-tuned computation. However, as well as an optomotor turning response, flies slow down in response to motion in the environment (Creamer et al., 2018). The neural circuits that control this behaviour are velocity-tuned, that is independent of the pattern of the stimulus (Creamer et al., 2018). Indeed, other insect responses also appear to be velocity dependent and independent of the spatial structure of the stimulus, for example the centreing response in honeybees (Srinivasan et al., 1991), and peering behaviour (Srinivasan et al., 1999). So the circuitry for velocity-dependent responses is either present already, or can plausibly be developed in an insect brain; this is an open question.

1.1.8 Active Vision

In active sensing, the actions of the sensor directly sample the environment, as opposed to passive sensing, in which a sensor that has no influence on how information reaches it. Active sensing is found widely in nature, for instance in electroreception in fish (Zweifel & Hartmann, 2020), echolocation in dolphins (Moore et al., 1984), and whisking in rodents (Bush et al., 2016), as well as in robotics (Bajcsy et al., 2018).

Vision can also be considered active, since the actions of the the agent controlling the sensor can affect what arrives at the sensor. In flies this can occur via self-generated movements, from the photoreceptors themselves (Juusola et al., 2017; Kemppainen et al., 2022), to the eye muscles (Fenk et al., 2022; Franceschini et al., 1991), head movements (Hateren & Schilstra, 1999) and body position (Cellini & Mongeau, 2020). These allow the fly to modify

what is shown to each eye, which can allow for a number of different properties of vision that are not available to the passive sensor. One of these is roles is gaze stabilization, which seems especially suited to movements that move the entire field of view, which head and body position movements can achieve. Depth information can also be extracted when the sensor has independent control of two different sub-sensors. This can be individual photoreceptors, or the two eyes.

Finally, active sampling allows the fly eyes to see in higher resolution. As each photoreceptor is a discrete sampling unit it only has a limited resolution. By incorporating active mechanical movements both at the photoreceptor level and each eye, this discrete unit is transformed into a continuous sampling unit that allows for a much higher resolution. This has also been proposed as a mechanism that is for mammalian eyes to increase edge-detection during whole-retinal microsaccades (Donner & Hemilä 2007).

1.1.9 Microsaccades

When light is absorbed by the rhodopsin pigments, PLC is activated cleaving PIP2 from the membrane (Bloomquist et al., 1988) and initiating the signal transduction pathway that eventually leads to the depolarisation of the photoreceptor (Hardie & Minke, 1992; Ranganathan et al., 1995). The cleavage of PIP2 itself causes contraction of the microvilli. The contraction of the microvilli activates the mechanosensory TRP and TRPL channels which then go on to effect the rest of the phototransduction pathway (Hardie & Franze, 2012).

A consequence of the photomechanical nature of the phototransduction pathway is that there is a physical contraction of the photoreceptors themselves, resulting in a modification of the receptive field location over time (Juusola et al., 2017; Kemppainen et al., 2022). The photoreceptor movement consists of a waveform that rapidly deflects and returns more slowly to its baseline position over time. Each photoreceptor's movement direction is stereotyped

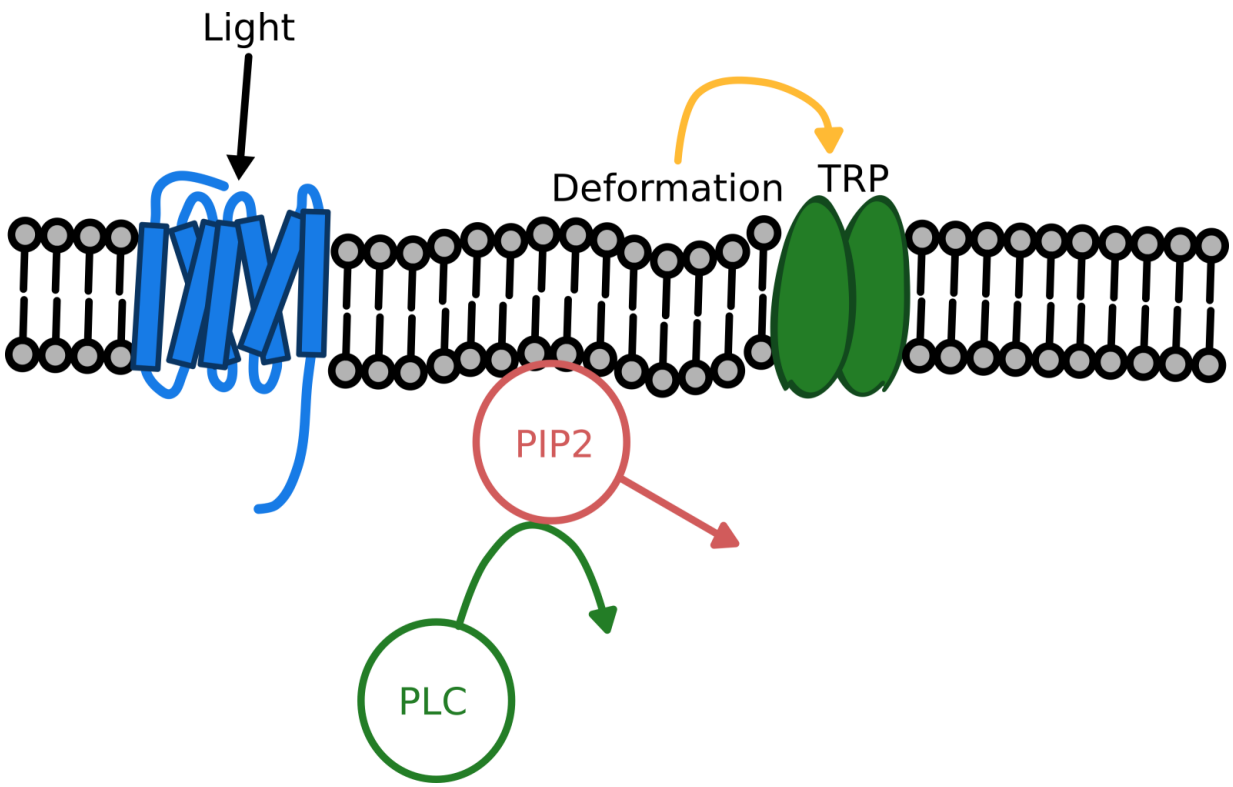

Figure 4: In Drosophila*, light is absorbed by rhodopsin molecules; this causes the transformation into metarhodopsin. Via Gq, PLC is activated, which reacts with PIP2, cleaving it from the membrane and transforming it into DAG and IP3. The cleavage from the membrane causes a mechanical deformation detected by the TRP and TRPL ion channels.*

by its location within the eye. This aligns the photoreceptors' deflection direction to the optic flow field during forward flight (Kemppainen et al., 2022). Yet, each photoreceptor's movement speed is adaptive and depends on its light/dark adaptation state, being the fastest in fully light-adapted cells (daylight conditions) (Kemppainen et al., 2022).

Because of this movement, the output of a photoreceptor output does not just encode light intensity changes within a small spatial area. Instead, it encodes a complex time-dependent function of its receptive field (RF) moving over a region of space. This function is made more complex by the fact that a light change initiates the microsaccade itself. A light increment transiently moves a photoreceptor in its eye-location-specific direction, say north (0°), and pulls it axially (narrowing the RF), whilst a light decrement shifts it in the opposite direction (south, 180°) and extends it axially (widening the RF) (Kemppainen et al., 2022). So this complex function is a function of space, time, and light intensity change.

1.1.10 Retinal Muscle Movements

Flies have muscles that move the retina underneath the lenses of the ommmatidia (Fenk et al., 2022; Franceschini et al., 1991). Each eye is controlled by two muscles, that move each retina laterally in contrasting directions, reaching a 15 degree peak displacement (Fenk et al., 2022). The eye muscles are of a very different nature to microsaccades, since they globally happen within each retina, are generally slower, and can be initiated via top-don control, rather than being an intrinsic part of the signal transduction pathway (Fenk et al., 2022; Kemppainen et al., 2022).

Muscle movements can be used to track motion in smooth pursuit, as well as short sharp motion in response to visual scenes (Fenk et al., 2022). Both these characteristics are remarkably similar to vertebrate saccadic and smooth eye movements, and also show nystagmus-like activity, which is also known to occur in head movements in blowflies (Longden et al., 2022). The eye muscles, at least some of the time, are likely to have a similar gaze stabilisation role, along with head movements.

1.1.11 Head Movements

The final axis on which the fly is able to manipulate its own visual input is its body and head movements. The head moves is able rotate around the yaw and roll axis. As it is only able to move the whole retina, it cannot be used to achieve higher acuity or depth perception, but can still be used for gaze stabilisation (Land, 1999).

1.1.12 Evidence for Hyperacute Vision

As a result of the microsaccadic photomechanical contractions, the fly's photoreceptor signal contains much more information than in a static model (Juusola et al., 2017), and allows flies to see in a more detail visual acuity (Juusola et al., 2017; Kemppainen et al., 2022), as

well as allowing binocular stereopsis for depth perception for flies when both eyes are intact (Kemppainen et al., 2022). The key assumption that fly vision is low-resolution has previously underlined many further assumptions within the field of fly vision. For instance, the assertion that head-movements do not improve visual performance is dependent assumption that vision is low resolution (Geurten et al., 2014). Re-interpreting these findings in the context of flies with high-resolution vision will be required.

However, hyperacuity is not always observed, for instance on a study on eye-muscle movements, the authors did not observe any walking optomotor response to hyperacute patterns (Fenk et al., 2022). Where hyperacuity has been observed, it has only been observed in flying flies (Juusola et al., 2017; Kemppainen et al., 2022). While there is no reason to think that microsaccades are dependent on the behavioural state of the fly, since they are an intrinsic part of phototransduction, it is possible that the expression of behaviours at such resolutions is modified by the behavioural context; leading to the two different findings.

1.1.13 Optomotor Reversal

The optomotor reversal effect is an apparent reversal of the optomotor response found at certain grating wavelengths (Fenk et al., 2022; How & Zanker, 2014; Kunze, 1961). One explanation for this effect is aliasing caused by the Moirè effect (See Figure 5).

This occurs when two repeating patterns of different frequencies are overlaid. In this example, one pattern is rotated, producing a pattern of slightly different frequency in the x-axis. The overall intensity of the superimposed patterns over the x-axis is described by:

$$Intensity = \frac{1 + sin(Ax)cos(Bx)}{2} \tag{1}$$

Equation 1: The intensity of light passing through two filters at different frequencies. A is the average of the two frequencies, and B is the halved difference of the two frequencies.

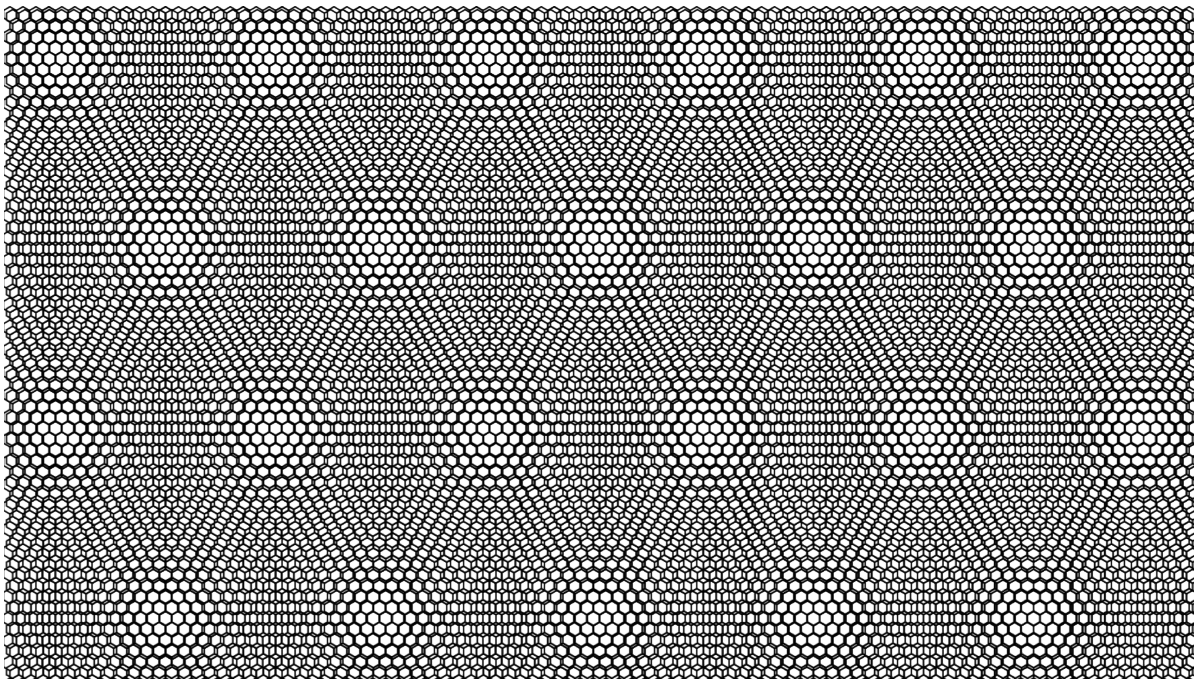

Figure 5: "When light hits the fly, under the limit of its compound eye, that's a Moirè"
Moirè pattern produced by placing two hexagonal lattices of slightly different sizes over each other.

Where A is the average of the frequencies, and B is the halved difference of the frequencies. The cosine term describes the low-frequency component of the Moirè effect. Whilst the sin term describes the high-frequency component of the pattern. Thus if the difference in frequencies is very large, the cosine term will generate a slower-wavelength Moirè pattern.

In the compound eye, samples are taken by the photoreceptors, and in the classical view, the limit of the sampling resolution is defined by the interommatidial angle. This repeated sampling pattern, combined with the repeated pattern of a grating can produce aliasing at certain wavelengths (specifically those 2x the interommatidial), giving the impression of a grating moving in the opposite direction (Horridge, 2009).

The alternative hypothesis for the optomotor reversal effect is that it arises from the action of microsaccades (Kemppainen et al., 2022). In this interpretation, microsaccades move over the object at 40°/s. Because these movements are mirror-symmetric between the two eyes, when the velocity of the stimulus and matches that of the microsaccades, one eye will be in lock-step with the moving grating, perceiving no motion, the other eye will therefore have

the opposite effect, perceiving high motion in the opposite direction. This means that the fly perceives motion in the opposite direction to the stimulus. Although this model does not fully explain why the effect is pattern dependent. One prediction of this model is however, that the optomotor reversal effect should be speed-dependent and also disappear when one eye is occluded. Both of these predictions seem borne out by the data (Kemppainen et al., 2022). If the stimuli shown to each eye could be controlled independently, we would also expect to notice no optomotor effect when the left eye is shown a grating of 40'/s moving right, and the right eye the same grating moving left.

One assumption of microsaccadic optomotor reversal explanation is that photoreceptor microsaccades are the only component of active vision that is not either stationary or in lockstep with the grating motion. If any part of this pathway (body, head, or eye-muscle movements) does not have this characteristic, the velocity at which the reversal will occur will shift away from the velocity of the motion of the photoreceptor contractions. In the case of most flight-simulator experiments, the head is fixed in place, however, eye muscle movements can occur, and although these generally track global motion (Fenk et al., 2022), in this case the stimulus motion is not being accurately being transmitted.

In (Fenk et al., 2022), they find optomotor reversals that occur in the 5-10° range, as others have found. In (Kemppainen et al., 2022) the authors test multiple different grating speeds, and find that only some velocities elicit optomotor reversals. (Fenk et al., 2022) uses 4Hz stimuli, which at the reversal wavelengths should produce a range of velocities from 36-100°/s. This stimulation corresponds reasonably closely to (Kemppainen et al., 2022) reversals at 45°/s & 6.6° wavelength, so it is not necessarily the case that the two results are incompatible. To test this, we would need to repeat the walking paradigm seen in (Fenk et al., 2022) on hyperacute gratings of different velocities.

One problem with (Kemppainen et al., 2022) is the velocities tested were very fast. This could

be a problem since fast movements of the drum might add air movements, which could lead the fly to choose the correct optomotor response rather than the illusory reversal. Indeed velocities of 300°/s at 6.6° wavelength produces a temporal frequency of 45.5Hz which is well above velocities found to elicit the most strong optomotor responses (Duistermars et al., 2007).

1.1.14 Other Anti-Directional behaviour

As well as the optomotor reversal, there are other contexts where the fly moves against the rotational optic flow of the world (so called anti-directional behaviour). When flying flies are shown a rotating full-field grating, they behave in the normal, optomotor way. When rotation is restricted the rear portion of the fly's field of view however, the fly turns anti-directionally (Tammero et al., 2004). They interpret the behaviour of the fly under normal, full-field rotation as being the end result of the sum of the optomotor frontal and anti-directional rear-field rotation.

Flies being shown a moving grating have a smooth optomotor response, but it has also been noted that this behaviour is interspersed with anti-directional saccadic turns in both flying (Heisenberg & Wolf, 1979), and walking flies (Williamson et al., 2018). In the case of walking flies, these saccades were occasionally so large and fast that sometimes the trial-averaged behavioural response was anti-directional, even though the fly spent most of its time doing optomotor course-correction. In this paper, they did not find that the likelihood of the saccades correlate with the frequency of the stimulus, in contrast to the optomotor response (Duistermars et al., 2007). It is unclear as to whether these anti-directional saccades are initiated by the same optomotor mechanisms that results in the optomotor behaviour, although this is unlikely to be a linear function of LPTC activity, since the saccadic frequency did not correlate with the stimulus frequency (Williamson et al., 2018).

Very recently another anti-directional response was uncovered. During walking behaviour, a moving grating stimulus caused an initial optomotor response, however after roughly 1 s, this syn-directional response changed into an anti-directional response (Mano et al., 2023). The anti-directional response disappears when the contrast is reduced. The response shares some of the same circuits as the optomotor response, as it is dependent on the T4/T5 cells. Inhibiting HS cells with shibire, while reducing optomotor behaviour, did not have an effect on anti-directional behaviour, while inhibiting CH does seem to reduce the anti-directional response, it also appears to strengthen the optomotor response.

Two external modifications affected the anti-directional response. First, presenting translational back-to-front gratings before presenting a rotatory grating caused the fly to perform the anti-directional behaviour immediately after motion onset (as opposed to after 1 s of optomotor behaviour), although the resulting anti-directional behaviour was weaker than in the rotation-only case. Second, changing the rearing conditions affected the likelihood of finding anti-directional responses. Older flies showed less anti-directional behaviour. Flies reared at 25° C also showed less anti-directional behaviour. Developmental processes are surprisingly susceptible to temperature in flies (Kiral et al., 2021).

Other labs have also reported long-lasting anti-directional behaviour (Personal Communication: Roshan Satapathy & Victoria Pokusaeva, ISTA), under experimental conditions different to that shown above, suggesting that this behaviour is robust under many different laboratory conditions, although given the types of stimulus that appear to cause it, it is unlikely to be found in the wild (Mano et al., 2023).

1.1.15 Body and Head Saccades

Flies tend to move in straight lines, interrupted by short, sharp turns called saccades, in a so-called fixate and saccade strategy. This pattern of behaviour is true for both flying (Fenk

et al., 2021) and walking flies (Censi et al., 2013; Cruz et al., 2021; Geurten et al., 2014). Saccades can occur spontaneously (Heisenberg & Wolf, 1979; Maye et al., 2007; Muijres et al., 2015), or they can be evoked by the environment (Censi et al., 2013; Fenk et al., 2021).

Where it is clear that the visual environment causes turning decisions, these happen in order to avoid objects such as walls (Censi et al., 2013), or large looming stimuli (Fenk et al., 2021), otherwise saccades can also be exploratory (Cruz et al., 2021). The probability of saccades away from a wall can be described as a linear function of the optic flow resulting from that wall (Censi et al., 2013). Because of the fixate-and-saccade strategy, the optomotor response must be engaged during the fixation portion, but if it were engaged during saccades, it would work against the direction of the intended saccade. For this reason, the optomotor response must be suppressed when turning. It has been found that flies are non-responsive to visual stimulation during saccadic movement (Bender & Dickinson, 2006), and there have been a number of studies linking this to the neural mechanisms behind optomotor behaviour (see Integration of Visual and Motor Signals below). On the other hand, saccades in flies are very rapid, reaching a rotational speed in the region of 1,000°/s in fast-bhevaing flies (Blaj & van Hateren, 2004; Schilstra & van Hateren, 1998). The resultant high temporal frequencies would result in very small optomotor responses. Thus the suppression of the optomotor response may only be necessary be necessary, or perhaps is only necessary at the initial phase of the saccade. In accordance with this view, flies are known to produce a visually-evoked rebound optomotor response at the end of a saccadic turn (Stewart et al., 2010), suggesting that at least at the final stage of the saccade, some optomotor information is available. An alternative hypothesis is that motion vision is not suppressed during the saccade, rather afferent feedback acts to cancel out the expected optic flow that would be associated with a yaw head turn (Kim et al., 2017).

Head saccades are of a similar nature to body saccades, they consist of rapid deflections of

the head, interspersed with smooth fixating behaviour. In flight, head-saccades turn faster than body saccades (Duistermars et al., 2012; Fenk et al., 2021), presumably stabilising the image seen on the retina, especially when tracking objects that move differently from the background (Fox & Frye, 2014). There is inconsistent evidence as to whether this is true in walking behaviour, with some reporting that body and head-saccades do not associate together in free walking fruit flies, with the further conclusion that a head saccade would not stabilise vision very much if we assume fly vision is low-resolution (Geurten et al., 2014). However, others report that head-saccades do co-occur with body-saccades, where they precede the body movement by approximately 45ms (Williamson et al., 2018). Complicating matters further, others have found that the head saccade follows the body saccade by 66ms (Cruz et al., 2021). Since these both studied exploratory saccades in free-walking flies it is unclear why this difference should arise. In fixed setups, the blowfly (*Calliphora*), head-movements do accompany body saccades as they do in flying *Drosophila* (Blaj & van Hateren, 2004). It has been found however, that head-movement dynamics differ when the body is allowed to rotated freely in flying flies (Cellini & Mongeau, 2022; Tuthill et al., 2013), so any experimental effort to characterise head and body co-ordination must take into account the experimental settings when attempting to extrapolate out general principles.

1.1.16 Integration of Visual and Motor Signals

In mammals, motor-related signals are ubiquitous in the brain, such that the sensory signals are accompanied motor signals at different scales (Stringer et al., 2019); an association that only makes sense from an active-sensing point of view. The subject is less well studied in insects as it is in mammals. Despite this, recent evidence shows that both short and long-scale motor context signals are globally present in a similar manner in the insect brain. In butterflies, compass cells change their tuning preference, depending on the animal's internal

state (Beetz et al., 2022). More recently, behavioural activity has been shown to have a wide-reaching signal that can be detected in disparate brain regions (Aimon et al., 2022; Brezovec et al., 2022; Schaffer et al., 2021). One study shows that movement signals can be detected in 40% of brain regions (Brezovec et al., 2022). In the same study, they show that this motor activity is spatially and temporally structured within the brain, and corresponds to the real and anticipated movements of flies (Brezovec et al., 2022). Some sensory information in *Drosophila* is also globally available (Pacheco et al., 2021), although this has not been yet found to display as much detail and structure as shown by motor activity (Brezovec et al., 2022).

As well as these signals that act across the entire brain, a number of studies have shown that the LPTCs integrate information-rich signals into their motion detection response. Flies selectively modify their responsiveness to external rotation when they perform flying body saccades (Wolf & Heisenberg, 1990), this modification may be a necessary step, since the optomotor response would act against the fly's course-changing turns. The optomotor suppression has been shown to be neurologically based in feedback inhibition to HS cells during turning behaviour in flight (Fenk et al., 2021). The HS cells have a strong gain in their sensitivity to visual motion when the fly is walking, compared to when it is still, and this gain change is strongest at the higher temporal frequencies likely to be experienced during walking behaviour (Chiappe et al., 2010). As well as active locomotion, flight also changes the gain of the HS cell response (Maimon et al., 2010). This broad gain in sensitivity is accompanied by highly phasic modulation of the HS activity during walking behaviour, with stride-by-stride signals from the legs reaching the HS cells (Fujiwara et al., 2017), brought by mechanosensory feedback, via the ascending LAL-PS-ANContra neurons (Fujiwara et al., 2022).

LAL-PS-ANContra terminates in the posterior slope. What is intact and identifiable of the

HS cells in the hemibrain dataset (Li et al., 2020) shows that they receive many inputs from the posterior slope, suggesting that this premotor area provides information about intended locomotion to the HS cells. Given the HS cells are an unusual cell type; they are very large, they have gap junctions (Cuntz et al., 2007), and exhibit graded potentials but also spiking responses (Hengstenberg, 1977), it is possible that this sensory-motor motif is unique to these cells. On the other hand, given that information about locomotion is found all over the brain, it is would require some explanation as to why HS cells would be the only cell type to integrate this information into their response pattern, and indeed evidence for integration of motor signals into visual glomeruli have also been found (Turner et al., 2022), as well as the identification of areas into which motor and sensory signals are integrated (Chen et al., 2023).

1.1.17 Experimental Aims

Given the existence of the anti-directional response, the following questions are left thus-far unanswered. Firstly, why do flies sometimes turn in the opposite direction to that predicted by the optomotor response? Secondly, Is the behaviour of flies during these behaviours similar to that seen during the optomotor response? Thirdly, under what conditions can the response be modified? Fourthly, to what extent do active sensing mechanisms impact both the optomotor and anti-optomotor response? Specifically, we seek to determine if the microsaccadic sampling theory can account for the enhanced visual resolution evident in the optomotor responses of flies.

1.2 Methods

1.2.1 Behavioural Measurement

The optomotor response can be tested in the 3 following ways: in a flight-simulator system, in a trackball system, and free walking. We opted for the trackball system to allow for better corroboration between previous efforts where anti-optomotor behaviour has been observed. In the trackball system, the fly walks on an air-cushioned ball (6mm, HDPE or PTFE), which is able to rotate in the yaw, pitch, and roll axes to allow for a full 2-dimensional plane of locomotion. The rotation of the trackball is recorded by two infrared cameras, placed 90' from each other, a black marker was used to pattern the ball to provide high-contrast features with which the optic flow could be tracked; these features are also visible to the fly when behaving. Each camera measures the vertical and horizontal optic flow of the trackball, These signals are then used to calculate the yaw (turning), pitch (forward walking), and roll (sideways walking).

The ball was illuminated by a 720 nm wavelength LED, split into two channels by an optic fibre, and directed on the sides of the ball where the IR tracking cameras face. The experiments were run with a custom MATLAB script, and the controllers for the tracking cameras were polled after every frame presentation. Most of the time, data had not reached the buffer on every frame presentation, and was usually pulled at around 40Hz, however, since the sampling rate from the cameras is at a constant rate this could be reconstructed into a 120Hz signal. A final IR camera, placed 15 cm behind the fly was used to position the fly onto the ball.

1.2.2 Head Tracking

Head-movement data was collected with a raspberry-pi camera. The infrared-filter to the camera was removed so that it could film when there was no visible light. The camera was placed above the fly and its position was controlled by a micro-manipulator. The video stream was recorded via a raspberry-pi zero using a custom script written in python. Recordings began up to 2 s before the onset of the stimulus, since there was some variation in the initialisation time for the camera. Videos were later synchronised to the trackball traces by recording the time at which the projector screen turned on, which is synchronised to the trackball data. Videos were recorded at 40 Hz, which was of a sufficient temporal resolution for head-movements but still high enough in spatial resolution to allow the tracking software to accurately track the head movements. During tracking, two symmetrical regions on the head were manually selected and an openCV (Bradski, 2000), CSRT-based tracker (Lukezic et al., 2017) was used to track the regions throughout the video. Manual selection of the same regions occurred 3 times per video to ensure the tracker was maintained its accuracy throughout. Since behaviours like head-grooming tended to disrupt the tracking process, these were identified and manually re-tracked after they have completed. As a final test to ensure the trackball data was synchronised to the camera data, we calculated the ball motion and compared this to the ground truth of the trackball data. These two measures were cross-correlated to fully align the traces.

Item	**Source**
Raspberry pi Zero	RS-Components
Raspberry pi Camera	RS-Components
Micromanipulator	Thorlabs

Table 1: Head-Tracking Parts

1.2.3 Stimuli

Projecting Stimuli: The projecting display was constructed from an acrylic (7.5 mm diameter, 7.5 mm height) half-tube, covered with diffusing paper. The screen was placed in front of the fly with the fly at the centre of the half similar, giving a distance of 7.5 mm to the screen. We used a DLP lightcrafter projector (EKB Technologies Ltd.), with blue, and green, and UV LEDs. Unless otherwise stated, stimuli were preprepared and shown to the fly at 120 Hz. The stimuli were calibrated to project onto the cylindrical screen with the *DisplayUnderstortionHalfCylinder* function in Psychtoolbox (Brainard & Vision, 1997). In order to allow sufficient resolution to display the hyperacute stimuli, the projector was placed close to the screen, which meant that the angle subtended by the display covered only 110°.

Open-Loop Grating Stimuli: Flies were shown each stimulus, with a 4 s gap between each stimulus presentations. Each square-wave grating stimulus began with a 4.2 s motion-free adaptation period, followed a counter-clockwise motion stage for 8.3 s, a second 4.2 s adaptation period, and then a clockwise motion stage for 8.3 s. We tested grating wavelengths of 5.2°, 10.2°, and 16.8°, along with grating velocities of 26.5°/s, 51.0°/s and 106.0°/s, as well as an additional hyperacute 2° wavelength at 10°/s and 20°/s for the head-tracking experiment.

Forward Walking Experiments: At the beginning of the experiment, a motionless grating was presented to the fly. We recorded the behaviour of the fly via the trackball, when the fly walked forward more than 2 mm/s over a period of 333ms, the stimulus was triggered and the grating moved either clockwise or counter-clockwise. The order of rotation was randomised within sets of four (this was to ensure the number of clockwise and counter-clockwise recordings was approximately balanced since the length of the experiment was not guaranteed). Flies were tested for up to 40 minutes at a time, but if a fly did not show sufficient walking

behaviour by not triggering the stimulus for more than 6 minutes, the experiment was ended. We removed the data for flies for which we recorded fewer than 20 'walks'.

High Frame Rate Experiments For the fast-grating experiments, running the projector at 120 Hz resulted in each grating moving over half the thickness of the grating per frame, so we presented the stimulus at 360 Hz to avoid this. As the data transfer rate out of the display ports is limited, the projector was setup to receive 6-bit data so that each frame could still be transferred at 360 Hz. The stimuli were rewritten into a 6-bit format. This reduces the colour range that can be displayed to the fly, but since we used square wave gratings with only 2 brightness levels this was an issue.

Starfield Experiments In order to simulate a less periodic environment, to test anti-optomotor effects, we used a starfield stimulus (Lyu et al., 2022). For these controls, we used psychtoolbox's wrappers for OpenGL (Woo et al., 1999). Square points were generated at uniform random locations around the virtual camera. In order to create an infinitely traversable environment, but optimised to run at a high enough frame rate for closed-loop experiments, the environment was reused as soon as it disappeared from the view of the virtual camera. To prevent items from appearing suddenly on the screen as they were reused, the lightness of the points was set proportional to the distance away from the camera. These features were implemented in a custom GLSL shader.

Looming Stimuli For the experiments that tested the effect of a looming stimulus on the optomotor and anti-directional responses, we generated a stimulus consisting of a white circle, increasing in size from a diameter of 0°, to a diameter of 40° over the course of 100ms. The increase in the size of the radius of circle was a function of arctan, to simulate the size of a real life object coming towards the fly at a constant speed, and was presented to the left or

right of the fly at 25° eccentricity. To test the fly's responsiveness to environmental rotation, we presented square gratings at the same time as the looming circles, 30° wavelength and at 4 Hz temporal frequency. The gratings were presented at 40% contrast to allow the looming stimulus to be visible. Some of the 'saccadic' stimulation comes from the grating itself, as we found during presenting high-contrast and fast gratings over longer periods, as well as the fact that saccadic responses were enhanced in the looming + grating condition compared to the looming condition alone. For this reason, the lower contrast grating was also used to ensure most of the saccadic stimulation came from the looming stimulus rather than the grating.

1.2.4 Analysis

Head-Saccade Prediction We identified head saccades using a continuous wavelet transform of the head-position traces and the Ricker wavelet over varying scales. This identifies peaks in the data at different scales, the locations of which were then identified using the ridge-detection algorithm as described previously (Du et al., 2006; Fischer & Schnell, 2022). Saccade magnitude sizes were measured as the difference between the peak of the saccade, and the most distal head position within a 125 ms window.

Tracking Analysis The trackball was analysed by binning all the data into 8.33 ms segments. Sometimes the buffer data is not read onto the computer by the time that the next frame of the video is read, resulting in data from one frame being collected in the packet of data in the next frame. Because the controller generates the tracking data at a constant rate however, this was fixed with a simple interpolation of the frames at the end of data collection. To calculate optomotor responses we took the response to each motion presentation relative to the response 1 s before the presentation of the motion, the response to counter-clockwise motion was then subtracted from the response to clockwise motion to generate a

single optomotor measure.

Fly Genetics & Husbandry Wild-type Canton-S flies were reared in a 12 hour light-dark cycle at 21 ℃. Flies were behaviourally tested at 2-5 days old, and within 3 h after lights on or 3 h before lights off since these are the most active times, thus allowing us to test more of the behaviour.

Item	**Ingredient**	**Source**	**Supplier**
Cold tap water	1 Litre		
Medium Cornmeal	80g	Triple Lion	Lembas/Easton Enterprises
Dried Yeast	18g	Kerry Ingredients	Regina
Soya Flour	10g	Lembas Wholefoods	Lembas
Malt Extract	80g	Rayner's Essentials	Lembas
Molasses	40g	Rayner's Essentials	Lembas
Agar	8g		Regina
10% Nipagin in Absolute Ethanol	25ml	Clariant UK Ltd; Fisher	Chemolink Specialities Ltd; Fisher
Propionic Acid	4ml	Fisher	Fisher

Table 2: Fly Food Material (from the Sheffield Fly Facility)

Name	**Genotype**	**Source**
Canton-S Wild Type	Wild Type	
BPN Drivers	w1118; R11H10-p65ADZp(attp40);VT033947-ZpGal4DBD(attp2)	Bidaye Lab
csChrimson	UAS-CsChrimson-tdTomato(VK5)	Lin Lab
Elav-GCaMP	elav-Gal4/Fm7a;+;lexAop-P2X2,UAS-GCaMP6m/Tb	Yunqi MA
BPN>csChrimson	w1118/+; R11H10-p65ADZp(attp40)/+;VT033947-ZpGla4DBD(attp2)/UAS-CsChrimson-tdTomato(VK5)	This study

Table 3: All the Genotypes Used in these Experiments

1.2.5 Fly Preparation

Flies were held in ice for around 4 minutes and transferred to a Peltier-cooled fly-holder. The condensation that appears around the cooled-holder allows the fly to adhere to the

holder while it is rotated into position. After this, a pin is lowered to the dorsal side of the fly's thorax and glued to the fly with low-temperature melting wax. Images were taken each time to assess the accuracy of the waxing and positioning on the pin. The pin was then attached magnetically into the behavioural rig, and the fly is centred on the ball with a micro-manipulator. The fly was oriented on the pitch axis horizontally. The flies were allowed to acclimatise to the ball for 5 minutes before recording began. For the head-fixed experiments, we made a specialised pin that attached to both the thorax and then bent horizontally to attach to the head, again with wax.

1.2.6 Optogenetic Experiments

Flies used in the optogenetic experiment where reared on fly food as described above, but with 0.4 mM of retinal (Hindmarsh Sten et al., 2021). Flies were reared in the dark to avoid activation of the neurons expressing csChrimson. During the behavioural experiment, we activated the csChrimson expressed in the BPN cells with a 680 nm Cairn LED, fixed 40mm directly above the head of the fly. The power used to drive the LED was sufficient to generate small behavioural responses in wild type flies, potentially via the heat generated from the LED, or its long red tail marginally activating Rh1 pigments. These responses tended to increase activity, but not to generate the strong forward-walking behaviour as exhibited by the BPN>csChrimson flies. The LED control was integrated into the experiment protocol with a national instruments board, which turned the LED on at the beginning of grating motion.

Item	**Source**
LEDs 680nm	Cairn
LED Driver	Cairn
Controller Board	National Instruments

Table 4: Parts for the Optogenetic Stimulation System

1.2.7 Statistics

For almost all of the behaivoural experiments, we measured the optomotor strength during a relevant period of time as our measure. Optomotor strength was calculated as the turning rate per second for flies responding to leftward motion, subtracted from the turning rate per second for flies responding to rightward motion, since the trackball system generates positive numbers for clockwise motion of the ball. For each experiment the optomotor response was calculated by comparing the responses to rightward and leftward gratings within each parameter, such as a certain wavelength or speed of grating. For the initial optomotor experiment, the optomotor response was taken over the entire period of grating motion presentation, tested with a two-way ANOVA, and then post-hoc independent T-tests carried out with the bonferonni correction for multiple comparisons. The same tests were carried out with the peak frequencies and powers of the calculated power spectra. In addition, we tested the optomotor response between flies following the calibration grating to ensure there were no differences in innate ability to perform the test. For the head-tracking experiment, we carried out two-way ANOVAs on the sizes and frequencies of the head-saccades. We took the head-optomotor response as the difference between left and right head turning during the first 3 seconds of grating motion presentation, which was chosen to because after this period head-saccades tended to disrupt the measures of smooth head-movements. Dependent T-tests were used to test the difference between the optomotor strength before the head-saccade and afterwards. For the head-fixed experiments we carried out two-way ANOVAs to test for effects of wavelength and speed, testing the optomotor response over the whole stimulus presentation period. For the forward-walking experiment, we calculated the optomotor response strength from the two seconds of motion presentation, as well as the slowdown response over the same period. The slowdown response was calculated as the average forward walking rate prior to the beginning of stimulus motion, minus the aver-

age forward walking rate over the motion presentation. We carried out two-way ANOVAs on both the optomotor strength and slowdown responses, with independent T-tests, with corrections for multiple comparisons for the optomotor responses. To calculate the correlation coefficients between the forward and turning behaviours, we carried out a linear regression with a single coefficient and intercept using the GLM package in Julia (Bezanson et al., 2017). For the comparisons between walking and non-walking flies, we used a repeated measures ANOVA to compare optomotor responses at the first second vs the last second of stimulus presentation, with dependent T-tests as the post-hoc tests. We used the same statistical tests to test the 5Hz amplitude time series. For the optomotor responses tested at the reversal wavelengths, we used a repeated measure two-way ANOVA with dependent T-tests as post-hoc. For the high-speed gratings, we used a one-way ANOVA on the forward walking and optomotor responses, with dependent T-tests used to test between the leftward and rightward turning responses for the optomotor behaviour. For the optogenetic experiments, we used dependent T-tests to compare between the forward walking and optomotor behaviour, when the LED was on vs when it was off. For the looming experiment, we used a repeated measures ANOVA to test between the early optomotor and late anti-optomotor responses with the loom present or not.

Two-Way ANOVAs, independent and dependent T-tests, and tests for multiple comparisons were carried out using the SciPy python package (Virtanen et al., 2020), with repeated measures ANOVAs carried out using the python package Pingouin (Vallat et al., 2018).

1.3 Results

1.3.1 The Anti-Optomotor Response

For each fly, we wanted to record the optomotor and anti-optomotor responses to moving gratings of various grating diameters and speeds. During pilot experiments, we noticed that flies tended to stop responding at all during certain periods. So we tested the differences in optomotor responses between-flies, testing only two grating parameters per fly. One set of parameters was kept consistent between flies to get a baseline optomotor response, the other was modified between flies to test the effect of grating diameter and speed on optomotor and anti-optomotor responses.

We found that under these conditions, the anti-optomotor responses dominated the behaviour (figure 6). That is, flies turn in the opposite direction to the grating, which under free-moving conditions would increase the optic flow perceived by the fly. These responses were unexpected, as most studies of optomotor behaviour rarely report any of anti-optomotor behaviour, although it is not entirely unknown (Mano et al., 2023; Tammero et al., 2004; Williamson et al., 2018).

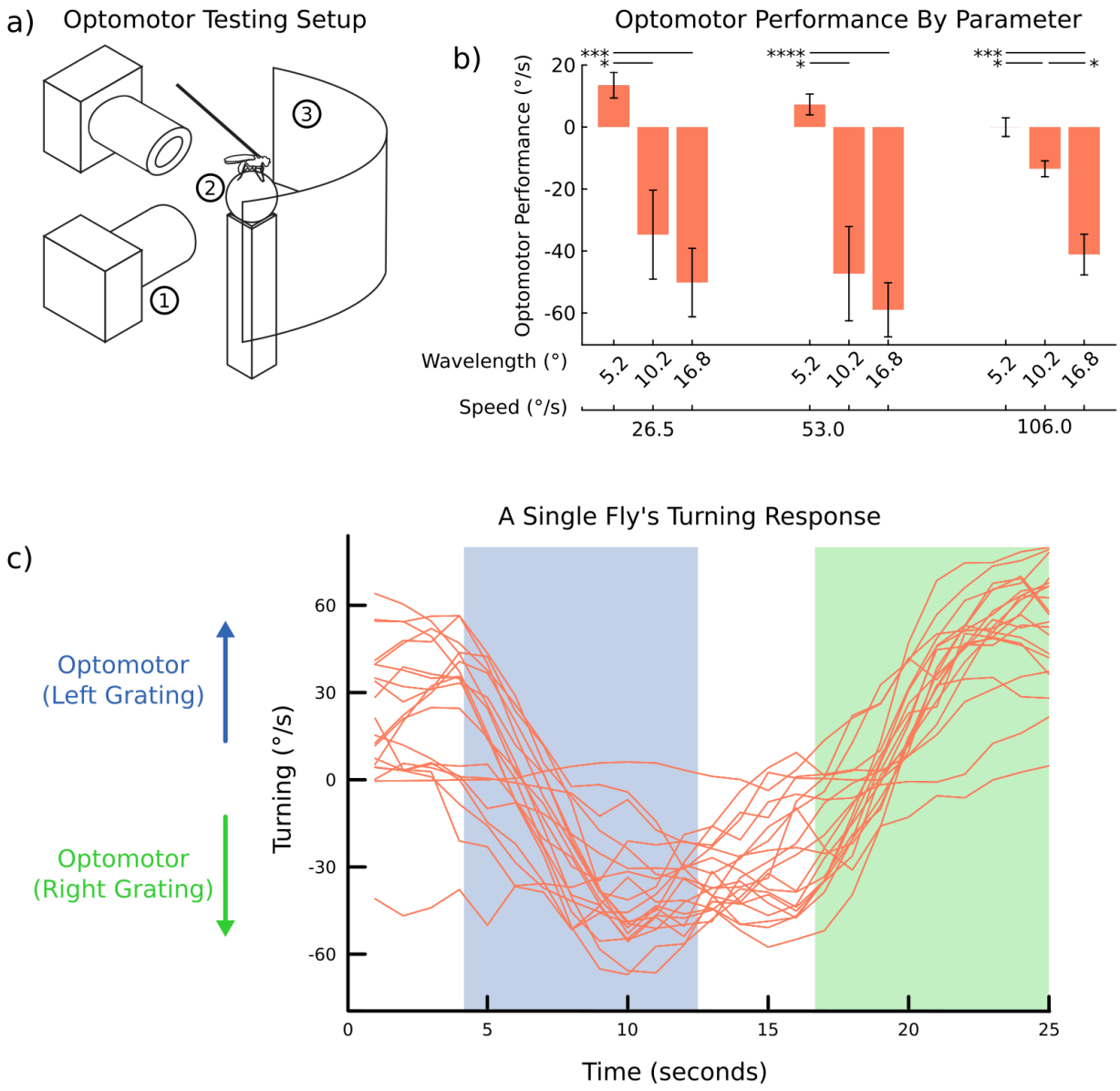

Figure 6: Flies turn in the anti-optomotor direction to rotating gratings
(a) Schematic showing the trackball system. The motion of the trackball is detected by two infrared cameras (1). The fly moves around on the air-cushioned ball (2) and is presented with stimuli projected onto a semi-cylindrical screen (3). A third camera position is behind the apparatus to position the fly (not shown)
(b) Optomotor responses of flies responding to the stimulus. At diameters 5.1 and 8.4, the responses are anti-optomotor.
(c) Turning response of a single fly in response to the stimulus. Turning indicates the turning of the ball. Positive turning indicates the ball turns clockwise, meaning that if the fly were not restrained, it would turn anti-clockwise. For the left grating (blue period), the response should be positive if the fly performs the optomotor response and negative for the right grating (green period). In this example, the fly tended to continue rotating, albeit at a lower rate, after the offset of the stimulus. We found this could occur with flies with particularly strong and consistent turning behaviour.

The traces appear to show an initial anti-optomotor response to the stimulus, which on average sees an increase in turning in the anti-optomotor direction for approximately 3 seconds

(figure 6c). After which, the response stabilises and remains anti-optomotor until the offset of the grating motion. The offset of the motion results in a slowdown of similar slope, which for some flies does not fully recover to baseline, but in other flies overshoots before returning to baseline before the start of the next grating motion onset.

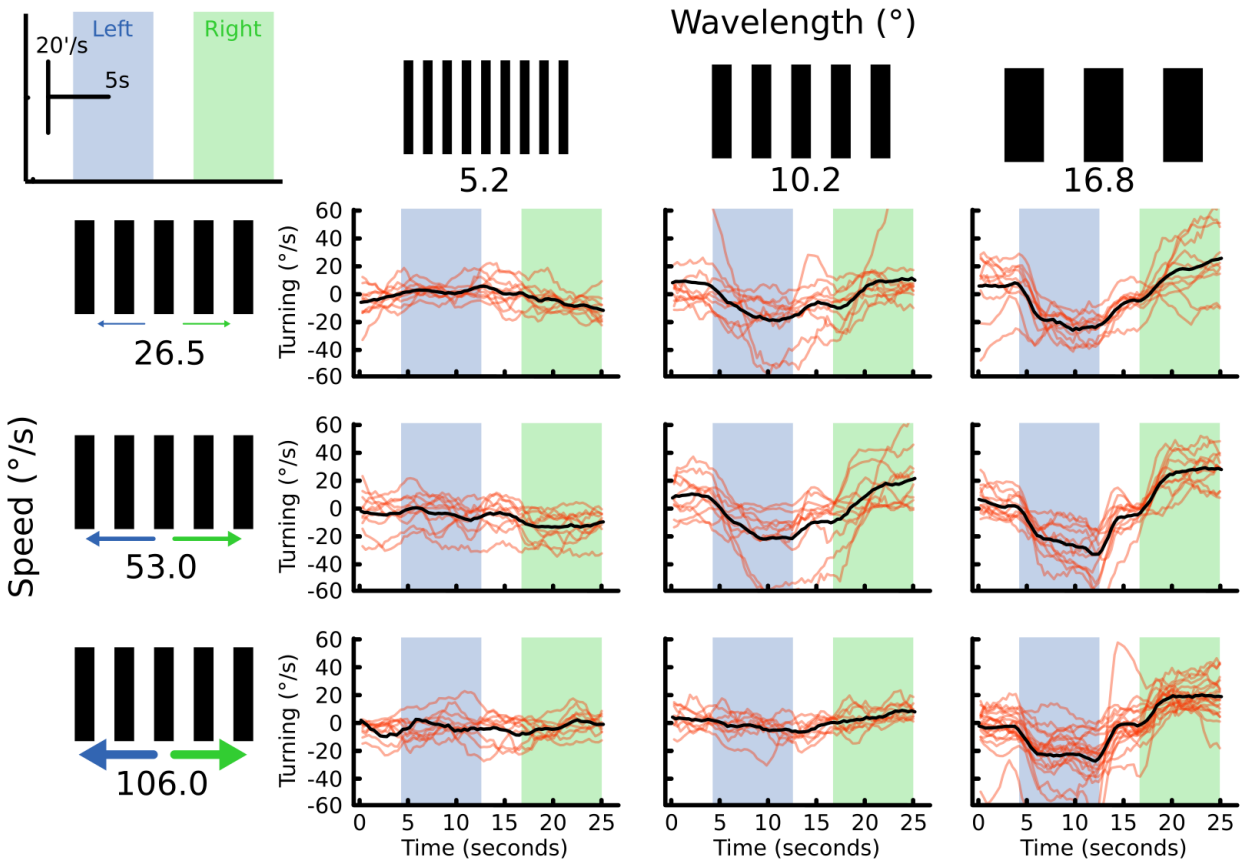

Figure 7: Average turning traces for flies shown grating of different wavelengths (across) Speeds (down).
Each line represents the average turning response of a single fly.

The strongest responses were seen in the largest gratings, at 16.2° wavelength (figure 7), with the strongest speed being observed at 53°/s, corresponding to a temporal frequency of 3.3 Hz, which is reasonably close to the 4Hz maximal stimulation found elsewhere (Duistermars et al., 2007). Averaging over the trials flies were rarely observed to maintain a rotational velocity above 25°/s, which would not counteract even the slowest grating speed we tested. This was however, more likely to be the result of averaging traces in which flies rotated a lot

faster, with traces in which the fly does not respond at all.

While the responses to gratings at 16.8° were very clear, responses at other grating thicknesses were much less clear. At 10.2°, the response to a 106°/s grating is very weak, but clearly present at 53°/s and 26.5°/s. At the 5.2° wavelength, there was no detectable anti-optomotor response, however there did appear to be very slight optomotor responses to the onset of the grating.

A two-way ANOVA revealed a significant effect of thickness on the overall optomotor response ($F = 32.59$, $P < 2e\text{-}10$, $n = 10$ flies per condition), with no significant effect of speed or an interaction between thickness and speed. Post-hoc tests show that the 10.2° and 16.8° responses were significantly different from the 5.2° responses for all speeds tested, with a significant difference between the 10.2° and 16.8° responses at 106°/s only.

In addition to the turning responses of flies, we also investigated their forward locomotion. The forward walking was generally low, and the grating did not tend to elicit changes in forward walking, except for the calibration stimulus, for which we had a large number (90) of samples. Different flies also appear to have different baseline walking speeds. Occasionally, flies had extremely strong forward walking speeds, averaging over 20°/s.

In contrast to other findings, the anti-optomotor responses dominated the responses at all timescales, unlike the anti-optomotor effects that have previously been found for which the anti-optomotor responses were preceded by optomotor turning (Mano et al., 2023). Since we observed this effect for gratings well above the diameter at which optomotor reversal normally occurs (Kunze, 1961), and for a range of different gratings diameters and speeds, the results are not likely to stem from a simple aliasing effect (optomotor reversal). We did observe a significant difference in the sign of response between the 5.2° wavelengths and the other wavelengths (figure 6b), this is consistent with an optomotor reversal wavelength,

i.e. the effects sum up to produce the 'correct' optomotor respons, suggesting that the anti-optomotor effect is downstream of the mechanism that results in the optomotor reversal effect.

Anti-Optomotor Responses are not the result of Discrete Short-Term Saccades Other studies have reported that saccadic behaviour is often anti-optomotor, whilst smooth behaviour is often optomotor (Williamson et al., 2018). And it has also been noted that the saccadic behaviour, being of a larger amplitude, might tend to dominate responses when pooled together, even if the optomotor behaviour is actually more common in terms of time spent doing it (Mano et al., 2023). One method to sidestep this problem is to take the valence of responses, that is whether the response is left or right, ignoring the magnitude. This method should better represent what the animal is doing most of the time.

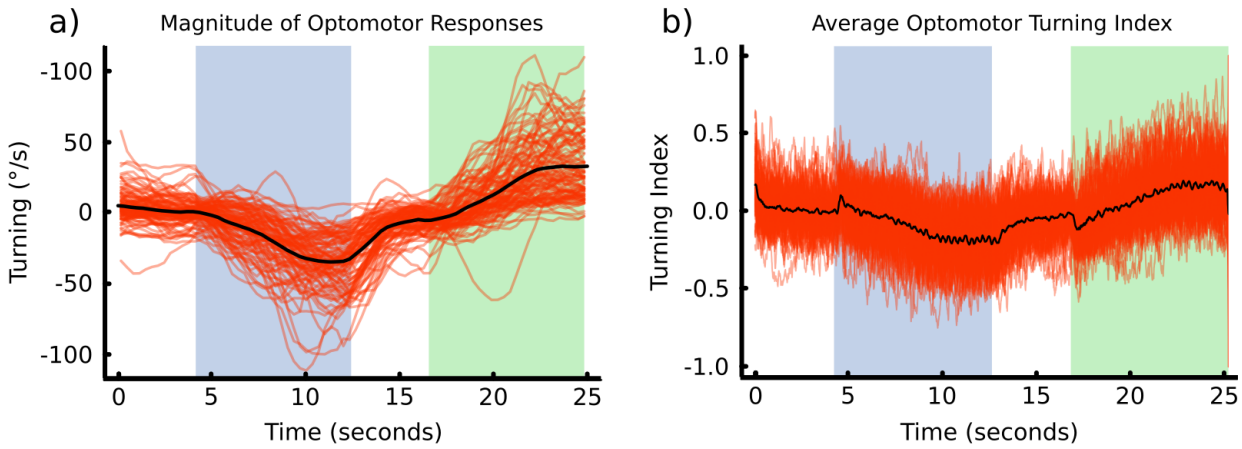

Figure 8: Average responses of flies shown the calibration grating.
(a)(i): The average turning response of flies to the calibration grating. Each line is the average trace for a different fly; overall, there is an average turn in the anti-optomotor direction.
(b)(ii): Flies' average turning index (left or right) to the calibration grating. An initial optomotor response appears immediately and decays slowly, followed by an anti-optomotor response.

When we observed the average valence of the fly turning, we see that for most of the parameters there is no visible optomotor response. However, for the 8.4°, for which the anti-optomotor response was strongest, there appears to be a small period of optomotor

behaviour until around 1 second after the onset of the grating motion, before returning to zero, and then into anti-optomotor behaviour. For the other parameters, where there was any strong response in the valence, it was anti-optomotor. Some of the time we observed no, or very little reaction from the fly to the grating, the valence method would add random noise to the data under these circumstances, so it is likely that the valence analysis reduces the signal-to-noise ratio of the data. For each of the parameters we tested, we tested an individual parameter on each fly, but we also tested another grating, the calibration grating; this was a grating with wavelength 30° and velocity 20°/s. We tested this to ensure that flies differences in performance between flies were not because of individual differences in the ability to respond to gratings, but it also meant that we had a large number of samples for this particular grating type (Figure 8).

For the calibration grating, we were able to observe other characteristics of the response not present in the rest of the data, probably on account of the very high n-number. We observe some slowdown during the stimulus presentation and recovery of forward-walking speed after offset in this data. In addition, the overall magnitude of turning still suggests an anti-optomotor response (figure 8a). However, the valence analysis shows that there is a clear, immediate short sharp optomotor response (figure 8b), that decays over the course of 2 seconds, into a primarily anti-optomotor response, which is immediately extinguished at the offset of the grating motion. This pattern is not obvious from the magnitude of the optomotor data, suggesting that in the initial period there are at least some anti-optomotor responses which are of a larger amplitude than the optomotor responses, although they are apparently less common than the optomotor responses, similar to behaviour found elsewhere (Mano et al., 2023).

Power spectra of responses shows a stimulus-invariant behaviour A Fourier transform of the data can allow us to see the dominating frequencies in the data. Short sharp saccades should show up as higher frequency spikes in the power spectrum. We calculated the power spectra of turning behaviour with a window length of two seconds, with the data binned to a sampling rate of 30 Hz. Other have found that saccadic behaviour consists of short sharp spikes lasting roughly 200 ms (Williamson et al., 2018). This should show up as a 5 Hz spike in the power spectra.

For all of the parameters tested, there was a peak around the very low frequencies, as well as one that surrounded about 2 Hz (figure 9), which indicates behaviour that is of a slower time-frame than we would expect from previous studies. A two-way ANOVA showed that there was no effect of the thickness or speed on the location of the spectral peak, although it did find a significant effect of thickness on the power of the peak ($F = 8.61$, $P < 0.0005$, $n =$ 10 flies per condition), although no post-hoc test revealed any significant difference between any of the thickness when correcting for multiple comparisons.

Another suggestion is that most, although not all (Creamer et al., 2018), experiments on the optomotor response fix the head in place, this means that only the external motion of the grating is detected by the fly, rather than, in our experiment where the heads of the flies were allowed to move, the sum of the head-motion and the grating motion. In order to investigate this further, we tracked the heads of flies performing the same experiment.

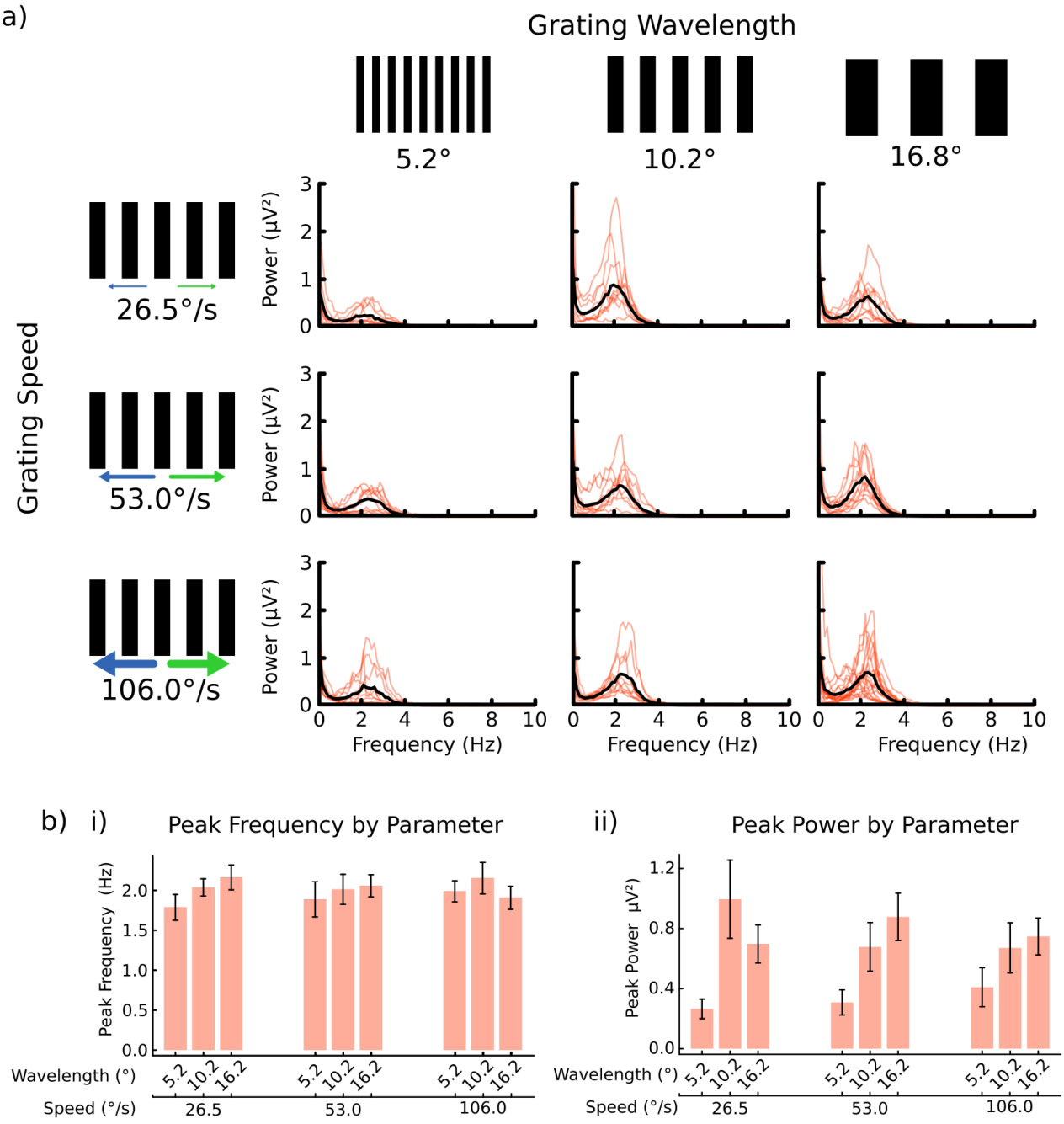

Figure 9: Power Spectrum analysis of flies responding to gratings of different thicknesses and velocities.
(a) The power spectrum for each grating parameter. Each line is the spectrum over the entire trace for each fly.
(b)(i) The average peak frequency for each parameter remains consistent for each parameter at around 2Hz.
(b)(ii) The average peak power for each parameter, there is some variation, with flies shown 5.2° wavelength gratings consistently showing the lowest peak power.

1.3.2 Head Movements During Optomotor behaviour

There are two ways that anti-directional behaviour during the presentation of a rotating stimulus can arise: perceptual or behavioural mechanisms. Perceptual anti-directional behaviour suggests the existence of a visual illusion, such as that occurring at the optomotor reversal wavelengths. In behavioural anti-directional behaviour, the fly is not mistaken about the movement of the world, but behaves in a non-optomotor manner. In order to distinguish between the two types of behaviour, we tracked the head movements of the flies performing the same optomotor experiment. If the response we observe is a perceptual response, we should see that the smooth tracking of the optomotor stimulus (Longden et al., 2022) is reversed during the anti-directional behaviour. If it is behavioural however, we should expect normal smooth tracking of the gratings during both syn- and anti-directional behaviour.

The Anti-Directional Response is not a Perceptual Illusion We measured the head directions of flies under the same experimental conditions as the previous experiment. The heads of the flies followed a consistent pattern throughout the experimental setup, with flies slowly turning the head in the same direction of the stimulus (Figure 10 & 11).

Across the different widths and grating velocities, there was a response to the grating motion. For all the grating parameters tested, the head-movements were syn-directional. That is, the head turns in the same direction as the optic flow of the world. This suggests that the flies perceive the direction of the stimulus correctly, and this is true even for gratings shown at 5.2° wavelength for which the behaviour in the previous experiment was reversed compared to the others. Thus, this shows that the anti-directional behaviour in the previous experiment is likely to be a behavioural, rather than a perceptual optomotor reversal.

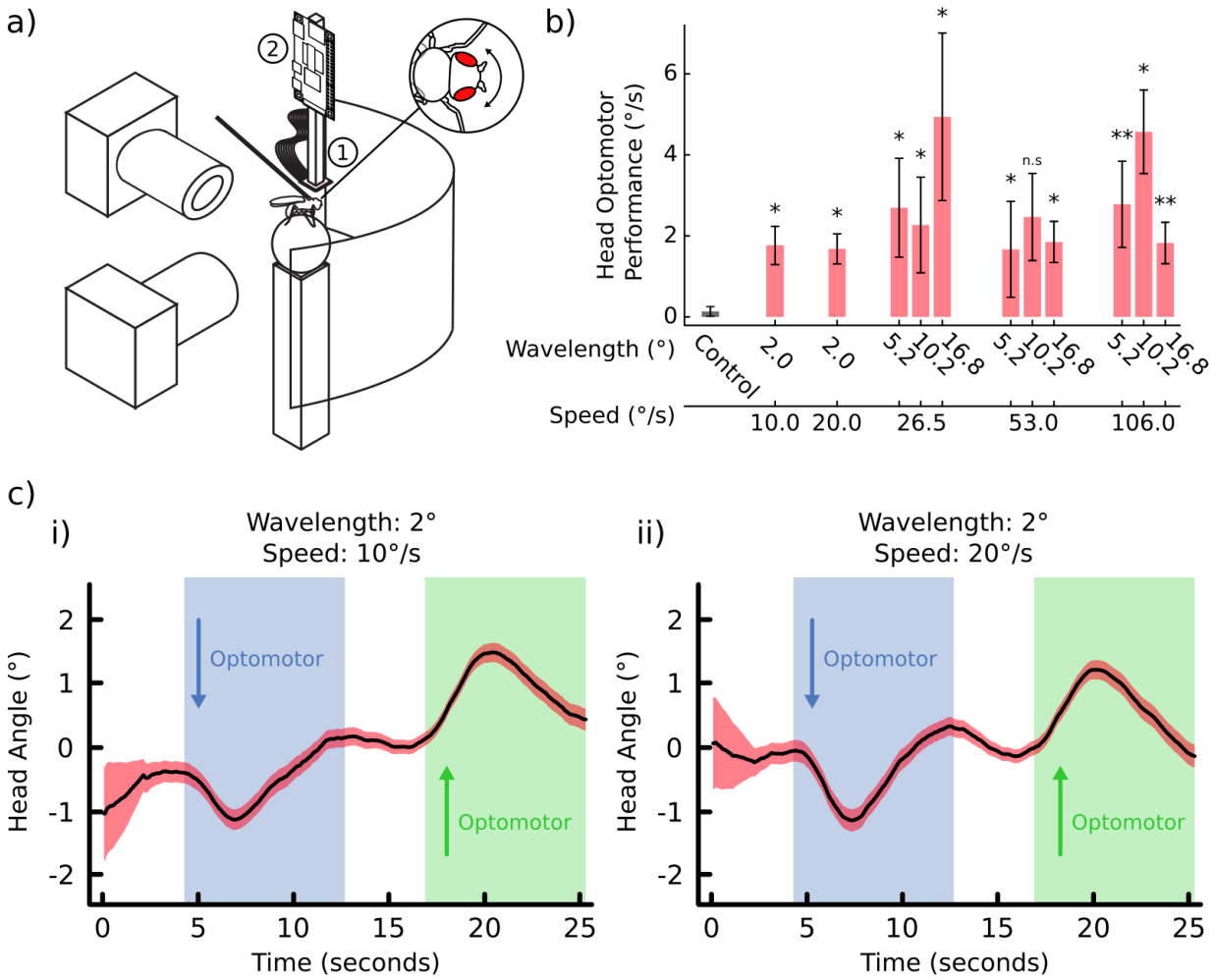

Figure 10: Average head movements during grating presentations.
(a) Schematic showing the head tracking setup. A camera is placed above the fly head, which can move freely (1), and the video stream is recorded by the raspberry pi attached above (2).
(b) The average head optomotor responses to the gratings. Each thickness and grating is significantly different from a control grating, which contained no motion, except for the flies shown a 10.2° grating at 53.0°/s (although the response is still in the same direction as for the other parameters).
(c) The average head traces for flies shown hyperacute gratings. Positive represents the head-turning clockwise. Thus, the optomotor response should be negative for a left stimulus (blue) and positive for the right stimulus.

Head Movements Show *Drosophila's* visual perception is Hyperacute We tested two additional grating parameters, at 2° wavelength, well below the theoretical minimum for fly resolution (a.k.a hyperacute). We used lower velocities in these relative to the other gratings because of limitations with the frame rate and resolution of the screen. Even for these hyperacute gratings there was a significant optomotor response, with flies turning their head

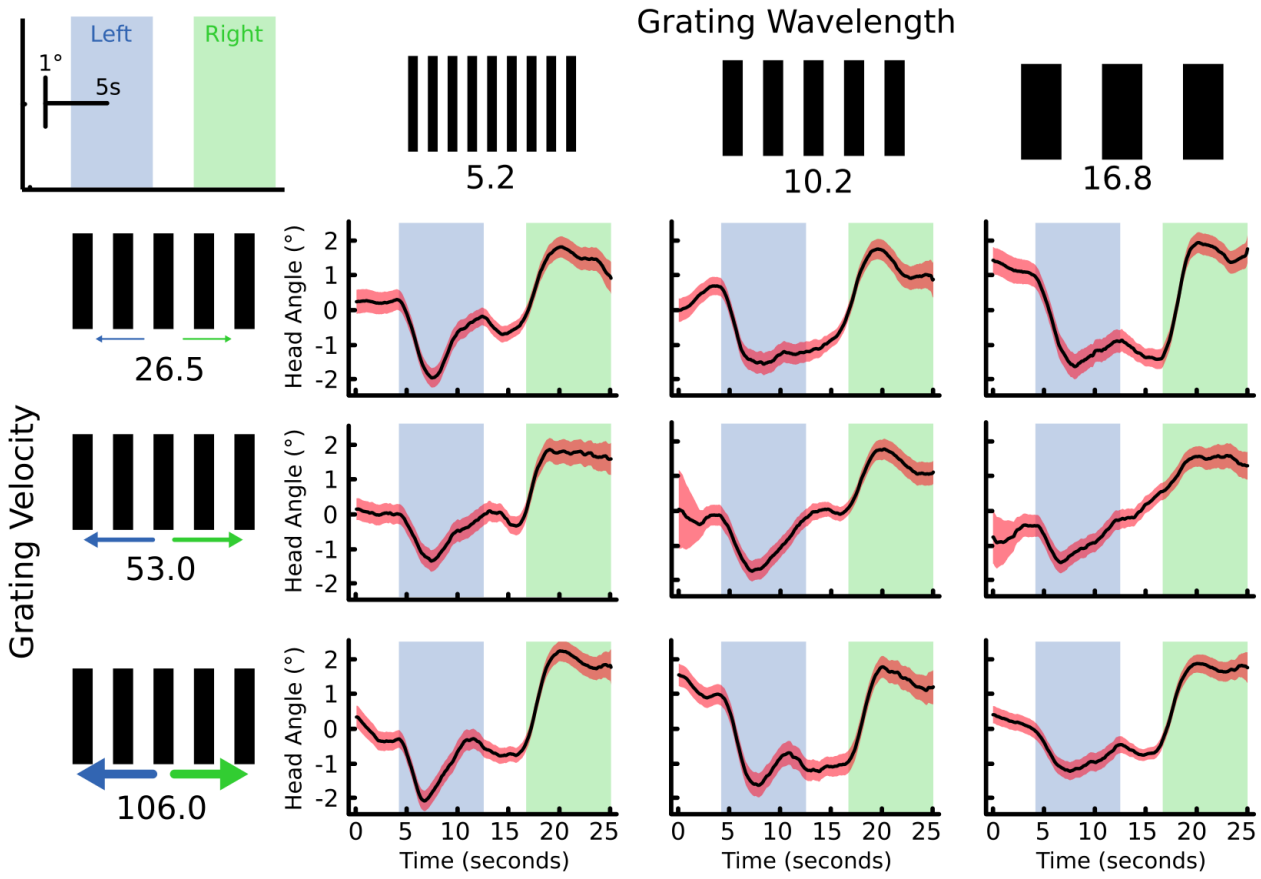

Figure 11: Average head directions for flies shown gratings of different thicknesses and velocities. Each fly responds similarly to the gratings, with heads initially following the direction of rotatin. For some parameters, the head direction maintains its position (e.g. 10.2° at 26.5°/s). But the heads return to baseline for other parameters before the grating presentation is complete (e.g. 5.2° at 106°/s).

in a syn-directional manner for both velocities (figure 10c). This is a clear sign of hyperacuity, suggesting that the walking optomotor response is not a full representation of the rotational optic flow being perceived by the fly.

Fruit Flies Exhibit Head-Nystagmus Flies also exhibit head-saccades, with the heads quickly flicking back against the grating rotation, before slowly turning again syn-directionally (figure 12a). This appears similar to visual nystagmus to that seen in *Calliphora*, where the smooth pursuit of an object that moves outside of the visual field is interrupted by short sharp saccadic movements in the opposite direction.

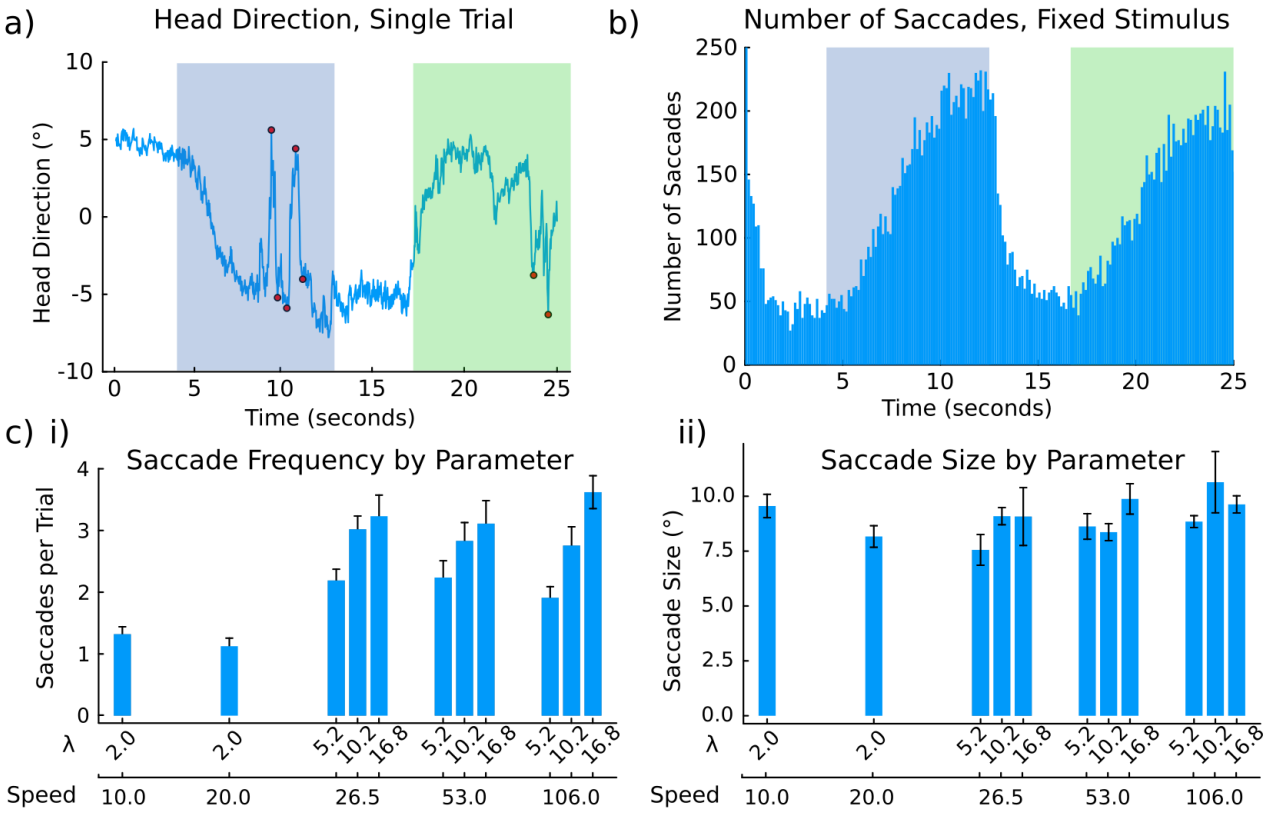

Figure 12: Flies show head-nystagmus during motion presentation
(a) Example trace showing the head direction of a fly (blue trace). The head initially smoothly follows the grating until the head reaches about 5 ° eccentricity, at which point the head rapidly snaps back in the opposite direction. The head trace following this saccade moves more quickly to the syn-directional direction. Detected saccades using the saccade detection algorithm are shown as red points.
(b) pooled number of traces for flies being shown the calibration grating at each time-point. The number of saccades gradually increases over the course of the grating presentation, dropping off rapidly at the offset of the motion.
(c)(i) The average number of saccades per trial for each fly at different parameters. Saccades tend to increase as the grating thickness increases.
c)(ii) The average size of the saccade at different diameters. The head saccades are the same size (10 °), regardless of the used grating parameters.

We wanted to examine these nystagmus-like movements further. We hypothesised that if the head movement were driven by the same circuitry that controls optomotor locomotion (for instance the HS cells), the movements should track with temporal frequency. On the other hand, if the head movements are directed towards particular objects (in this case the bars of the grating), the size of the saccade should decrease with increasing temporal frequency (speed being fixed, a thinner grating).

We detected individual head saccades by thresholding the continuous wavelet transform of the head-traces, this picks up and identifies the peaks in the trace that are characteristic of the saccades, (see markers on figure 12a).

Grating Motion Causes Head Saccades For the thicker wavelengths, there is a strong relationship between the presence of grating motion and the saccades. There is a main effect of thickness on the frequency of saccades (Figure 12c.i) ($P < 0.05$, $F = 25.98$), with many more saccades being detected for the 16.8° than the 2° wavelengths. There was no effect of speed on the likelihood of head-saccades (figure 12c.ii). The frequency of head-saccades gradually increased throughout the motion portion of the stimulus presentation, although the rate of increase slows down towards the end of the period (figure 12b). There were also a large number of saccades detected at the beginning of the trials, this is probably a reaction of the flies to the stimulus appearing at the beginning.

The Head Saccade Waveform is Stimulus Invariant We looked at individual head-saccades for each grating diameter thickness and speed. Neither of these paramaters affected the magnitude of the head-saccades, which tended to be around 10°, roughly in line with what others have observed (Williamson et al., 2018). Similarly, the head-saccade shapes were unaffected by the grating diameter or speed, with all saccades appearing roughly similar (figure 13).

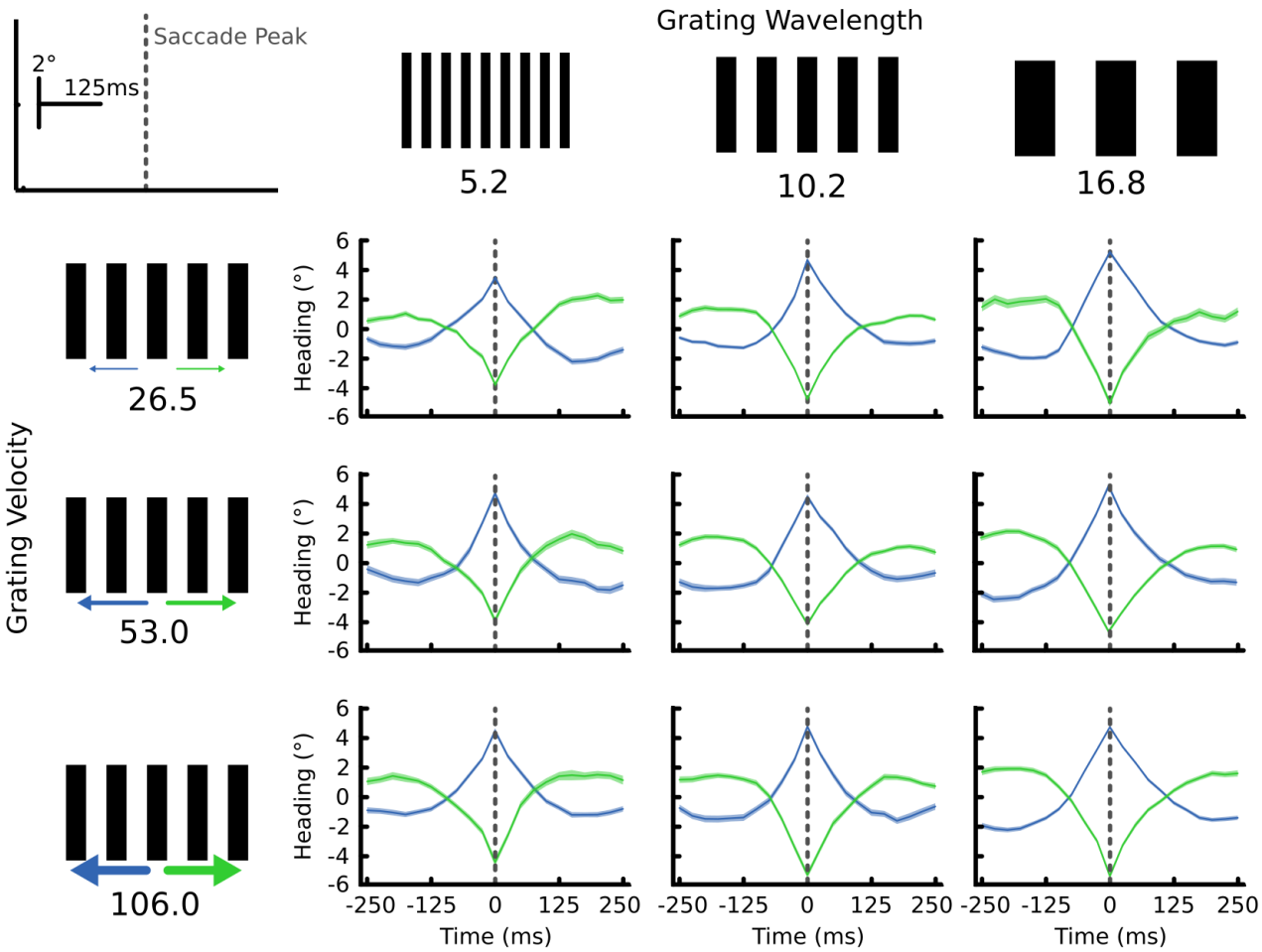

Figure 13: Average head saccade waveforms for flies for different parameter gratings. Saccades are clockwise for flies shown the left grating and anti-clockwise for flies shown the right grating, which goes against the direction of the grating motion. Each head saccade is roughly the same shape regardless of the grating parameter, having a peak centred around 0 ms and rapidly returning after the saccade.

Head Saccades Precede Anti-Optomotor Turns We identified the head-saccades over the whole dataset, and aligned the trackball-motion to the peaks of these saccades, this was to see if the head-saccades were related to the locomotion of the fly. We found that flies tended to increase their turning for approximately 125ms after the peak of the saccade. This was true for all grating parameters tested (figure 15), including the calibration grating (figure 16). The increased turning was always in the anti-optomotor direction, regardless of whether the fly was already turning in the anti-optomotor direction. For wavelengths 10.2° at 26.5 °/s, 5.2° at 53.0 °/s, 5.2° and 16.8° at 106.0° the anti-optomotor turning was significantly greater

after the saccade than before it when corrected for multiple comparisons. Interestingly, for the 5.2° wavelengths, the turning preceding the saccade was optomotor, and the turning after the saccade anti-optomotor.

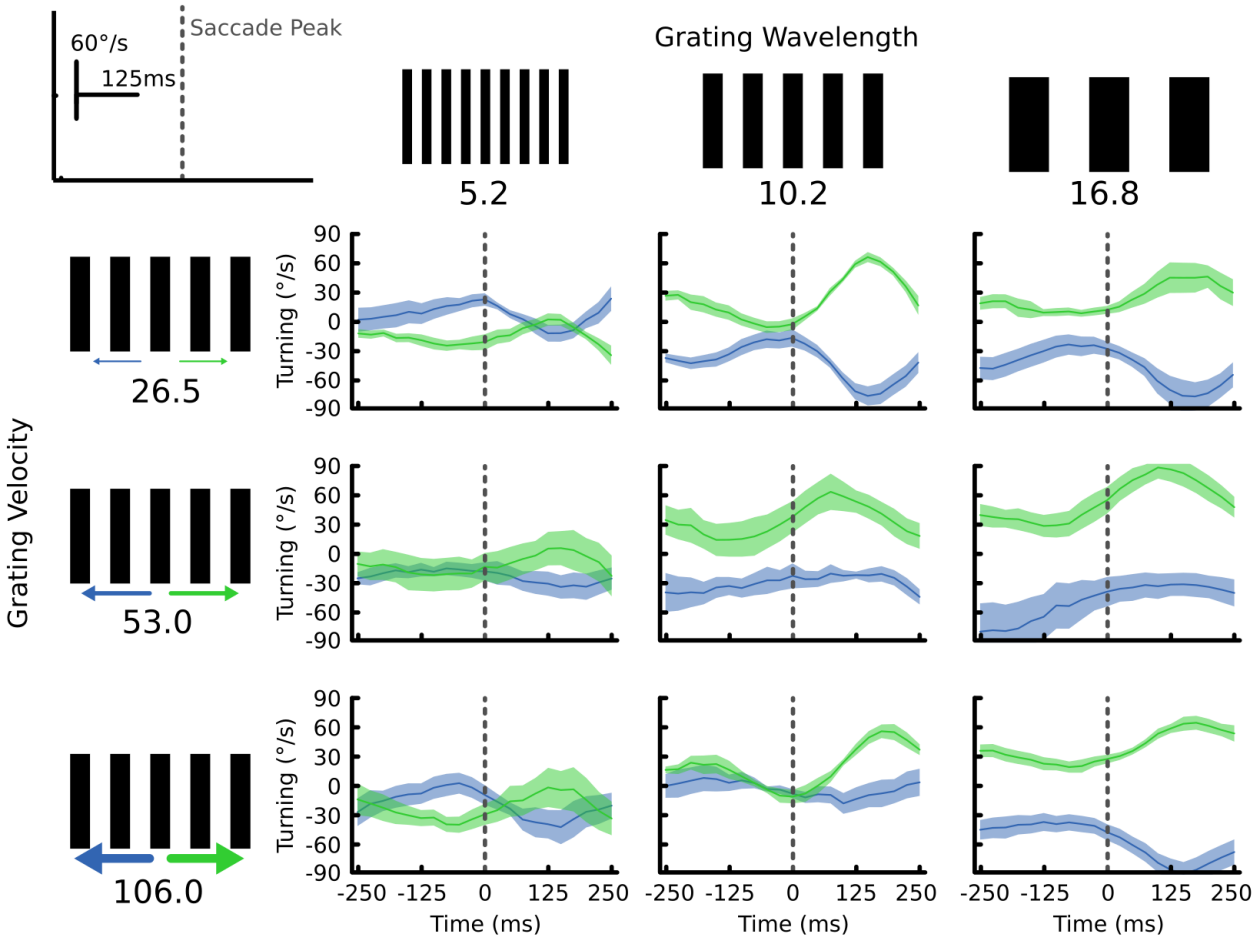

Figure 14: Average trackball traces for flies centred around the head-saccade peak (dotted line) time. Regardless of the thickness or velocity of the grating, flies turn more strongly in the anti-optomotor direction after the saccade peak. The baseline turning is different for different parameters, however.

These results suggest a common behavioural motif that has been reported elsewhere, where animals first move their head in the direction of the motion, and then move their body (Williamson et al., 2018). Where this motif has been seen in flies it has been seen in the context of the fly performing a saccade. This observations suggest that while the anti-optomotor shown by flies is not composed of the classic behaviour of saccades, interspersed with optomotor behaviour (Mano et al., 2023), it seems that the behaviour does otherwise resemble

saccadic behavioural sequences.

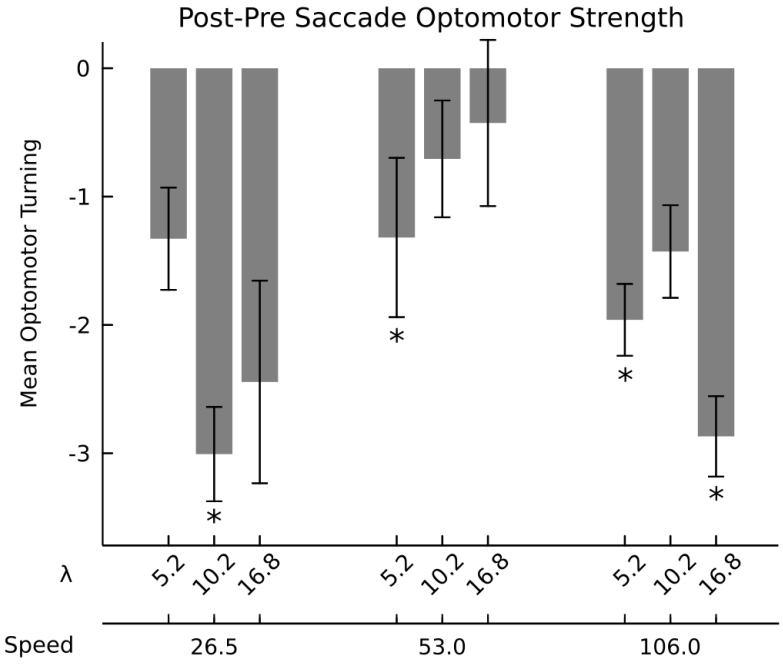

Figure 15: Average optomotor turning difference between the post- and pre- head-saccade. At all the wavelengths and speeds tested, the post-saccadic (at 130ms after the head-saccade peak) optomotor turning was more negative than the pre-saccadic turning.

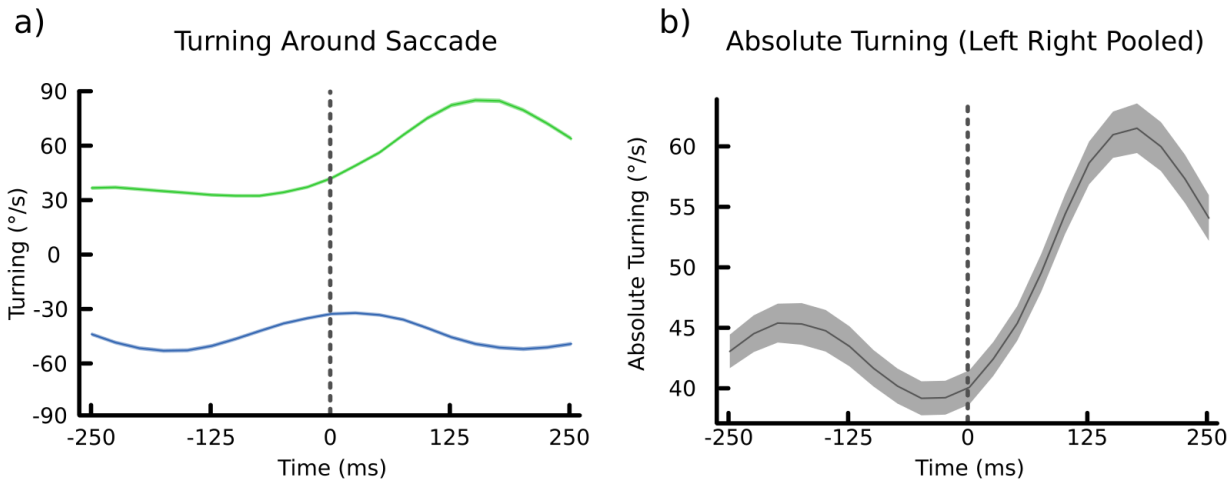

Figure 16: Average trackball responses of flies shown the calibration grating, centred around the saccade peak.
a) Average turning responses. Flies, on average, are already turning in the anti-optomotor direction before the grating onset, but this increases after the peak.
b) Absolute turning magnitude. Flies increase the amount of turning that occurs after the saccade peak.

1.3.3 Fixed Head Optomotor behaviour

In the natural state, the fly is free to move its body via leg movements, its head via neck muscles, its retina via eye muscles, and its individual photoreceptors via microsaccades, all contributing to the final light absorption that is observed by the photoreceptors.

In the previous experiments, we kept all of these components of active vision free except for the feedback the fly receives between walking and world motion. This combination of open-loop feedback for walking behaviour, and closed-loop feedback for the remaining elements of active vision, may affect the behaviour of the fly in some hard-to-predict way, potentially producing the anti-optomotor behaviour we observed. Indeed, flies tend to behave differently under open and closed loop conditions (Cellini & Mongeau, 2022; Heisenberg & Wolf, 1988; Reiser & Dickinson, 2013). In addition, we found that head-saccades preceded the anti-optomotor behaviour, and so we hypothesised that it could be the head-movements themselves that might be the cause of the behaviour.

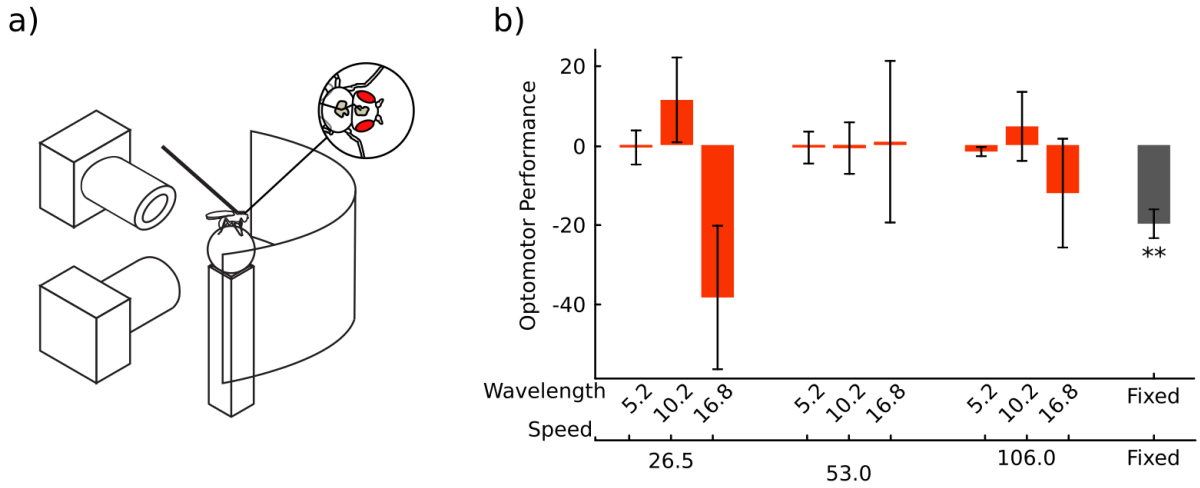

Figure 17: Effect of head-fixing on the anti-optomotor response.
(a) Schematic showing the wax locations on the thorax and head during the head-fixed experiment.
(b) Average optomotor performance of head-fixed flies. Overall, the optomotor performance is poor amongst the flies tested, with only the calibration grating and the 16.8° grating exhibiting strong optomotor response, both in the anti-optomotor direction.

Head Movements do not cause Anti-Directional Turning As in the previous two experiments, each fly was shown two sets of stimuli, the first kept consistent between flies, and the second varied between flies to observe the effects of grating size and velocity on the behaviour. We found that the performance of flies under head-fixed conditions was severely reduced. However, where there were strong responses, they were largely anti-optomotor. Flies exhibited stronger responses for the calibration gratings, which had a larger diameter than the others, and there was a significant optomotor effect here in the anti-optomotor direction ($F = 8.92$, $P < 0.005$, $n = 10$ flies per condition) (figure 17b).

Anti-optomotor responses to the calibration gratings were seen for almost all of the flies tested (figure 18). However, two individuals exhibited behaviour that was not consistent with the rest of the cohort (outlying points in figure 18b). At the onset of motion, the flies show optomotor behaviour, which is primarily not followed by anti-optomotor saccadic movement. There was nothing unusual about these flies, except for the fact that they had greater forward motion than the other flies in the cohort.

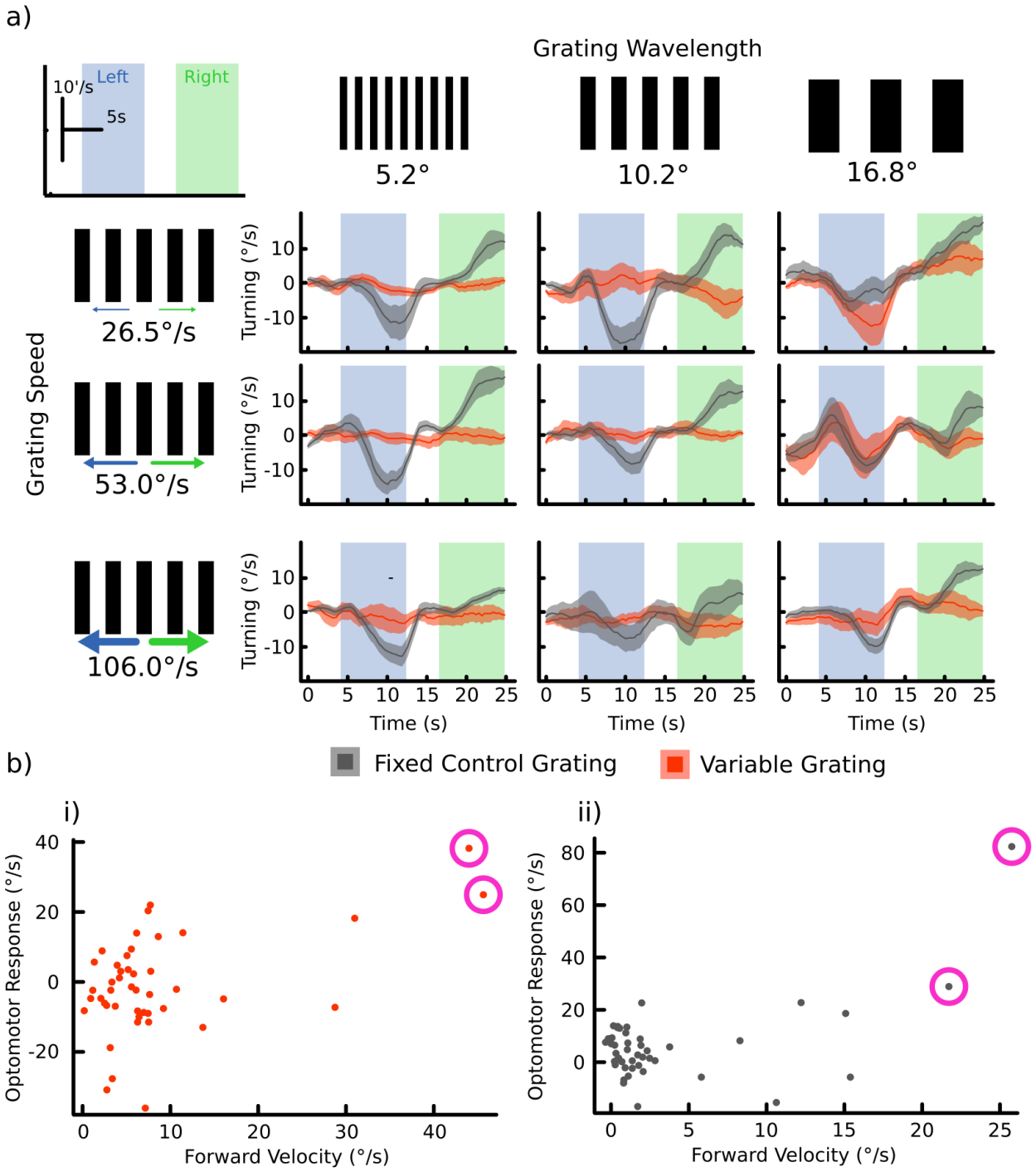

Figure 18: Average trackball traces of head-fixed flies shown moving gratings.
(a) Average traces of flies at different grating parameters (red) as well as the calibration grating (grey). Performance for the calibration grating was fairly consistent among flies, with each fly showing an anti-optomotor response. The exception to this rule is the gratings at 10.2° at 106°/s and 16.8° at 53°/s, which show an initial optomotor response to the calibration grating. These contain the two outliers shown in (b).
(b)(i) Average turning vs forward walking responses to the variable grating. Most flies do not exhibit strong responses, with the distribution centred around 0. The exceptions to this behaviour are the two outliers shown in pink, which exhibit strong optomotor responses and forward walking.
(b)(ii) Average turning vs forward walking responses to the calibration grating. Outliers in pink are for the same flies as in (b)(i).

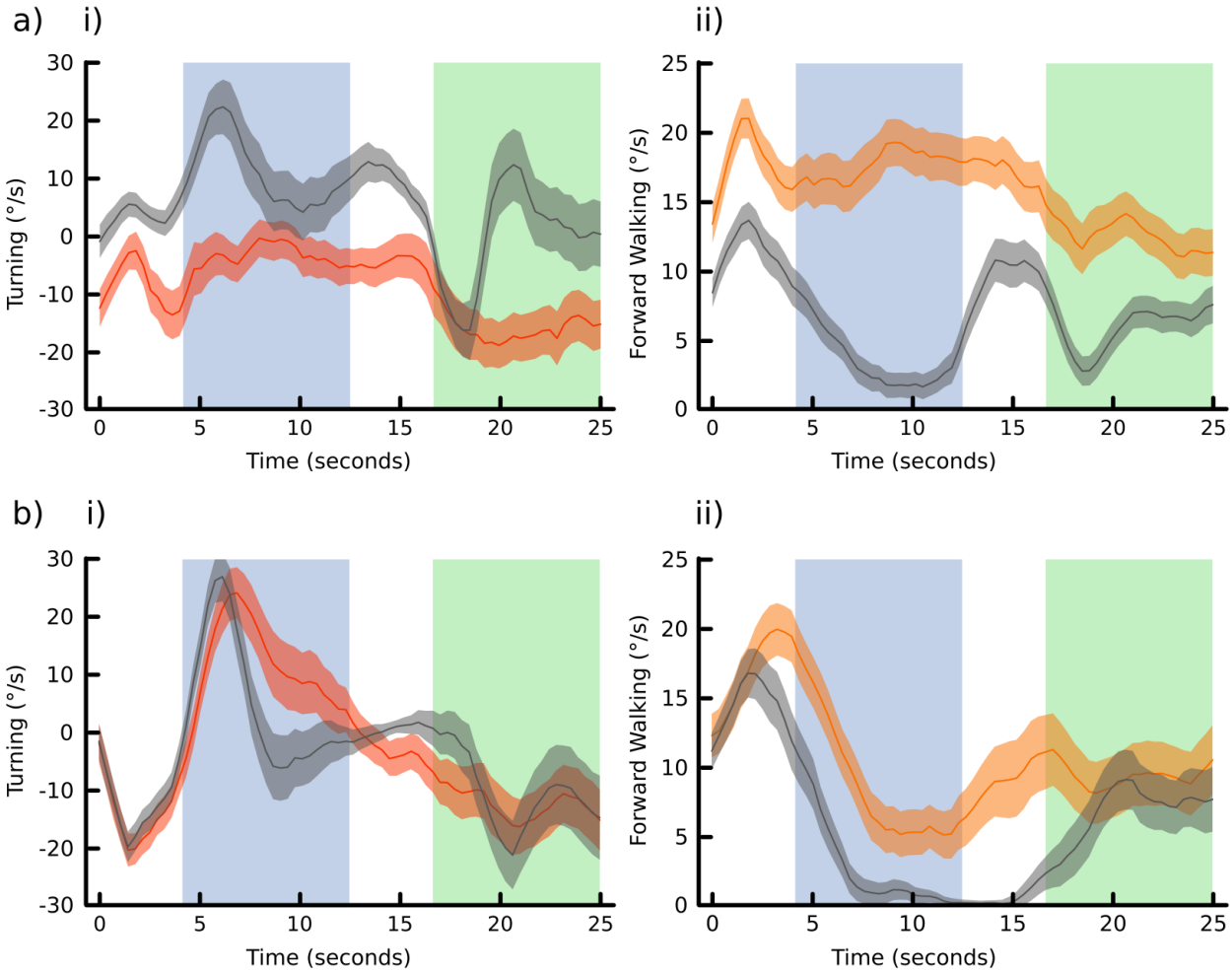

Figure 19: Traces for individual outlier flies found in the fixed-head experiment
(a) The average turning (i) and forward motion (ii) for fly A. The calibration grating (gray) shows optomotor responses to both the left and right gratings
(b) The average turning (i) and forward motion (ii) for fly B. The calibration grating (gray) shows optomotor responses to both the left and right gratings, and the variable grating (red) shows weaker optomotor responses as well.

Fly A exhibits strong forward walking behaviour in the pre-motion phase before the onset of both the left and right gratings, while fly B exhibits forward walking in the pre-motion phase before the left grating, and then doesn't show strong walking until the onset of the rightward moving grating (Figure 19). Fly A's behaviour is more consistent with other findings that flies tend to slow down in response to motion (Creamer et al., 2018). Tying this to the turning behaviour, fly A shows optomotor turning behaviour at the start of both motion onsets, whilst fly B shows a large optomotor turn starting at the beginning of the leftward motion, but

only shows an optomotor turn to the rightward-moving grating a few seconds after motion onset, roughly around the same time that the forward-velocity begins to increase to levels comparable to those seen in the initial segment of the leftward-moving grating.

Overall, these result suggest that while head-movements were associated with anti-optomotor turns in the previous experiments, fixing the head in place does not prevent the anti-optomotor behaviour. The two individuals that behaved differently suggest that forward motion relates to the propensity to perform optomotor behaviour.

1.3.4 Optomotor behaviour During Forward Motion

The previous experiment suggests a link between forward motion and optomotor behaviour. To further elucidate this connection, we designed an experiment that would ensure we observed behaviour during forward motion.

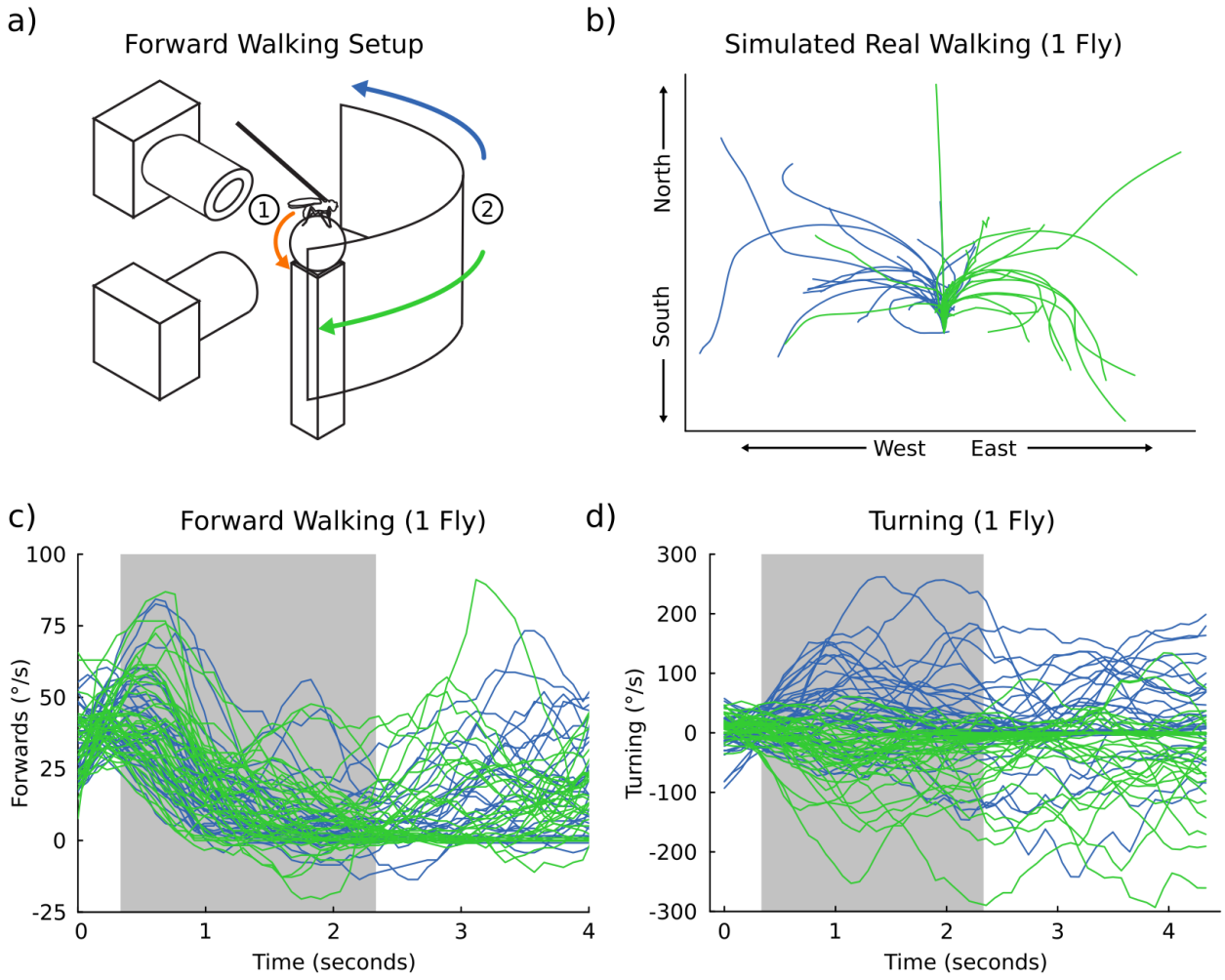

Figure 20: Forward walking experiment, example traces.
(a) Schematic showing the forward walking experiment. The fly begins to walk forwards on the ball, and (1) this is detected by the cameras, which initiates the onset of grating motion (2) in the left (blue) or right (green) direction.
(b) Absolute motion for a single fly. Each trace represents the real-world motion of a fly in response to the gratings.
(c) Raw traces of forward walking responses for a single fly. The fly initially accelerates before the grating motion begins, at which point the fly slows down.
(d) Raw turning traces for a single fly. Flies turn at the onset of the grating in the optomotor direction.

Forward Motion Enhances Optomotor behaviour The onset of grating motion was triggered after the fly moved consistently for 333 ms (figure 20a). We tested the optomotor

behaviour over the first 2 s of this motion, as this was the optomotor period for the outlier flies in the previous experiment. Since this experiment was triggered in a closed-loop manner, we presented left or right gratings randomly, as opposed to sequentially in the previous experiment. Example traces for a single fly are shown (figure 20b,c,d). We measured these optomotor responses under the same velocity and thickness parameters that we had previously measured. As before, we did not observe any strong optomotor responses at a 5.2 degree wavelength (figure 21). There was a significant effect of thickness on the optomotor responses ($F = 8.27$, $P < 0.0005$, $n = 10$ flies per condition).

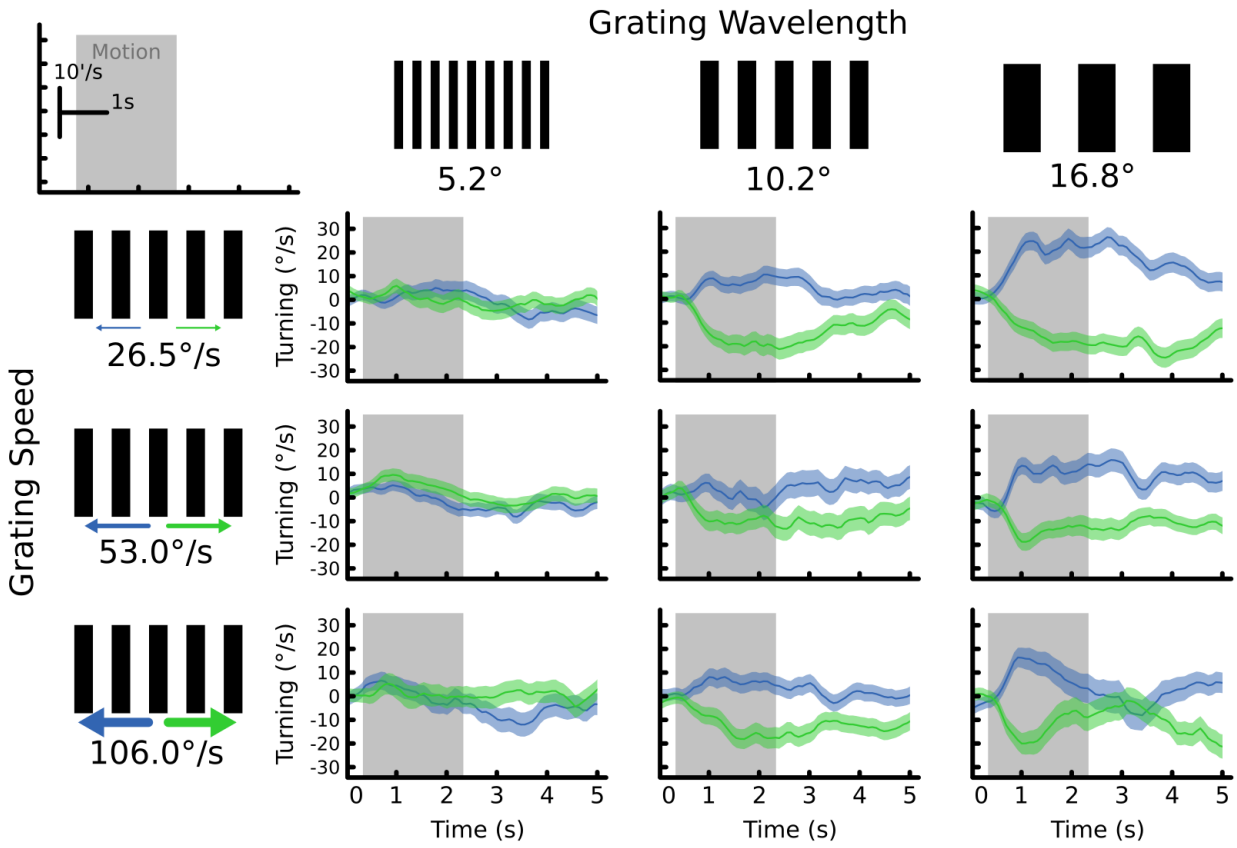

Figure 21: Average turning responses of flies to different grating parameters. Responses to the 5.2° grating do not appear to be present. Responses to the 10.2° and 16.8° gratings appear strong and in the optomotor direction

At a 10.2° wavelength the optomotor response was present, lasting for the 2 s motion duration. At 16.8° wavelength, the optomotor response was strong (which is the same pattern-dependence effect seen in the anti-optomotor behaviour). The turning responses tended

to average 25°/s, which was of a similar magnitude to those seen in the anti-optomotor responses. Turning responses often took several seconds after motion offset to extinguish, and occasionally didn't at all (e.g. 16.8° at 26.5°/s), this was potentially due to inertia of the ball. At the 16.8° wavelength at 106°/s the optomotor response was extinguished before the end of the motion stimulus, possibly suggesting that flies were beginning to initiate the anti-optomotor response by this point. However, flies under this forward walking paradigm were not actually observed to carry out any anti-optomotor responses for any of the parameters tested.

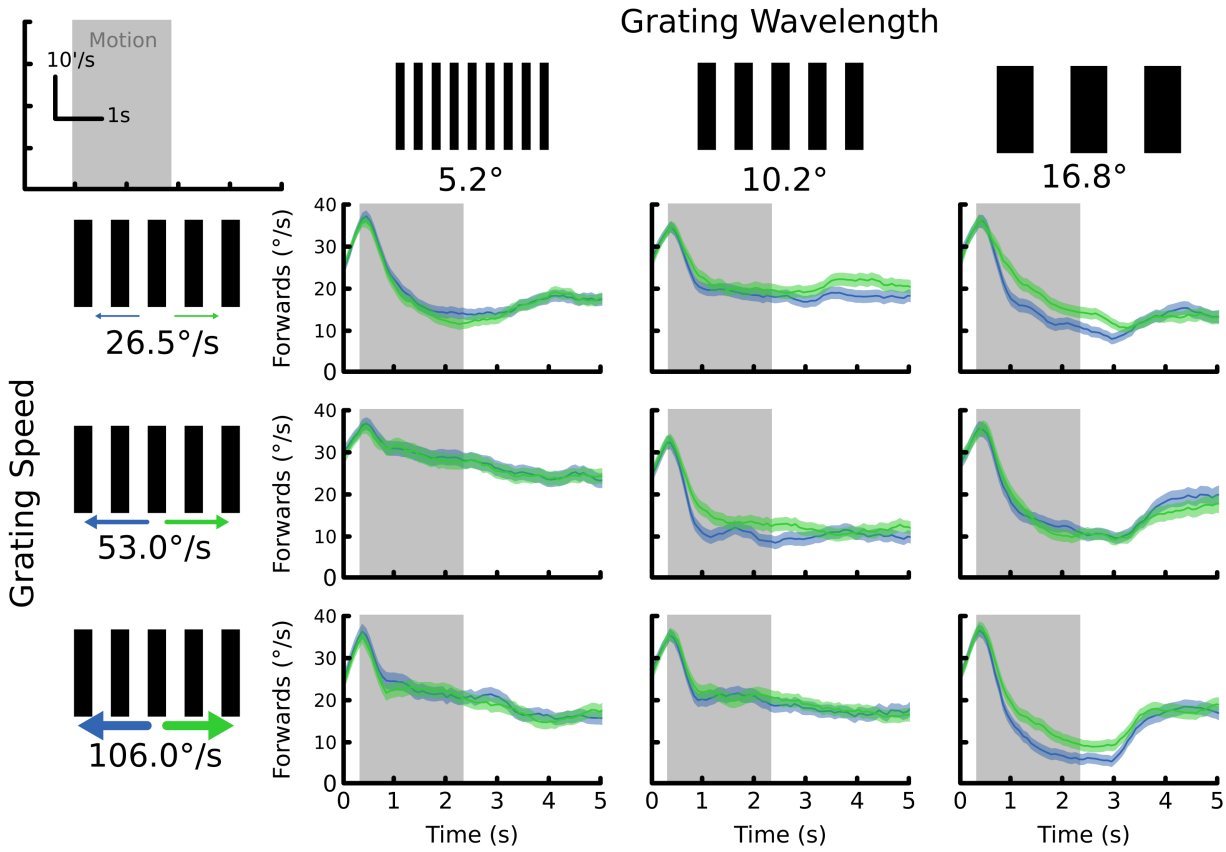

Figure 22: Slowdown traces of flies at different grating parameters. Flies slow down in response to the grating motion. This behaviour is clearly present for the larger gratings and the 5.2° grating, particularly at 26.5°/s, despite having no optomotor response at this wavelength.

Flies slow down to small gratings despite having no optomotor response When we examined the walking speed of the flies, we found that although flies did not produce optomotor responses to the 5.2° wavelengths, at the slowest velocity, flies showed a strong

slowdown effect (figure 22). This slowdown effect, reported elsewhere by (Creamer et al., 2018) was also seen in the other conditions. In parameters that saw a stronger slowdown response, we also observed a weaker optomotor response. For instance, the small optomotor response of the slowest, largest diameter grating was mirrored by the strongest slowdown of the cohort, almost dropping to a complete stop.

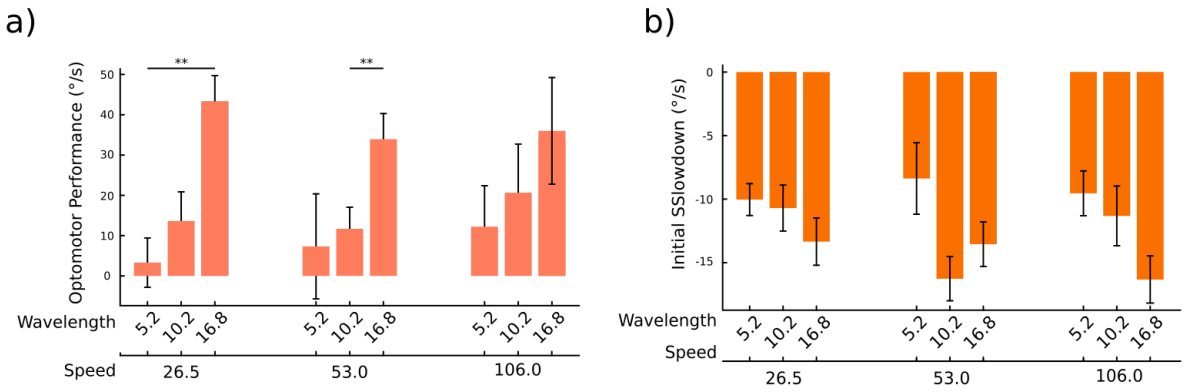

Figure 23: Average optomotor and slowdown responses of flies.
(a) Flies perform in the positive optomotor direction for all the gratings shown, with the 16.2° significantly different from the 5.2° grating at the two lower speeds. Optomotor performance generally increases at thicker gratings.
(b) Slowdown responses of flies at different parameters. Slowdown responses appear broadly similar, regardless of the grating parameter.

Optomotor Strength is Proportional to Forward Walking Speed We wanted to examine this relationship between the turning response and forward motion further. We segregated fly behaviour throughout the entire task into individual time-points. We took the rotary motion and forward motion for all of those time-points for each fly. We found that for all of the conditions under which we observed an optomotor response, there was a correlation between the forward walking and the turning (figure 24). This is a relationship not predicted by the average curve of the responses. The relationship predicted from the average curves would result in the opposite correlation, since (within a single parameter) the strongest turning generally occurs at the end of the slowdown period. This result corroborates the finding that behaviourally, the optomotor behaviour is strongest when the fly is walking forwards.

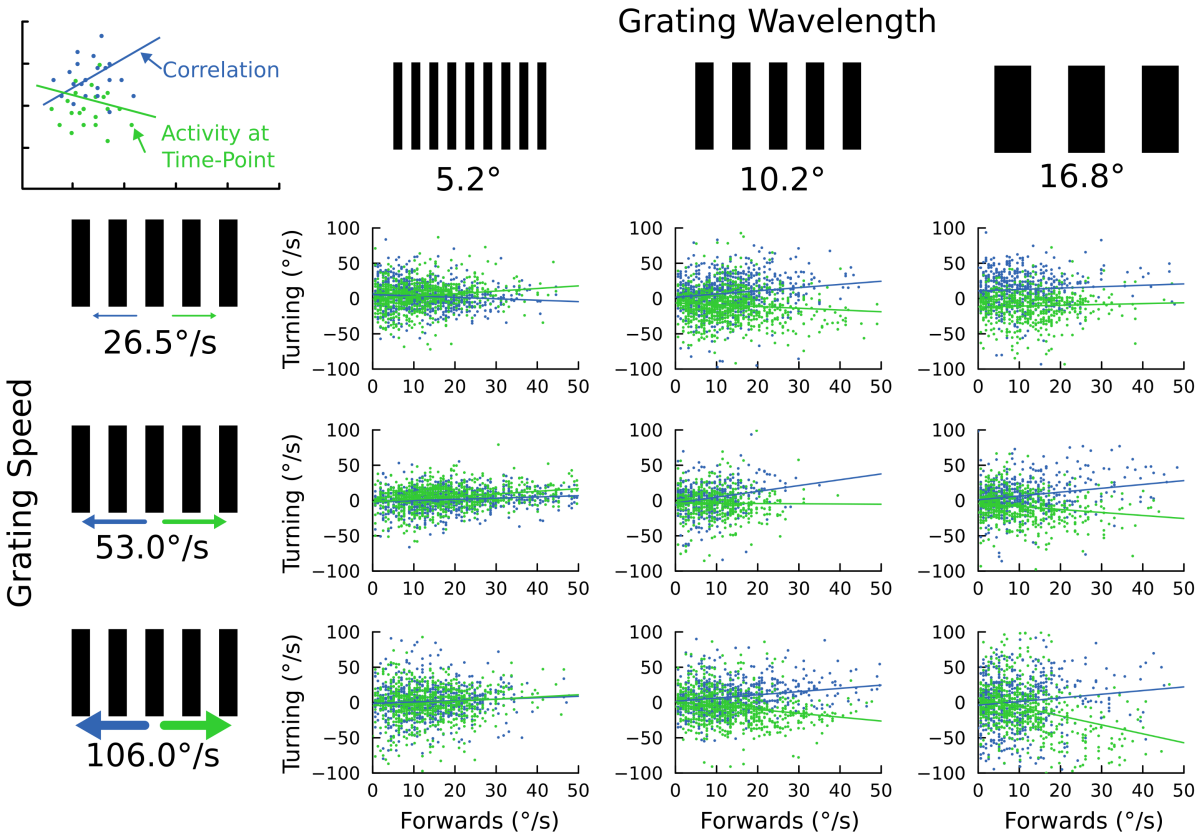

Figure 24: Correlation between the forward walking and turning. Each time-point during motion presentation is represented by a single dot. For the parameters at which we observe strong optomotor responses, we see a positive correlation between optomotor performance (positive for left, negative for right), and forward walking.

1.3.5 Optomotor and Anti-Optomotor Responses

In the previous experiment, the optomotor response was present when we restricted the behavioural testing to times at which flies were walking forward. We did not observe any anti-optomotor effects in this experiment. We hypothesised that forward walking would prevent the anti-optomotor response from arising, or perhaps prolong the optomotor stage; due to a context-dependent modulation of the optomotor circuitry. In the previous experiment, however, we did not directly compare the optomotor responses of non-walking flies to walking flies.

We decided to repeat the forward walking experiment. This time, however, we triggered the presentation of motion whilst the fly was either walking, or not at all, and compared re-

sponses within-subject. In pilot testing, we found that we could generate both optomotor and anti-optomotor responses in a short time frame if we used a lighter trackball. Because of the previous relationship we found, we predicted that the optomotor response would be greater in those flies that experienced the motion whilst they were walking quickly, but wouldn't be present in still flies.

Forward Walking Does not have a Lasting Effect on the Anti-Optomotor Response

Flies which were presented rotary motion while walking experienced a slowdown as in the previous experiment, and both groups recovered some speed after the presentation of the stimulus (figure 25, a & b). Flies that were walking forward at the time of stimulus onset tended to turn in the optomotor direction. Whereas flies that were not walking when the stimulus presented do not exhibit this early optomotor behaviour.

Both sets of flies, however, start to turn in the anti-optomotor direction after about 1 s. In the walking flies this response occurs after most of the slowdown has occurred. We took the average turning during the first second of stimulus presentation and the end of stimulus presentation (figure 25c-f). A repeated measures ANOVA showed that the time since stimulus onset was significant factor in the optomotor response ($F = 12.3$, $P < 0.005$, $n = 12$ flies), and the post-hoc tests showed this effect for both the walking ($F = 3.59$, $p < 0.005$, $n = 12$) and for the still flies ($F = 3.136$ $p < 0.05$, $n = 12$). In addition there was a significant interaction between the locomotory state and the time period between stimulus onset ($F = 4.75$, $P < 0.05$, $n = 12$).

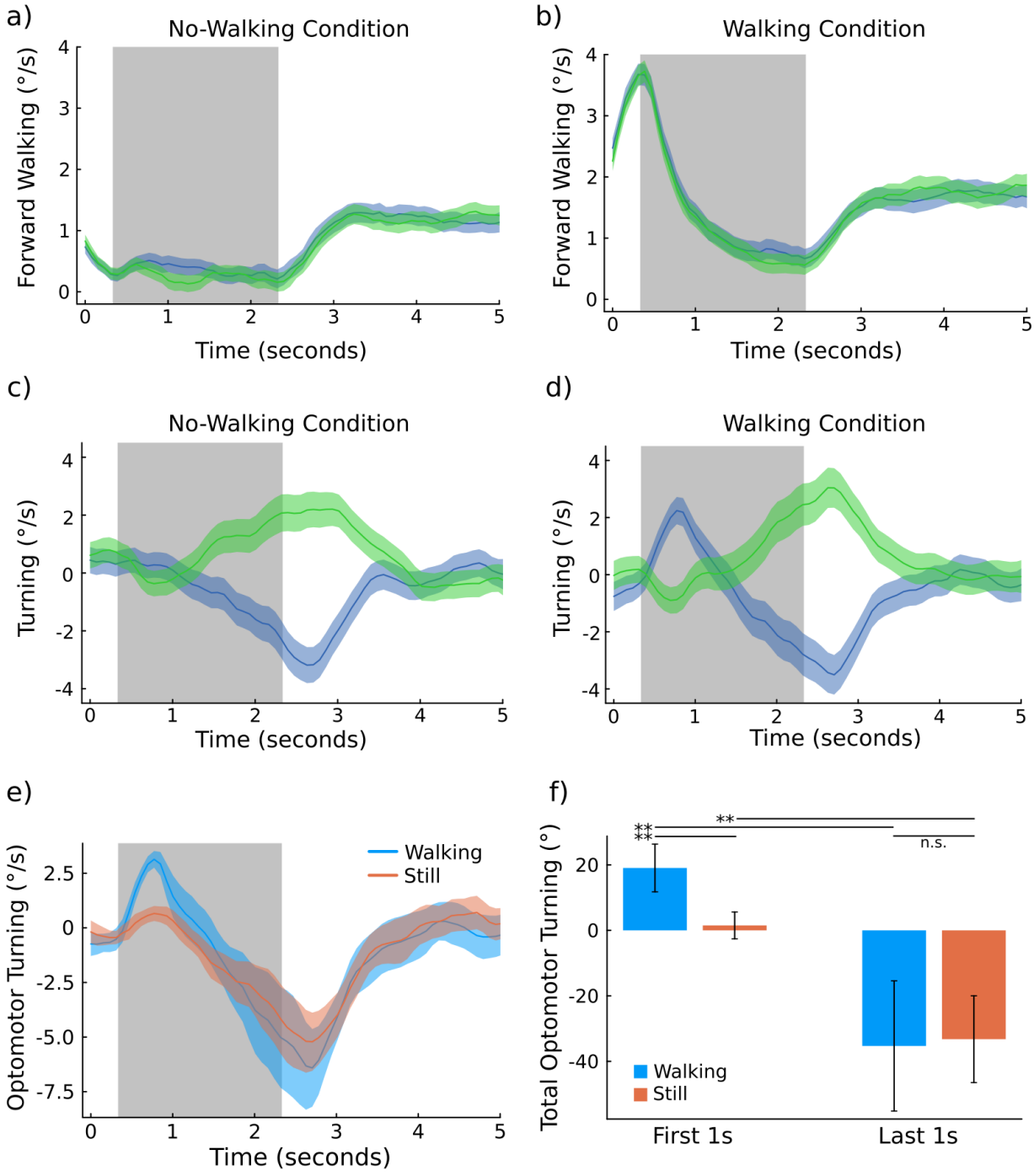

Figure 25: Optomotor and Anti-optomotor responses of flies.
(a) Forward walking of flies in the non-walking condition. Flies maintain a low speed before and during the grating motion and start to walk forward more after the grating motion offset. (b) The forward walking of flies in the walking condition shows similar slowdown effects as seen in figure 22.
(c & d) Turning responses of flies. Non-walking flies exhibit only an anti-optomotor response, while walking flies exhibit an initial optomotor and late anti-optomotor response.
(e) Still flies show a small optomotor response.
(f) Overall Optomotor turning by condition and stage (first or last second).

Non-walking flies do not perform the optomotor response, whereas walking flies do, this could suggest an increased engagement of the optomotor circuitry, that leads to this show-

ing up in behaviour (Chiappe et al., 2010). However, the fact both groups of flies performed a similar anti-directional response, shows that whatever mechanism results in the anti-optomotor response can be engaged when the walking speed is low. This could potentially be rationalised as the optomotor effect being an additive effect on behaviour: that is, it does not directly initiate any locomotory module, but rather acts to modulate existing activity. The anti-optomotor effect is however clearly an active response, and can be initiated whether the fly is walking forward or not. Secondly, the existence of both the anti-optomotor and optomotor behaviours within this dataset show that the increased walking at the beginning of the experiment did not have any lasting effect on the anti-optomotor response once the slowdown had occurred. Although, the anti-optomotor response occurs only when the fly has slowed down, this observation does not contradict hypothesis that these two behavioural paradigms do not generally co-occur.

The Optomotor and Anti-Optomotor Response Are Associated with Distinct Temporal Features Since we have both optomotor and anti-optomotor responses in this dataset, we tested how the instantaneous amplitude of different frequencies changed over the course of the motion duration (Figure 26). As in the first experiment, the maximal power of the responses centred at around 2 Hz, with gradual increases over the course of motion presentation (figure 26a). When we compared the still and walking flies, we found that in the initial period, during which walking flies have an increased optomotor response, the frequencies between 0-4 Hz are upregulated (figure 26c). We found that at 5 Hz the frequency-time domain experienced a phase-transition, where the initial part of the stimulus showed stable (in the still flies) or reducing amplitudes (in the walking flies). In the second half of the trial, during which the anti-optomotor response was seen, the 5 Hz signal started to increase (figure 26d). There were significant differences between the early and late stages at the 5 Hz signal for both sets of flies (figure 26b). This is notable because the 5 Hz component of the

behaviour would be represented by flies performing continuous behaviour of a period that lasts around 200ms, which is the average length of a body-saccade in flies (Williamson et al., 2018).

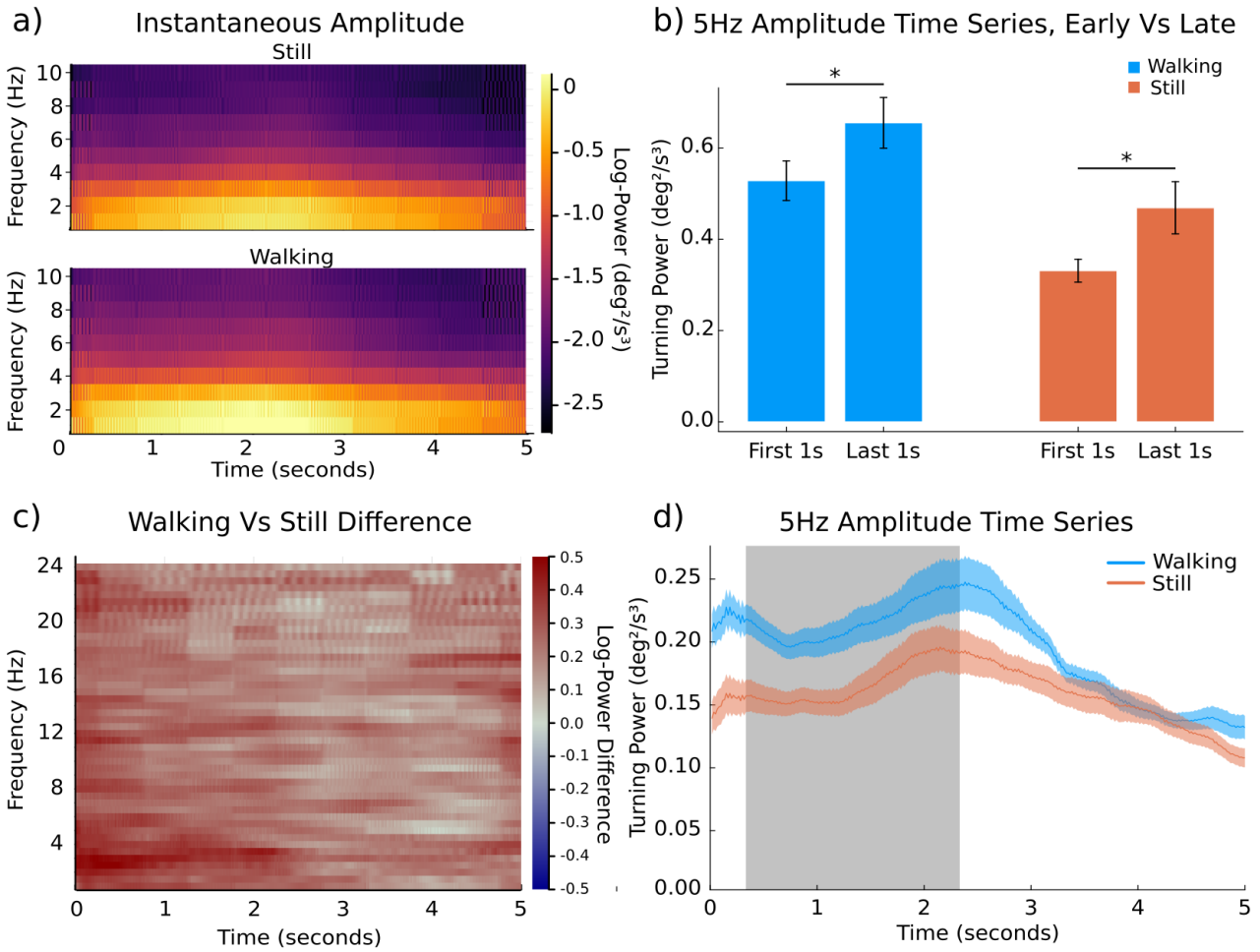

Figure 26: Frequency Analysis of Turning Behaviour.
(a) Instantaneous amplitude for still (above) and walking (below) flies.
(b) Comparison of power between early and late traces in the 5 Hz frequency range.
(c) Whole spectrum difference between the walking and still flies, showing an increase in the log-power in the early response of walking flies.
(d) 5 Hz time series showing state change between the early and late motion presentation.

A Non-Periodic Stimulus Does Not Prevent the Anti-Optomotor Response In order to assess whether the periodical grating stimulus causes the anti-optomotor response, we tested flies in a starfield environment (Fenk et al., 2022). The fly is surrounded by randomly arranged cubes with simulated real locations in space. Cubes closer to the fly appear larger, and during closed-loop forward translations, cubes closer to the fly move faster, this means

that the size and movement profiles vary as if they were in the real world (figure 27a-c).

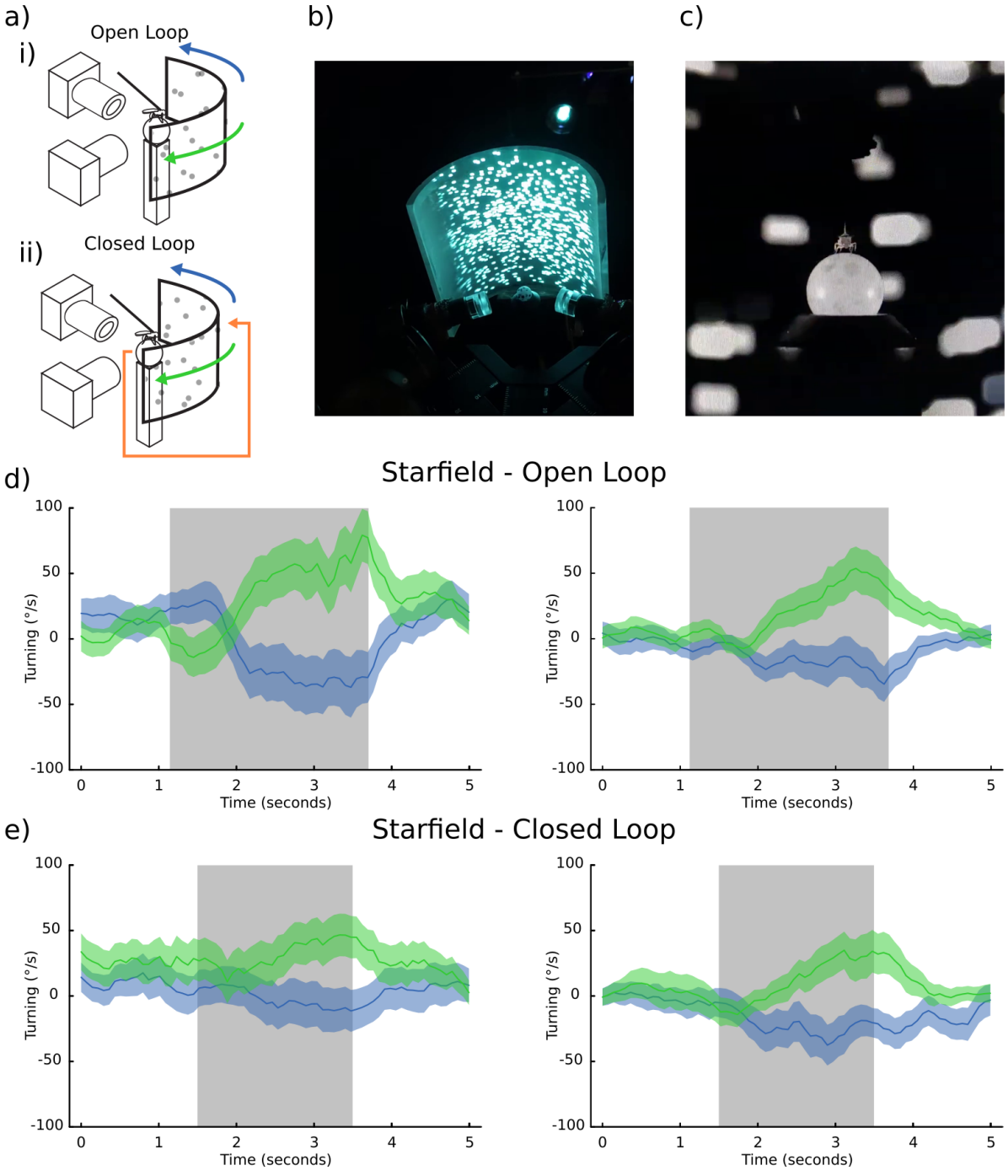

Figure 27: Example Traces Showing Flies behave Similarly when placed in a Non-Periodic Environment
(a) Schematic for experimental setup of the open-loop (d) and closed loop (e) paradigms.
(b) Image showing how the starfield environment appears over the whole screen.
(c) Close up view of the flies responding to the starfield environment.
(d) Example traces from two flies shown the starfield environment, the first fly exhibits an initial optomotor and late anti-optomotor response, whilst the second exhibits only an anti-optomotor response.
(e) Example traces from the same flies shown the closed-loop environment. Both flies only exhibit an anti- optomotor response.

When we presented rotatory motion to flies under the forward-walking paradigm, we observed both an initial optomotor response, as well as a late anti-optomotor response (figure 27d), but in other flies we observed only the anti-optomotor response, which starts 1s after the stimulus onset, as in our previous experiments. This result demonstrates that the anti-optomotor response is likely a response dependent on world-rotation, rather than specific to the type of stimulus being rotated.

A Closed Loop Experimental Setup Does Not Prevent the Anti-Optomotor Response Within the starfield environment, we set the rotary and translational and optic flow of the stimulus to be dependent on the movement of the trackball. We found that even when the fly experienced closed-loop re-afferent control of the environment, it still performed the anti-optomotor response (figure 27e).

The Anti-Optomotor Response Reverses at a Reversal Wavelength In the first experiment we observed only a very small, but potentially reversed optomotor response at a 5.2° wavelength when compared with the other wavelengths tested. This wavelength is below the standard wavelength that results in the optomotor reversal, therefore we wanted to test whether the anti-optomotor response is reversed at a reversal wavelength (6.6°). In addition to this we wanted to test the hypothesis that the optomotor reversal wavelength is speed-dependent (Kemppainen et al., 2022). We presented flies with gratings of either 6.6° or 20° at either 4 or 20 Hz. We found that both the optomotor response and the anti-optomotor response is reversed at 6.6° when shown at 4 Hz. Flies show an initial anti-optomotor response, and a late optomotor response (an inversion of the normal case) (figure 28a). We did not observe any strong responses 6.6° when shown at 20 Hz (figure 28b). There was a significant interaction between wavelength, temporal frequency, and optomotor response at different points in the stimulus presentation ($F = 5.77$, $P < 0.005$, $n = 11$ flies). With signif-

icant differences between the early and late trace for the 6.6° and 20° wavelengths at 4 Hz (F = -2.29, P < 0.05 and F = 2.9, P < 0.05 respectively, n = 11), but no difference at 20 Hz figure 28d. This result broadly agrees with existing literature that the optomotor response is reduced at high temporal frequencies (Duistermars et al., 2012; Fenk et al., 2022; Kunze, 1961).

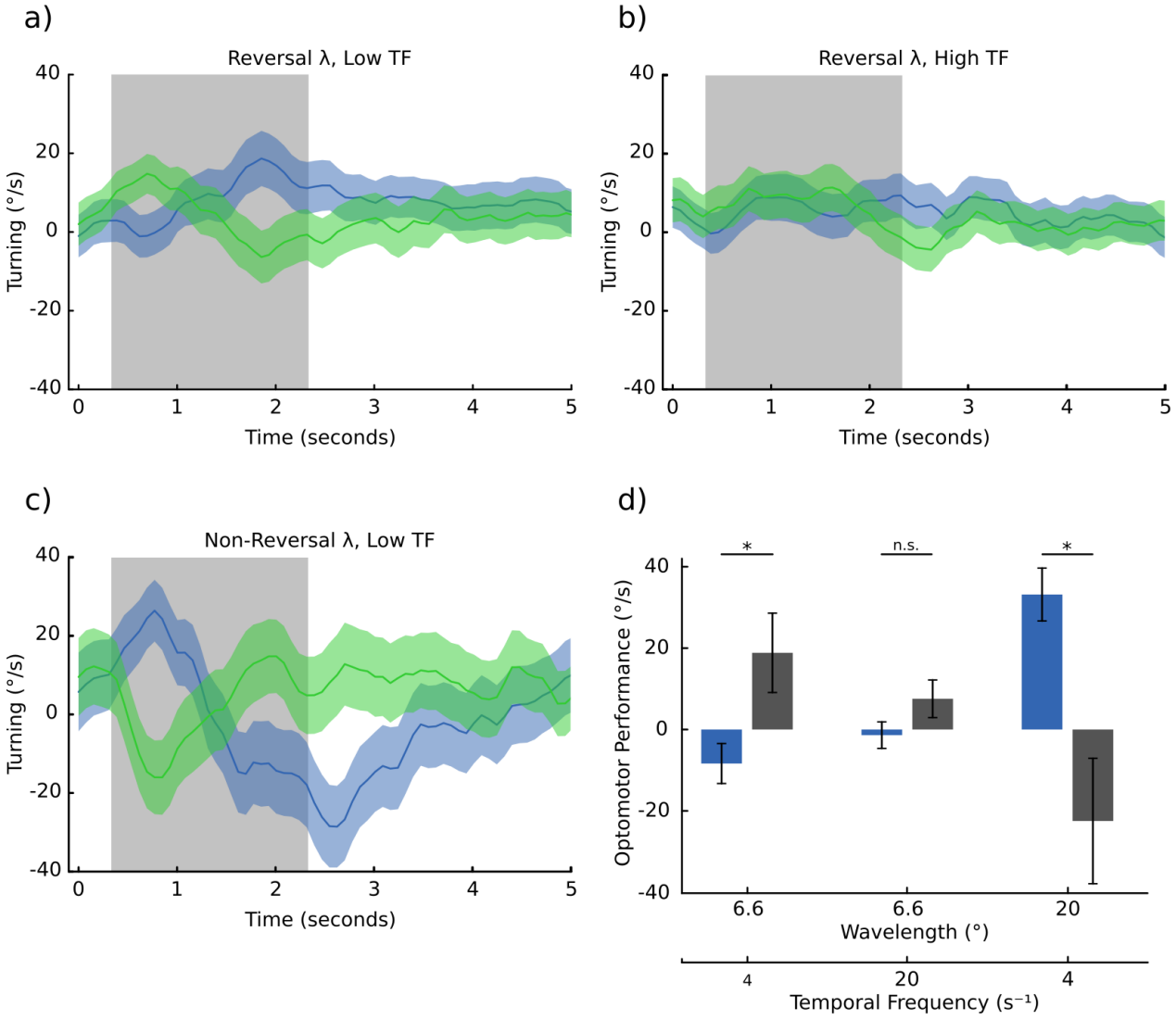

Figure 28: Flies Responding to Reversal Wavelengths at Different Temporal Frequencies.
(a) Flies responding to a low-TF grating at 6.6°, they exhibit an initial anti-optomotor response and late optomotor response.
(b) Flies responding to the same grating wavelength at a higher TF, responses are attenuated or non-existent.
(c) Flies responding to a low-TF grating at 20°, showing a stronger, and reversed case compared to (a).
(d) Overview of optomotor responses, responses at 6.6° are inverted compared to responses at 20° for the low temporal frequency, and non-significant at a high temporal frequency.

1.3.6 Optomotor Responses at Extreme Velocities

Our previous findings show some relationship between the forward walking and optomotor response. Personal correspondence (HaDi Maboudi, Opteran Technologies) suggested that the optomotor responses of other bumblebees might be constrained to naturalistic parameters of world motion likely to be experienced by that animal. Specifically, it was found that honeybees reduced their optomotor response at higher temporal frequencies, but bumblebees even exhibit anti-optomotor behaviours at very high temporal frequencies. One explanation is that the system estimates the likely range of world motion that might be possible, as a function of the natural limits that might be expected for an animal of that species, modulated by the level of world rotation that might be expected as a result of the animal's own actions. We decided to test similarly extreme grating velocities in fruit flies.

The Optomotor Response is Maintained at Higher Velocities than the Slowdown Response We tested gratings of 30° wavelength at 0, 400, 600, 800, 1,000, 1,200, 1,400 °/s velocities, using the same forward-walking trigger as in the previous experiment. In the control condition, for which no grating motion was displayed after the forward-walking threshold was triggered, the flies did not significantly slow down over the 2 s period of stimulus exposure. There was a significant effect of grating speed on the slowdowns observed ($F = 7.5224$, $P < 0.0005$, $n = 10$ flies). At medium speeds (400, 600 °/s), the flies exhibited a significant slowdown. At higher speeds (800, 1,000, 1,200, 1400 °/s), flies did not have significant slowdowns (figure 29b).

We observed responses for the majority of the velocities. There was a significant effect of the direction of motion grating ($F = 14.5043$, $P < 0.05$, $n = 10$), but not of speed, or an interaction between speed and direction. Given this there were significant optomotor responses in all of the conditions tested, except for the very fastest: 1,400 °/s, and of course the control

condition) (figure 29c). Although not significantly, the strength of the response did appear to be lower at the higher speeds.

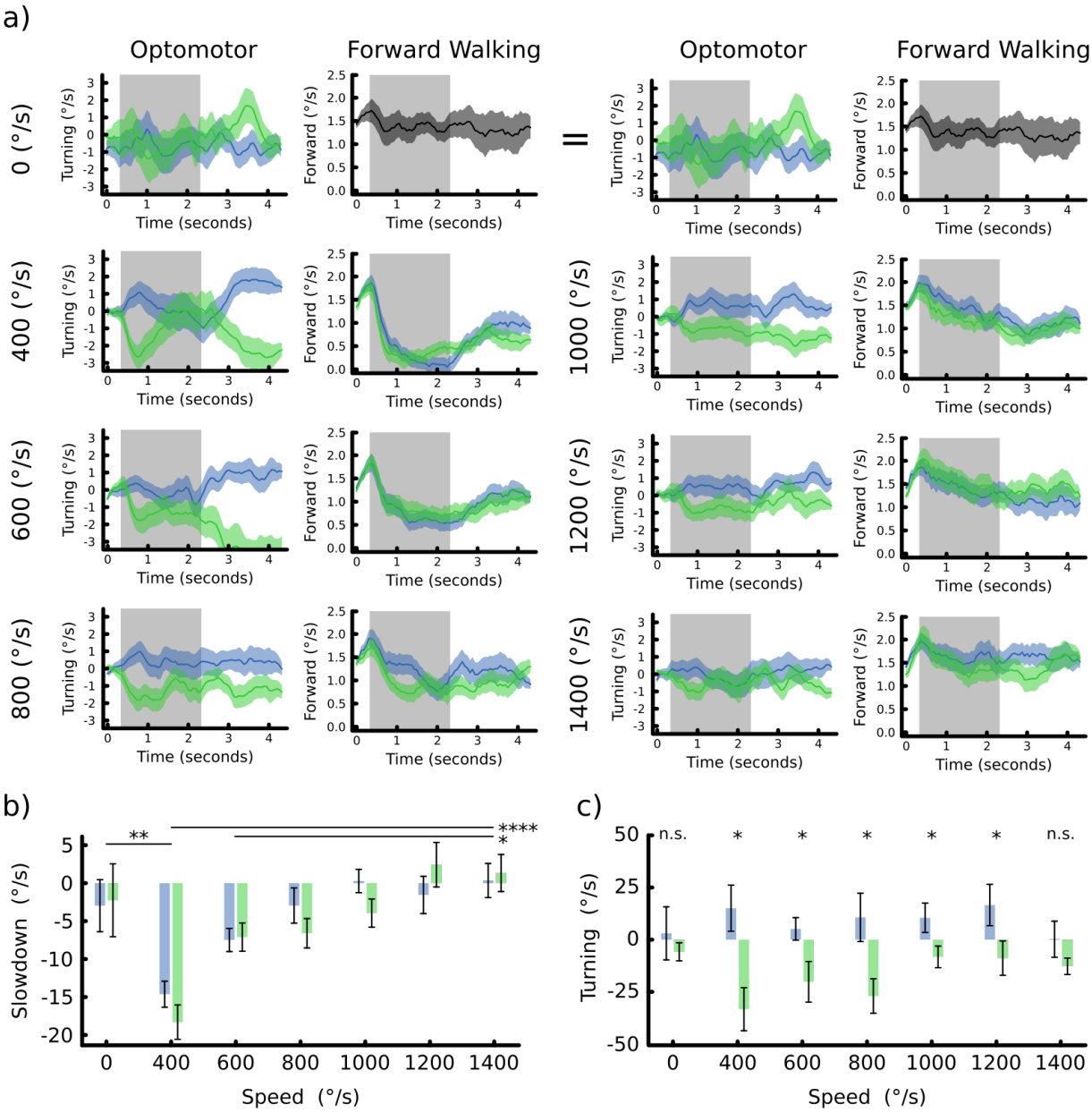

Figure 29: Optomotor and Slowdown responses of flies in response to fast gratings.
(a) Average turning (left) and slowdown (right) to different grating speeds. Control gratings with no motion are shown at the top.
(b) Overall slowdown responses of flies. Slowdowns at 400 and 600 °/s are significantly different from 0.
(c) Average Turning responses, Flies maintain an optomotor response until 1,200 °/s

At faster velocities, flies did not appear to exhibit much of a slowdown response, indicating the limit of their velocity tuning, although the optomotor response appeared more sensitive here up until the very fastest gratings. The temporal frequency was at maximum 10-50

Hz, given the large size of the gratings, so this could represent the difference between the temporal frequency tuning, and the velocity tuning of the two behaviours (Creamer et al., 2018). We did not however, observe the reversal effects that were seen in the bumblebee data.

1.3.7 Optogenetic Control of Optomotor State

The previous experiments show a relationship between the internal state, and the optomotor response. Walking, compared to standing still appears to initiate a state of higher optomotor engagement. Both low and high engagement states are likely to be encountered as part of normal behaviour in naturalistic settings. By waiting for flies to start walking forwards, we can observe stronger optomotor behaviour, but this does not exclude the possibility of a third factor (e.g. arousal) that might be causing both forward walking and stronger optomotor turns. It has been found previously that activating forward walking optogenetically can create lower-variance behaviour in a closed-loop setting (Fujiwara et al., 2022). Two classes of neurons have been found to modify walking behaviour in flies; one of these classes is BPN (Bolt protocerebral neuron) (Bidaye et al., 2020). When BPNs are activated the fly engages in fast, straight, forward walking behaviour. This state can be initiated from a standing-still position. The other neuron (P9) appears to be involved in object-tracking behaviour such as that found in mate pursuit during courtship (Bidaye et al., 2020).

We hypothesised that by activating BPNs, we would engage the fly in the optomotor state, accentuating optomotor behaviour. The alternative hypothesis is that there is some third factor e.g. arousal, that modulates both the forward walking and the optomotor behaviour that could confound our results.

Optogenetically Activating Walking Increases the Optomotor Response We expressed csChrimson in BPN neurons, which we optogenetically stimulated with an LED fitted above the head of the fly (figure 30a). We first confirmed that optogenetically stimulating the BPN neurons elicited forward walking responses compared to wild-type controls (figure 30b). After the onset of the LED turning on, flies exhibited strong forward walking responses (figure 30c-e).

In wild-type controls, the light did activate walking a small amount, but at a significantly reduced level when compared to the BPN>csChrimson flies. We did observe, however, that BPN>csChrimson flies appear to show much more reduced walking outside of optogenetic stimulation compared to wild-type flies.

We tested how BPN>csChrimson flies responded to a moving grating, when BPN is stimulated compared to when it was not. As expected, optogenetic activation of BPN significantly increased forward walking ($F = 3.24$, $P < 0.05$, $n = 6$ flies). Optogenetically activating BPN appears to enhance the optomotor response when compared to the when BPN is not activated ($F = 6.95$, $P < 0.005$, $n = 6$) (figure 31b-d). The onset of the LED elicited a ramp up of walking behaviour within 500 ms, this was mirrored in the optomotor response which began at the same time as the forward walking behaviour, since the onset of grating motion occurred at same time as the LED onset. The controls did not exhibit any forward-walking behaviour in response to the LED onset, which was expected. When the LED was off, the flies exhibited only very weak, but still present, optomotor responses.

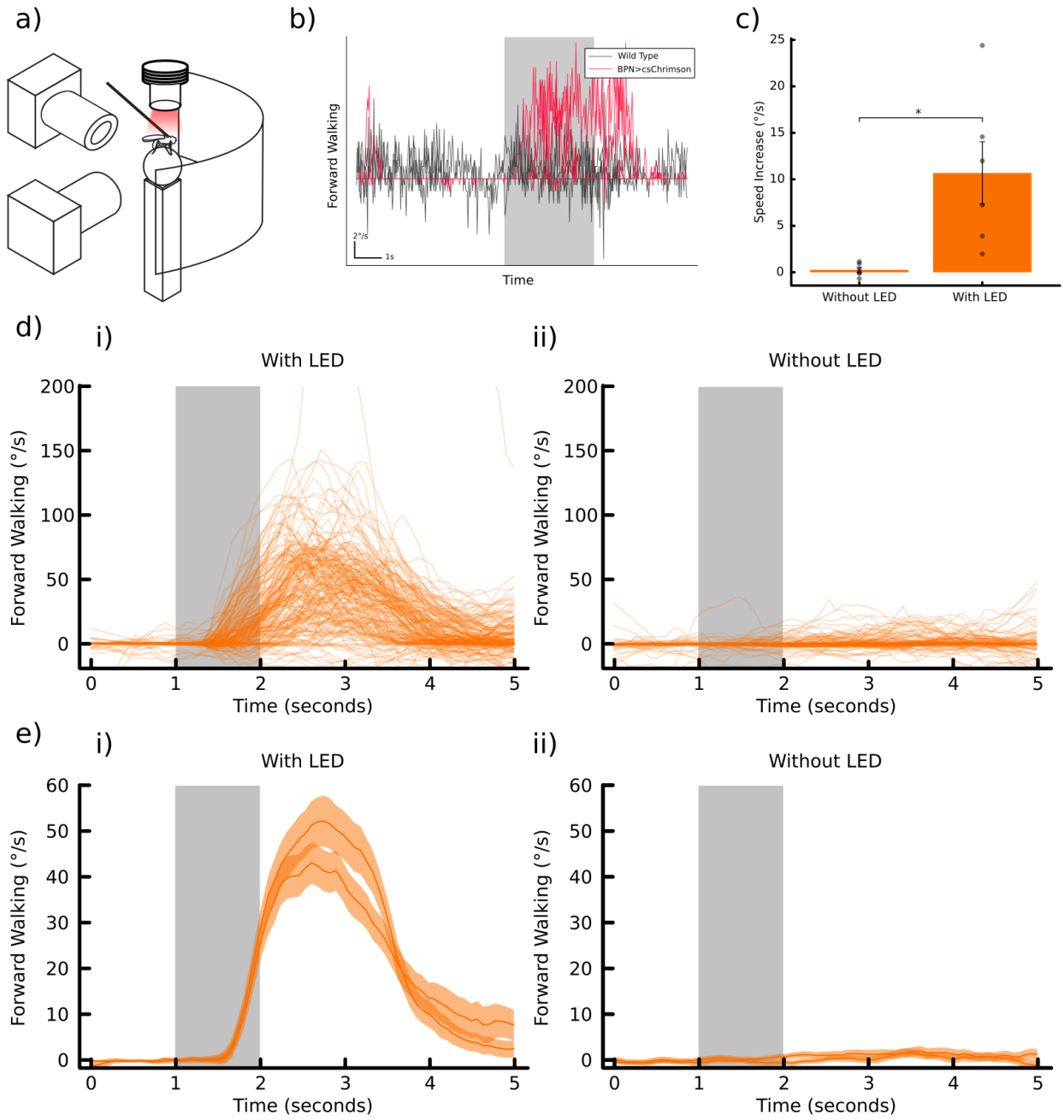

Figure 30: Forward walking responses to optogenetic stimulation.
(a) Schematic showing the LED placed above the fly during the experiment.
(b) Example trace showing the response of a transgenic (red) and wild-type (grey) fly to LED stimulation.
(c) Average speed increases after the onset of the LED; the LED significantly increases the walking speed of transgenic flies.
(d) Raw forward walking traces of flies in response to the LED. Transgenic flies begin to walk forward 500 ms after the onset of the LED, with minimal walking when the LED is off (ii).
(e) Average walking traces in response to the LED.

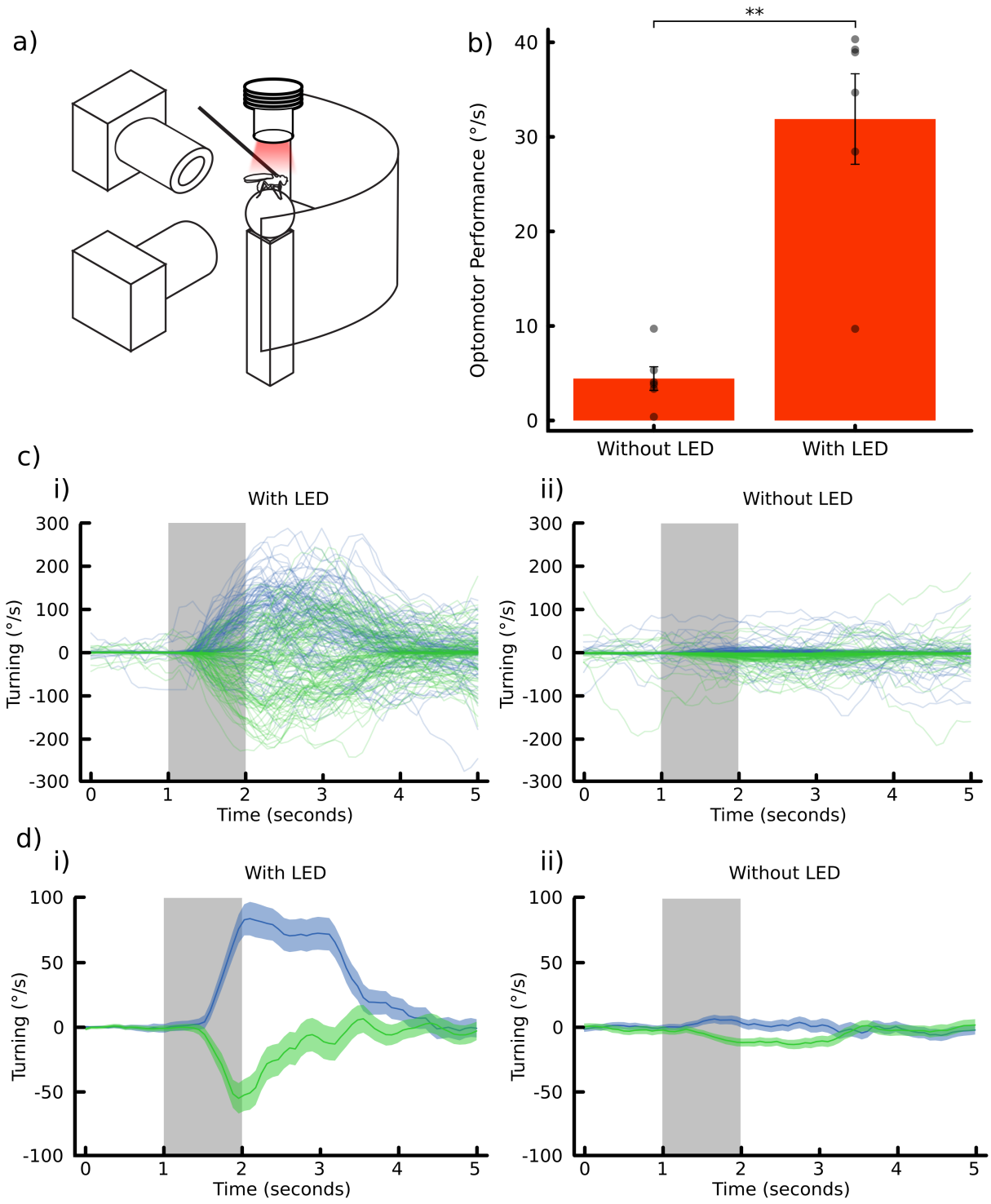

Figure 31: Average turning responses of flies in response to the LED and grating motion.
(a) Schematic showing the experimental setup.
(b) The average optomotor responses of flies are much greater when the LED is activated.
(c & d) Raw and average traces of flies in response to the grating motion and LED. Optomotor responses begin about 500ms after the onset of the grating. Responses are much larger when the LED is on.

We could confirm that the optomotor response is enhanced by forward walking, suggesting

that the circuits involved are more likely to be recruited to drive behaviour when in the walking state than when still. Furthermore, since this was initiated experimentally, it is unlikely this is the result of a confounding factor, such as arousal.

1.3.8 The Anti-Optomotor Response to Looming Stimuli

We found that when we tracked the head-movements of flies during the anti-optomotor, the head-movements preceded increased anti-optomotor turning, in a motif that resembles course-changing turning that occurs during exploratory behaviour. We reasoned that if flies were exposed to stimuli that also induced course-changing turns at the same time as being presented rotational grating stimuli, then the anti-optomotor response would be enhanced. Saccades can be induced by presenting a rapidly expanding stimulus (a loom) on one side of the fly (Fenk et al., 2021). Our hypothesis was that if we present this stimulus, in addition to a low-contrast grating, we would observe anti-optomotor saccades, but if we only present a low-contrast grating in the absence of a looming stimulus, then we will see only optomotor responses, as long as the flies are moving forwards.

A Looming Stimulus Recreates the Anti-Optomotor Effect We waited for forward-walking behaviour in flies as described in the previous experiments. When forward walking was detected, we presented a looming stimulus that increased to 40 degree diameter within 100ms, on one side of the fly, at 25 degree eccentricity. At the same time, we presented a 50% contrast grating, relative to the previous experiments (figure 32a). We compared the behaviour of flies that were shown only a low-contrast grating, to flies that were shown a low-contrast grating as well as a looming stimulus.

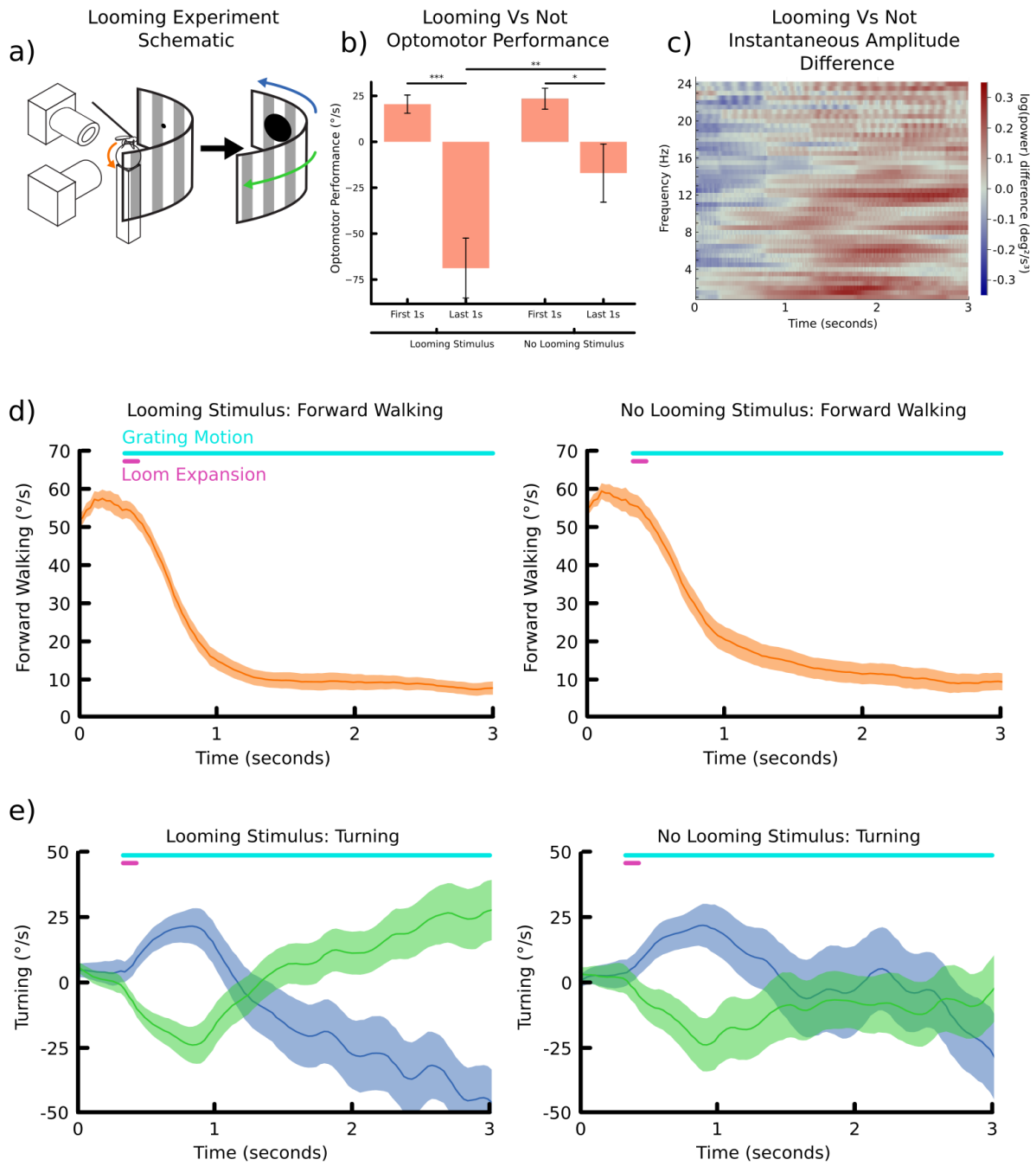

Figure 32: Responses of flies to a grating and a looming stimulus.
(a) Schematic showing the experimental setup. Forward walking triggers a low-contrast grating to turn at the same time as the expansion of a dark disc.
(b) Optomotor response of flies in the early or late stage of the stimulus.
(c) Difference between log powers of flies shown a loom and those shown no loom showing increases in the higher frequencies in flies shown the loom.
(d) Forward walking responses of flies in the looming and no-looming conditions.
(e) Turning responses of flies in the looming and no-looming conditions.

The effect of the looming stimulus did not appear to change the forward walking speeds of

the flies (figure 32d). In both cases the flies slow down in response to the stimulus, relative to the time at which the stimulus is triggered. When we look at the turning responses, both sets of flies appear to have an initial optomotor response to the stimulus which is not significantly different. In flies that are only shown a grating, this response reduces as the stimulus continues and the flies speed drops, which at the end of presentation is anti-optomotor, but not significantly so. In flies that are shown both the grating with the looming stimulus, the optomotor response is followed by an anti-optomotor response roughly 1 s after the onset of the stimulus. This anti-optomotor response is present regardless of which side the looming stimulus is presented on. The outset of this is that there was a significant effect on the optomotor turning depending on the presence of the loom ($F = 14.76$, $P < 0.005$, $n = 12$ flies), the difference between the initial and late response ($F = 22.73$, $P < 0.005$, $n = 12$), and an interaction between the two ($F = 13.00$, $P < 0.05$, $n = 12$).

Both groups have a more negative optomotor response between the first and last stages of the experiment, with the grating-only group dropping to near zero ($F = 3.21$, $P < 0.05$, $n = 12$), while the grating+loom group becoming anti-optomotor ($F = 5.13$, $P < 0.0005$, $n = 12$), and with a significant difference between the late stage responses for the grating vs the grating + loom groups ($F = 4.06$, $P < 0.005$, $n = 12$) (figure 32b). The response difference in the looming-group suggests that the fly is put into a different internal state in response to the looming stimulus. This state appears to result in an anti-optomotor response, which is not present in the control group. It is unclear why the anti-optomotor response only appears around 1000ms after the looming stimulus actually appears. This may be because the anti-optomotor stimulus can only occur when the fly is moving forwards slowly or stood still. The existence of a slowdown without accompanying anti-optomotor response in the control group however suggests that a slowdown is not sufficient to generate anti-optomotor saccades.

Higher Frequencies are Upregulated in the Anti-Optomotor Portion of Behaviour We had found previously when we compared the instantaneous amplitude spectra of walking an non-walking flies, that the low-frequency component of behaviour was higher in flies performing optomotor behaviour than in flies that did not on average turn in any direction. In this experiment we had the converse pattern, where both flies perform the optomotor portion of behaviour, but only the flies shown the looming stimulus demonstrated the anti-optomotor response. We compared the instantaneous amplitude spectra of these flies and found that the flies shown the looming stimulus exhibited greater amplitudes in the higher frequencies components of the spectra, with particular increases seen at 2 Hz, 6 Hz, and 12 Hz (Figure 32c).

We wanted to understand how the time-course of the presentation of the looming stimulus and the motion of the grating affected the anti-optomotor response in flies.

1.3.9 Time course of Saccadic Initiation

We found that in the previous experiment, we could enhance anti-optomotor responses by presenting a looming stimulus alongside a grating stimulus. One possibility is that flies go into an anti-optomotor state for a very short period of time during saccadic movement. If this is true, we should be able to test the time course of the anti-optomotor effect, there should be a period around the time a body-saccade is triggered where we should be able to cause the fly to behave in an anti-optomotor fashion. Any grating motion that occurs outside of this window is unlikely to cause anti-optomotor behaviour, and will cause either no, or optomotor behaviour.

Anti-Optomotor Responses to Grating Motion Only Appear after a Delay We presented looming stimuli to flies and triggered the grating motion at various time-points after

the loom began, to generate a dataset of responses where flies are performing turns in response to the loom and to the grating at different time-points. We presented the stimuli to flies without a forward walking condition, in order to ensure that the turning responses were not dependent on the fly's forward-walking state. We found that in this non-forward walking condition, flies do not exhibit optomotor responses at all. Instead only anti-optomotor responses are seen (figure 33). The anti-optomotor responses are seen on average within 1 second of grating onset. The looming stimulus, when presented alone, tended to slow down flies, sometimes causing them to walk backwards.

We took the movement data from the flies and identified the time at which flies performed the first body-saccade, if they did, defined as turning at 180°/s. We found that this method, along with triggering the grating motion at different delays from the looming stimulus generated a normal distribution of post-grating saccade latencies centred near 0 (figure 34b). On average, flies that perform a saccade, performed their first saccade within 1,000 ms after the onset of motion, broadly agreeing with the effect of the loom in the previous experiment.

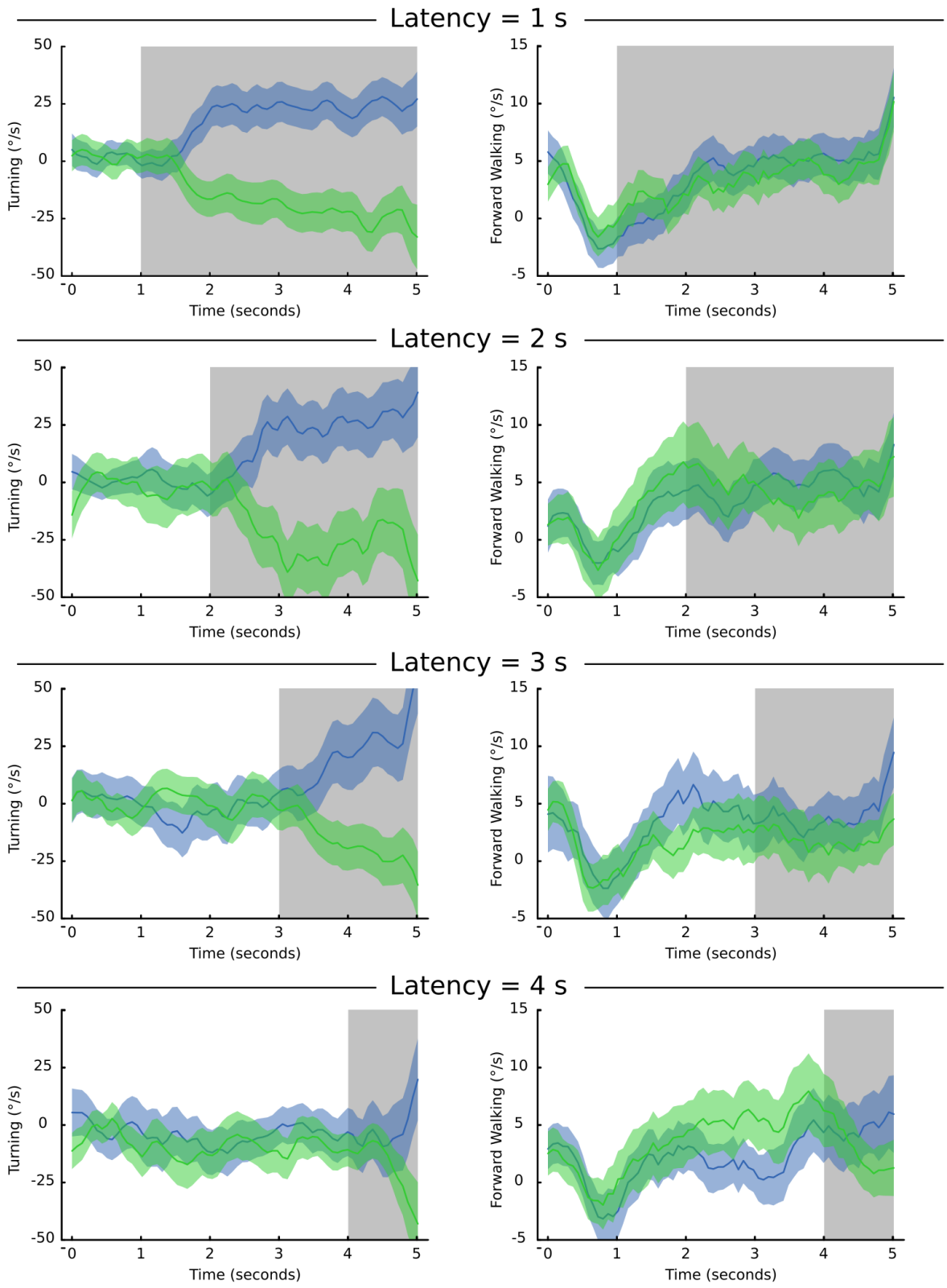

Figure 33: Average Responses of Flies to Grating Presentations at Different Latencies. Responses show the turning (left) responses and forward walking (right) of flies shown a loom within the first second, and a grating (grey bar). There is an initial forward walking response to the looming stimulus, as well as an anti-optomotor response to the grating motion onset.

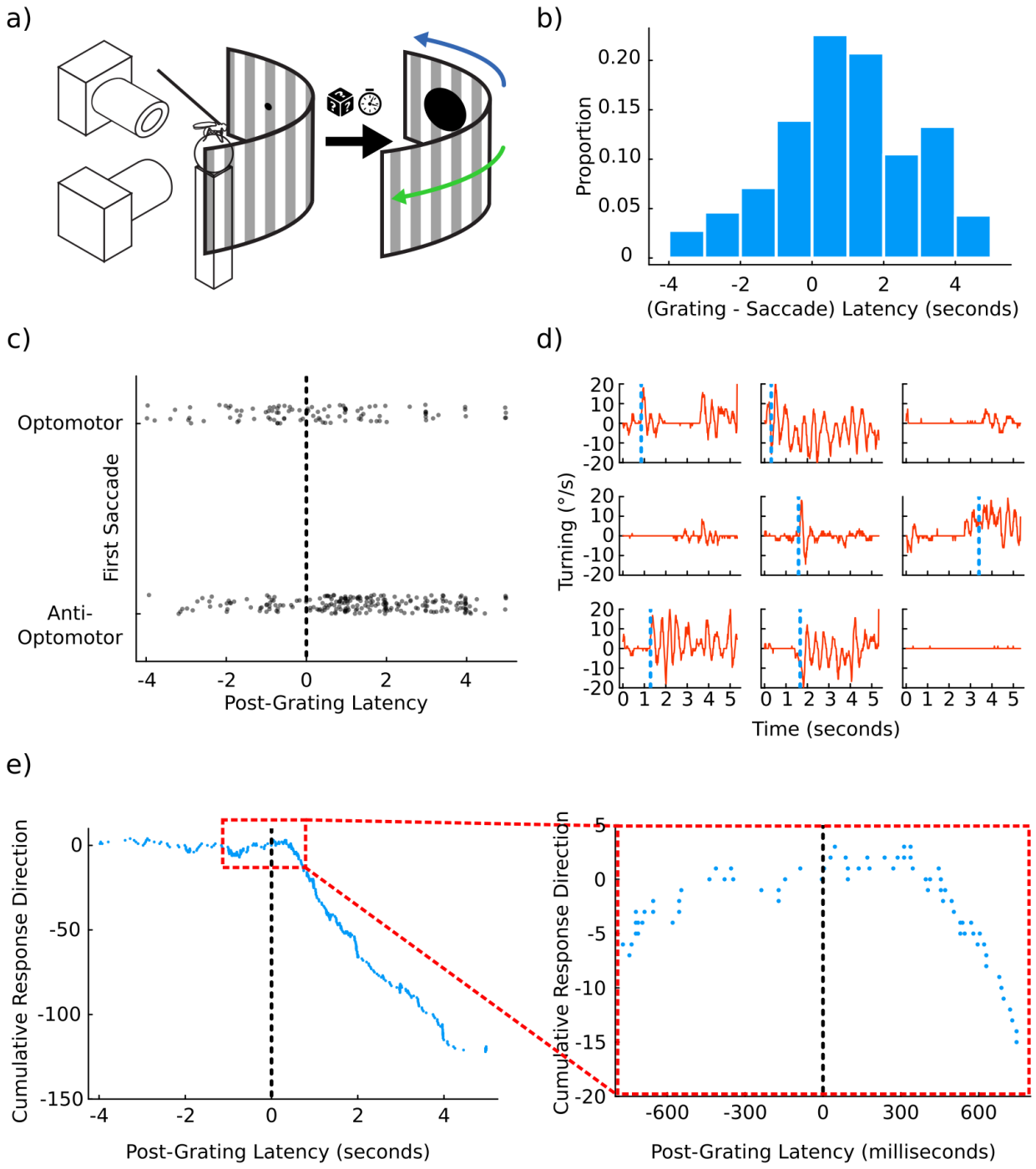

Figure 34: Grating motion only influences strong turning responses after a delay.
(a) Schematic showing the experimental setup. An expanding disc is shown at the beginning of the experiment, followed by a variable delay and then grating motion.
(b) Distribution of the first body-saccade latencies after motion onset.
(c) First Saccade directions and latency of responses, responses are random before the grating and appear anti-optomotor afterwards.
(d) Example traces showing turning responses and identified saccades.
(e) Cumulative turning responses by time. 300 ms after grating onset, flies do not show a bias.

We took these timings relative to the onset of motion, and categorised each initial saccade

as being optomotor or anti-optomotor. Clearly, if the fly performs the saccade after the onset of grating motion, the saccade will not be biased in the optomotor or anti-optomotor direction. From the previous experiment we know that if the motion proceeds the saccade by about 1 s then the saccade is generally anti-optomotor. However, what of the transition period? How long does the fly have to perceive the motion for to trigger the anti-optomotor response?

We took the timings, and whether the saccade was anti- or optomotor, and plotted the cumulative time-series (figure 34e). We can see that if the fly saccades prior to the presentation of the motion, the response is random, and likely results from the looming stimulus and internal stochastic processes. After the grating motion begins however, there is a 300 ms period before the grating has any overall effect on the direction of the saccades. This result shows either that there is a build-up of the optomotor stimulus until the saccade point, or that the saccade direction is locked in, for up to 300ms until the saccade actually occurs.

1.4 Discussion

1.4.1 Summary of Main Results

- Under certain conditions, flies show a consistent, large, and sustained anti-optomotor response.
- The anti-optomotor response is not a perceptual illusion, since the head moves in the optomotor direction.
- Head-saccades occur directly before increases in anti-optomotor turning.
- Optomotor turning is associated with low-frequency features while anti-optomotor turning is associated with high-frequency features
- Head movements do not cause the anti-optomotor response, since fixing the head in place does not prevent it.
- Low contrast gratings prevent the anti-optomotor response, but looming stimuli enhance it.
- Anti-optomotor turns only occur after a build of of exposure to rotary optic flow.
- Forward walking behaviourally enhances the optomotor response, and enhancing forward walking optogenetically brings about the same effect as naturalistic walking.
- Flies show head optomotor turning responses to hyperacute stimuli.

1.4.2 Initial Investigations into the Anti-Optomotor Response

We observed anti-optomotor effects with the first experiments we conducted into the optomotor behaviour of flies. Previously, anti-optomotor behaviour has been considered non-saccadic (Mano et al., 2023) because it is much more sustained than has been observed otherwise (Williamson et al., 2018). This observation holds somewhat consistent with our

results here, when flies begin to turn in the anti-optomotor direction, they continue to turn until the offset of the stimulus, which in our first experiment was over 8 seconds long. While the characteristics of the behaviour are not saccadic, in the sense that naturalistic saccades begin and end within a very short time frame (Williamson et al., 2018), we do not have any good evidence as to whether these two behaviours are driven by two completely separate systems. In particular, we believed the anti-optomotor responses observed in our experiments could be the result of the same saccadic system being triggered again and again.

In our first experiment, we observed no optomotor effects when we considered the magnitude of responses to the left and right gratings at any of the gratings types we observed. In the calibration grating, for which we had 90 flies, we did observe an optomotor directional response, suggesting that there was a small low-magnitude optomotor response, that was rarely present, given it was only observable at such a large sample size. The lack of real initial optomotor responses then suggests there was some difference in the experimental conditions between the conditions seen in our first experiment, and those used in other laboratories, which do observe an initial optomotor response, followed by an anti-optomotor response (Mano et al., 2023). The variety of factors likely that seem to affect the anti-optomotor response (contrast, rearing temperature, age) that have previously been found, suggests there are many more factors that can modify the response even further (humidity, background light levels), making comparisons between laboratories difficult unless all of these environmental factors are controlled for. Later on, we were able to observe both optomotor and anti-optomotor responses within single traces with the use of a lighter trackball and by testing responses during forward walking, so these may be plausible differences between the two procedures.

For the initial experiment, we tested three different grating sizes and speeds to test the optomotor response. It is known that the optomotor response follows a consistent bell-

shaped curve with respect to the temporal frequency of the stimulus (Duistermars et al., 2007), and this is caused by a bell-shaped response curve of HS cells to temporal frequency (Chiappe et al., 2010). We found that within a given thickness, increasing the speed of the stimulus did not have a significant effect on the size of the anti-optomotor response. Moreover, within a given speed, the size of the anti-optomotor response appeared to scale with the wavelength of the grating. For the 5.2° degree wavelength grating, we did not observe any strong optomotor responses, although the responses we did observe were slightly optomotor, it is unknown whether this was because the responses themselves were optomotor or, whether they were anti-optomotor responses to near-reversal wavelengths, we later clarify this by observing the head movements of flies in the same experimental setup.

This first experiment showed us the existence of the anti-optomotor responses, and was done without knowledge of the recently published paper into the subject (Mano et al., 2023). We were surprised at how consistently these responses were triggered, and at the size of the responses themselves, given that at the time, there was virtually no literature investigating them. We decided to investigate the cause and characteristics of the responses further.

In a similar intuition to (Mano et al., 2023), we thought that the head movements could have been the cause of these unusual behaviours. This turned out not to be the case, with most flies still performing only anti-optomotor behaviours in response to the turning gratings even when the heads were fixed. In fact, while the directionality of the responses was the same, we found that the responses themselves were much less consistent, with flies with fixed-heads often turning less overall than their head-free counterparts. (Duistermars et al., 2012; Kim et al., 2017). Since we later found that flies tend to follow the optomotor stimulus, fixing the flies heads in place should only serve to increase the optic flow perceived by the eyes; at least before the head reaches its maximal eccentricity, which should lead to increased compensation by the body position. This condition might be expected to increase both any

optomotor and anti-optomotor responses, though we actually observed weaker responses. These results demonstrate that the optomotor system cannot be viewed as a simple feed-forward response to the stimulus, but interacts non-linearly with the internal state of the animal to produce unexpected effects, as observed here.

We did however observe two flies from this cohort that did exhibit optomotor responses overall. We found that the average forward motion of these flies at the beginning of the stimulus was the highest out of the cohort, for both the calibration stimulus and the test stimuli. Neither of the flies displayed the same kind of anti-optomotor responses that we see in the other flies. We reasoned that it could be that the flies' forward motion dictates whether the optomotor or anti-optomotor response is performed; the optomotor response being an error-correction response. This error is produced by the difference between the internal intent (the afferent copy), and the actual result that occurs in the world (the efferent copy), which is made up of an interaction between the errors caused by carrying out the intent (e.g. incorrect co-ordination), and any external factors that may influence this as well (e.g. wind, barriers etc.). Without any internal motor signal, it seems that the error-correction system circuitry is not properly engaged. This hypothesis seems to hold for the gain-control of the LPTCs (Chiappe et al., 2010; Fujiwara et al., 2022; Maimon et al., 2010). And we show here that this link between locomotion and optomotor performance exists behaviourally as well.

1.4.3 Forward Motion and the Optomotor Effect

We tested the optomotor performance of flies while they were in the walking state, by waiting until a walking bout was initiated, and only then introducing grating motion. In contrast to the previous experiment, we found in these flies only optomotor performance over the course of the experiment, being analogous to the first two seconds of performance in the first experiment, in which we observed essentially no optomotor behaviour. It is known that

afferent activity about the front leg movements is phase-locked to the HS cell activity which can induce course-corrections (Fujiwara et al., 2022), and it has been theorised that this activity contributes to both the short and long-term motor context of these cells (Fujiwara et al., 2017). This result is a behavioural demonstration that the long-term motor context of the fly contributes to its optomotor behaviour during walking. Indeed, taking every time-point, stimulus-agnostically, there is a significant correlation between the forward motion of flies and their optomotor responses. The slowdown in response to motion that we observe here has been noted elsewhere (Creamer et al., 2018), and it seems the that optomotor response starts to reach a peak at the highest deceleration of flies. Interestingly, at the thickest and fastest grating (16.8° at 106°/s) showed the highest deceleration, and this was mirrored by a much shorter-lived optomotor response.

When we tracked the heads of flies we found that the head-movement response was much more stable than the walking response, and accordingly much less susceptible to modulation by motor context. Given that the gain of motion sensitivity is dependent on HS cells (Chiappe et al., 2010), and that head movements are dependent on HS (Haikala et al., 2013), it is possible that the head-angle is controlled by different circuitry, or is otherwise much more sensitive to the HS activity.

Given the motor context appears to strongly modulate the optomotor response in walking flies, we hypothesised that it would also modulate the anti-optomotor response. We found that the ball weight affected how quickly the anti-optomotor response appeared, and that even in the forward-walking protocol we could generate both optomotor and anti-optomotor responses within the 2 second motion period when we used a lighter ball. One explanation for this is that with a lighter ball, the frequency of the strides increases, and the mechanosensory feedback produces stronger HS cell activity, another possibility is that a lighter ball provides less inertia which might allow flies to slow down more quickly. The normal free-moving

walking speed of *Drosophila* is approximately 20-30 °/s (Mendes et al., 2013; Robie et al., 2010). In our experiments the walking speed was considerably lower (approximately 2-3 °/s). This is almost certainly a result of the weight of the air-cushioned ball requiring more force to move when compared to a fly in the free-moving state. This likely has an effect on the optomotor response, not only through the reduced forward-walking speed, but also through modifying the natural dynamics of the mechanosensory feedback that flies normally experience during free-walking (Fujiwara et al. 2017).

The optomotor and anti-optomotor responses with a lighter ball, show that the initial optomotor response is much more prominent when the fly is in the forward-walking state. The anti-optomotor response however, appears to be present between both conditions, indeed, with no difference in the anti-optomotor response of the latter part of the stimulus presentation. These results suggest that the initial forward-walking at the onset of the motion is not sufficient to prevent the anti-optomotor effect later on in the experiment. However, by the time the anti-optomotor effect occurs, the fly has decelerated substantially. and although the difference in forward walking between the non-walking and forward-walking conditions at this latter stage is significant, it is much smaller than in the initial stage of the experiment.

It is still plausible that a slow-walking motor-context allows the anti-optomotor effect to occur. The converse explanation, that the anti-optomotor effect induces the slowdown is not borne out from the data, since the slowdown occurs at the onset of grating motion, and the fly has almost completely slowed down by the time that the anti-optomotor response starts to begin. In the first forward-walking experiment, we observed slowdowns in response to the gratings, but no anti-optomotor effects. In experiment 1-a we observe anti-optomotor effects within the first few seconds of stimulus onset, so it is unclear why we did not observe it in the experiments in 1-c. Presumably if we had presented longer rotations, the anti-optomotor effects would have appeared.

The finding that the initial forward walking does not prevent the anti-optomotor effect from occurring later still leaves room for the slow-walking to be a permissive feature of the anti-optomotor effect. Others have found that the slow-down that flies perform in response to external motion is proportional to the velocity of the motion, rather than the temporal frequency (Creamer et al., 2018). This is reflected in the fact that the motion detection cells T4/5 are implicated in the slowdown rather than the LPTCs (Creamer et al., 2018). Drawing on this link, the anti-optomotor responses found by (Mano et al., 2023) show both a dependence on the T4/5 cells and the anti-optomotor response with respect to temporal frequency showed the same maximal response characteristics as those shown by the T4/T5 cells. Moreover, in (Mano et al., 2023), adaptation to a back-to-front translational stimulus for 5 seconds was sufficient to elicit anti-directional responses immediately upon switching to a rotatory stimulus. (Creamer et al., 2018) finds that this translational stimulus elicits the strongest slowing responses in walking flies, and is the only stimulus type to induce flies to come to a complete stop on average. In one explanation of these results, the back-to-front stimulus presented in (Mano et al., 2023) places the fly in the same motor context as sustained high-contrast rotatory motion, by slowing down the fly (or keeping the fly still if it was not already moving). Still, it is possible this is a coincidence of sharing some of the same circuitry, rather than the more direct explanation that the slowdown, resulting from T4/5 activity, is responsible for the motor context, which then allows the anti-optomotor response to happen.

In the wild-type forward-walking experiments, we could not infer causation between the optomotor response and forward walking from the correlation we found between these two measures. Because we waited for the fly to start walking forward, it is possible that there was a confounding factor that resulted in both the forward walking and optomotor response, such as arousal. To address this criticism, we initiated forward-walking experimentally by activating the BPN neurons. In order to run an optogenetic experiment, we reared the flies un-

der darkness to prevent the channels from being chronically activated by light and therefore affecting their function. Dark-rearing has been found to reduce the dependence of the anti-optomotor effect on the age of the fly, with dark-reared flies at 4 days post-eclosion having the same level of anti-optomotor behaviour as a 1 day post-eclosion fly (Mano et al., 2023). In our experiment, BPN>csChrimson expressing flies did not show any anti-optomotor effects. This was potentially because we ran the experiment at a lower contrast. This was done because the transgenic flies had a tendency to attempt flying escape behaviour whenever a high-contrast grating was presented. Moreover, the transgenic flies possessed very little motivation to walk whenever the BPN cells were not stimulated optogenetically. The reason for this is unclear, but one explanation is that the csChrimson, undergoes chronic spurious activation in the BPN cells, which might lead to a higher activation threshold via homeostatic compensatory mechanism, as has been observed in the mushroom body (Apostolopoulou & Lin, 2020).

Surprisingly, forward walking of flies began only after 500ms, which is too late to have arisen as a result of direct neural optogenetic excitation from the LED onset. It is possible that levels of csChrimson expression were so low that excitation only built up over time, particularly this may work in conjunction with a generally high threshold for walking activity for the BPN>csChrimson flies that did not tend to walk without stimulation.

Nevertheless, with this experimental paradigm, we were able to switch the fly between motor contexts optogenetically. In these flies, the optomotor response was strongly dependent on whether the fly was walking forward, showing that it is the motor context of the fly that determines the level of the optomotor response. It is unclear from this data whether this is the result of direct action of the premotor circuits that initiate forward walking or whether it is the feedback loop that is initiated when the fly starts to walk, and afferent information is sent back to the optomotor control machinery, which is difficult to disentangle from arousal.

behaviourally, this distinction would be difficult to test within the current setup we have used. In order to distinguish the efferent and afferent effects experimentally, we could activate BPN as here, but test behaviour on a trackball that only allows rotatory motion, not forward motion. If it is indeed the afferent activity that initiates the recruitment of the optomotor gain, activating BPN under these circumstances would not result in any optomotor gain.

Neurologically, this behavioural response could also be dissected by investigating the same neural pathways that are known to provide the HS cells with ascending signals from mechanosensory cells. For instance, LAL-psAN-Contra is known to provide signals to HS cells, and the inhibition of these cells disrupts the timing of discovered stride-coupled inputs to HS (Fujiwara et al., 2022). It is plausible that inhibiting these ascending cells abolishes the difference between optomotor performance in walking vs non-walking flies.

1.4.4 The Anti-Optomotor Effect

The discovery of the sustained anti-optomotor responses raised the initial question as to whether the results we observed were the result of a perceptual illusion, or whether they were part of a behavioural mechanism that received correct information from the motion-processing parts of the visual system, but responded to this differently. We found that the head-movements of the flies followed the direction of the grating, even when the fly's locomotion was anti-directional, suggesting a behavioural cause of the activity, rather than perceptual. One objection to the head-tracking approach could be that the head-movements and the locomotory movements are based upon segregated mechanisms, and the locomotory reversal is the result of a perceptual illusion that is not present in the head-movements because whichever system is dependent on the head-movements is not susceptible to the same illusory motion as the locomotory system. This is probably unlikely since the HS cells have been found to control head movements as well as the optomotor locomotory behaviour

(Haikala et al., 2013; Wertz et al., 2008, 2012).

We were surprised to find nystagmus-like activity in the head-movements, as these have not been reported in walking *Drosophila*, although they have been reported in flying *Drosophila* (Cellini et al., 2021; Cellini & Mongeau, 2022), and in walking *Calliphora* (Longden et al., 2022). These movements follow a pattern of activity where the fly head smoothly follows the direction of motion up until a certain angle, at which point the head-saccade occurs to reset the view in the anti-directional direction, similarly to that found in flying *Drosophila* (Cellini et al., 2021). The average rotatory velocity of these slow head-rotations were not sufficient to fully counteract the grating motion, and probably either acted in concert with muscle movements, or did not fully stabilise the image seen on the retina. We found that the thickness of the grating did have an effect on the frequency of the saccades found. Others have found that the rate of nystagmus can be modified by the velocity of the stimulus (Cellini et al., 2021). One objection to our thickness finding could be that when the fly resets the head this it tracks individual bars, and thus travels more to track thicker bars. This is not supported by the existing literature (Cellini & Mongeau, 2022), moreover, by our own findings that the size of the saccade is invariant to to the pattern. Taking these two results together, it seems likely that the rate of nystagmus is related to temporal frequency, which points to the control of nystagmus being the result of LPTC-dependent mechanisms (Duistermars et al., 2007). As has been found elsewhere (Cellini et al., 2021), we found that the actual shape of the head-saccade was invariant to the stimulus we presented. Given that it has been found that the saccade is dependent on the elasticity of the neck, this makes sense as a response to maximum eccentricity of the head, which is around 10° (Cellini et al., 2021), and is a necessary step in order to allow smooth tracking of the environment under sustained motion.

We also noticed that when the nystagmus-like activity began, this coincided with the time at

which the anti-directional behaviour began. It is unlikely to be the case that the movement of the head itself causes the anti-directional turns, since fixing the head in place does not stop the anti-directional behaviour. However, it is still possible that the internal state that is responsible for the head-saccades is also responsible for the anti-optomotor behaviour. It is also possible that other active vision mechanisms compensate during head-fixing that then also result in anti-optomotor behaviour, given the fact that the eye-muscles themselves appear to undergo a similar kind of optomotor nystagmus (Fenk et al., 2022), which might be enough to counteract the head-fixing, or may even be upregulated in the absence of any head-movement.

There is contradictory evidence about the role of head-saccades in course-changing turns (Cruz et al., 2021; Geurten et al., 2014; Williamson et al., 2018). The fact that we see strong evidence, both of the head-saccades themselves, and a tight correlation between the head-saccades and body-turns is probably a result of the experimental conditions. Principally a fixed body position in addition to the large high-contrast motion could be both responsible for nystagmus and anti-directional behaviour. If the anti-directional activity we observe here is the result of repetitive saccade-like behaviour, we would likely see the inter-saccadic periods being interrupted by small optomotor shifts. When we aligned the locomotory movements of the fly to the peak of the head-saccades, we found that flies were more likely to turn in the anti-optomotor direction directly after the head-saccade; suggesting that the anti-directional response is a form of a saccade, all-be-it a highly unnatural one, since it is so sustained. However, the turning in-between the detected head-saccades was for the most part also anti-directional, and so was not the result of smooth optomotor behaviour being obscured by anti-optomotor behaviour. The exception to this case was in the gratings presented at 5.2° wavelength, for which the movement was largely optomotor before a head-saccade and anti-optomotor afterwards. Anti-directional behaviour could therefore be the result of the

anti-directional saccades being triggered one after the other. In the 5.2° case, the frequency of saccade triggering is much lower than for the thicker gratings, which is the effect we observed, which explains why we see optomotor behaviour interspersed with anti-optomotor saccades, but for the thicker gratings, which exhibit on average higher-frequency nystagmus, the saccades could be triggered one after the other, leading to sustained anti-optomotor behaviour. This would be particularly prominent when the optomotor response is small, when the fly is not moving forward, as we have found.

This link to saccade-like behaviour alerted us to the possibility that the anti-directional behaviour itself might be triggered by a secondary stimulus that is also known to induce saccadic behaviour. Looming stimuli, presented ipsilaterally are well known to induce saccadic turns in the contralateral direction during flight behaviour (Fenk et al., 2021), these are referred to as loom-evoked turns. In walking flies, we found that when we presented with the looming stimulus on the ipsilateral side, we observed a similar loom-evoked turn in the other direction. We then tested what happened to this behaviour when we added a low contrast moving grating in the background of the looming stimulus. The low-contrast grating produced only optomotor behaviour, as has been found elsewhere (Mano et al., 2023). However, with the addition of the looming stimulus, the anti-directional behaviour was rescued. Puzzlingly, this anti-directional behaviour did not actually coincide with the expansion phase of the looming stimulus, which is where the turn usually occurred when only a looming stimulus was presented. The anti-directional phase appearing approximately 1 s after the onset of grating motion, as we have found with higher-contrast stimuli. One possible explanation that the presentation of grating motion alongside the loom acted to suppress course-changing turns until the fly had fully slowed down, since we waited until the fly walked forward to present these stimuli.

One explanation is the presence of the looming stimulus had an effect on the contrast of the

stimulus. With the loom, there is a locally increased contrast between the dark portions of the grating and the looming stimulus, but this is counteracted by a locally decreased contrast between the light portions of the grating and the looming stimulus, such that the global contrast of the stimulus is kept constant, so we deem it unlikely, although not impossible, that this is the cause of the appearance of the anti-directional behaviour.

Another explanation for these results is that the looming stimulus overexcites the motion-detection response of the fly, such that the optomotor and looming stimuli have an additive effect. This suggestion would help explain why high-contrast stimuli are more likely to initiate the anti-directional responses, since they elicit stronger responses in motion-sensitive cells (Duistermars et al., 2007). It has been observed that HS cells receive feed-forward visual input in response to looming stimuli, and this input sums linearly with motor-related feedback input (Fenk et al., 2021). If the effect we observed was due to feed-forward stimulus-evoked responses adding together, this would mean that looms on the right would enhance anti-directional behaviour with clockwise (right-moving) gratings, and act in the opposite way to anti-clockwise gratings. However, we found that the location of the looming stimulus did not have an effect on the probability of the fly displaying the anti-directional response. Simply the presence of the looming stimulus was sufficient, although it has been shown that hyperpolarisation to contralateral looms does occur in a subset of HS cells, but these are only dependent on motor feedback (Fischer & Schnell, 2022), and given the location of the projector not likely to be the primary drivers of the anti-optomotor response (Schnell et al., 2010). Moreover, the addition of the looming stimulus actually reduces the total world motion of the stimulus, and so is likely to have a reduced effect of global motion perception.

The remaining hypothesis is that the looming stimulus results in saccades via a different pathway than the optomotor response, but the feedback that results from the course-changing turns results in the sustained anti-optomotor response that we observe. It has

been shown that regularly repeating stimuli can result in oscillatory signals in HS cells (Fenk et al., 2021). If these cells are prone to oscillatory activity, particularly when gap junctions are inhibited (Ammer et al., 2022), then is it possible that the feedback response into them from the body-saccade, along with the addition of the optomotor stimulus puts the system into a rhythmic oscillatory feedback loop, resulting in saccade after saccade. This could occur with successive motor-related hyperpolarisation and stimulus-related depolarisation, entraining the HS cells into an oscillatory feedback cycle. Since it has been found that (Mano et al., 2023) the anti-optomotor effect is extinguished immediately on switching to a low-contrast stimulus, if a saccade-induced resonant circuit effect is to blame, then this would require a strong stimulus to be maintained.

During both body and head-saccades, world motion is induced, and afferent signals are sent to neutralise the predicted motion that is likely to occur as a result of the movement. This has been shown to be the case for body-saccades (Fenk et al., 2021; Kim et al., 2015), but not yet for head-saccades. The difficulty in recording from the brains of head-free flies is probably the reason for this, but it seems unlikely that such a mechanism would not exist, particularly since they seem to co-occur in our behaviours. This could help explain why anti-directional behaviour was reduced when we fixed the heads of flies, since there would be no afferent feedback from head mechanoreceptors.

A theory predicated on afferent feedback onto LPTCs would however require the HS cells to be involved in anti-directional behaviour. It was observed that silencing the HS cells with a temperature sensitive shibire (shibire^{ts}) did not have a strong effect on the anti-directional response (Mano et al., 2023). Although a small role was shown for the CH cells, which are known to be connected via gap-junctions in *Calliphora* (Haag & Borst, 2005), but are not thought to be in *Drosophila* (Schnell et al., 2010). It has been found however that the HS cells are connected to each-other via innexin-gap junctions, but also to other non-HS

cells, including descending neurons, although the exact identities have not been identified (Ammer et al., 2022; Haag & Borst, 2005; Schnell et al., 2010). Shibire is required to allow vesicle release from the presynaptic membrane, and as such is only able to block chemical transmission from neurons (Shyu et al., 2019). This leaves the possibility that the synaptic shibire^{ts} overexpression brought about by (Mano et al., 2023) was not sufficient to remove all of the HS cell output, since connections via gap-junctions could mediate the response; notable since the only neuron for which blocking synaptic output had an effect on the anti-directional response, is not connected via gap junctions to HS cells. Moreover, it has been previously noted that shibire$_{ts}$ block is only incomplete, and this is probably more severe in graded neurons (Gonzalez-Bellido et al., 2009).

One distinction between optomotor and saccadic behaviour, is that saccadic behaviour involves high-magnitude, high-frequency movements, while optomotor behaviour involves slower, more low-magnitude turning. For the first experiment, we ran a frequency power spectrum analysis on the turning behaviour of flies and found a normal distribution power with respect to frequency, centred around a peak at 2 Hz. Since body-saccades are thought to last approximately 200ms (Williamson et al., 2018), we should see increases in these frequencies when the anti-optomotor response occurs. This is indeed what we found when we observed flies performing both optomotor and anti-optomotor behaviour. This was corroborated when in the looming experiment, flies performing the anti-optomotor response exhibited increases in the higher frequency components of behaviour.

Since the onset of the anti-directional behaviour appears only some time after the looming stimulus appears, we wondered what effect the time-course of the grating onset had on the the start of anti-directional behaviour. In a pilot experiment, we attempted to wait until the fly initiated spontaneous high magnitude turns, and then initiated grating motion after the onset. We found that we could not affect these turns at the smallest latency which would

could initiate, which was 50ms, suggesting that this behaviour is locked in at the point of the turn. In order to test the time-course of these high-magnitude turns which are common in the anti-optomotor response then, we designed an experiment where we presented looming stimuli and grating motion at different offsets. Because we wanted to ensure that the fly's forward walking was the same at different offsets, we chose to perform this in non-walking flies. Surprisingly, up to 300ms before the onset of the turn, the grating motion appears to have no effect on the direction of the response, but any time after this point the fly turns in the anti-optomotor direction.

This findings suggest that for this experiment, for any given anti-optomotor turn, the opto-motor input before that turn must be present for an extended period of around 300 ms. If there is some kind threshold that must be reached to start resonant saccadic behaviour then this might represent the period in which the activity must be ramped up to initiate it. Indeed, tonic rotatory stimulation results in stronger afferent-feedback in HS cells (Fenk et al., 2021). Previously, it has been shown that presenting back-to-front motion prior to presenting a rotating grating can result in instantaneous anti-optomotor behaviour (Mano et al., 2023), it is possible that this stimulus has a similar ramping effect as a high-contrast rotating stimulus in HS cells, although since the stimulus is bilaterally balanced, does not actually result in any behavioural turning itself.

In our looming experiments, we found that overwhelmingly, while the loom did appear to bring about a change in the likelihood of a saccade, it did not affect the direction of the saccade. This is in contrast to other findings where presenting motion alongside a loom results in saccades that occur in response to the loom itself (Fenk et al., 2021). It is possible that there is a kind of push-pull relationship between the rotating stimulus and the looming stimulus, which in our case favoured the grating, but for other stimuli the result is likely to be different. This suggestion is indeed supported by our mixed-latency experiments, which

show an immediate response to the loom, and only later when the grating motion initiates does the response to the grating take over.

If we consider the possibility that the anti-optomotor response is part of the normal set of fly behavioural motifs, the available evidence points in the direction of a course-changing response, with sustained saccadic behaviour. Given the fly turns in the opposite direction to motion it could be considered an avoidance response. One behaviour which seems relevant to this family of behaviours is the insect object avoidance response to translatory optic flow on one side, which they will avoid in order to avoid hitting a wall or an object or avoid getting too close to obstacles (Srinivasan et al., 1998; Tammero & Dickinson., 2002). It is plausible that the circuits responsible for triggering this avoidance response are also involved in generating similar behaviour during full-field, high-contrast, sustained grating motion, leading to the observed behaviour in our experiments. Considering this as a possibility, several questions arise: Why does the response occur during full-field rotation? What is the underlying mechanism that allows the avoidance response to overrule the optomotor response? Why does the response only appear after a certain duration of exposure to motion?

An alternative behavioural cousin of our observed behaviours is the expansion avoidance response. The expansion avoidance response dictates that the fly is aversive to expansions in optic flow, that is optic flow that appears as if it emanating from a single point (Tammero et al., 2004). Aversion to expansion must be partially suppressed during forward motion, since this causes expansion optic flow to appear (Reiser & Dickinson„ 2010). In our current experiments, we have found that we have been unable to trigger the anti-optomotor response during forward motion, therefore it is possible that the circuitry responsible for avoiding expansions to stimuli might be being triggered here. If expansion avoidance arises from a comparison of the overal optic flow between different regions of space, then a comparison between the frontal rotary optic motion which we observe and the absence of any motion

anywhere else would lead the focus of expansion as occuring to the side of the fly (to the right if the motion is anti-clockwise and vice versa). However, evidence against this perspective is the finding that anti-optomotor saccadic behaviour in other contexts has been found even when panoramic stimuli are used (Heisenberg & Wolf., 1979).

Up until very recently, the sustained anti-optomotor responses that we have observed here have not been reported elsewhere, although various other forms of anti-optomotor behaviour have (Tammero et al., 2004; Williamson et al., 2018). Work on the optomotor response has been carried out over many years, so it requires some explanation as to why we are only just now starting to investigate this consistent and easy to study form of behaviour. Firstly, of all anti-optomotor behaviours investigated most, although not all (Censi et al., 2013; Williamson et al., 2018), have been studied in walking flies. We could find the first trackball systems that were used in the virtual reality setups as far as 1973 (Götz & Wenking, 1973), although they have become more popular in recent years with the refinement of the technique. Thus, it could be a focus on the flying optomotor response that has led to the neglect of the responses seen here.

Second, the behaviour is highly contrast-dependent (Mano et al., 2023). The use of projecting or screen displays is common among the studies that have found evidence for the anti-optomotor effect, previously the use of either paper gratings e.g. (Dill et al., 1995), or an LED matrix were used (Haikala et al., 2013), which may have been unable to deliver the same level of contrast on account of backlight leakage in the paper displays, or light dispersion in the off-led region in an LED matrix display.

Finally, the temperature of the fly during development appears to have an effect on whether the anti-optomotor effect appears (Mano et al., 2023). This suggests we should be paying much more attention to this aspect of development. A growing picture is beginning to emerge that the temperature of development can result in changes to both the connectiv-

ity of neurons, and factors that we have been found to influence the optomotor response, such as amount of walking (Kiral et al., 2021). Since many laboratory conditions are kept consistent over decades, it is unclear that the more recent timing of these discoveries could be attributed to any change in the rearing of flies, although the impact of lock-downs for covid-19 may have encouraged labs to reduce the temperature of incubators to increase the life-cycle and reduce the need to enter the labs, although this is only speculation.

1.4.5 Limits of Fly Motion Detection

In addition to our studies on the internal state of the fly and its relation to the optomotor response, we also investigated the limits of the fly's visual motion detection ability. We measured this for both grating speed and grating diameter. Flies have traditionally been thought to be blind to repeating patterns of a wavelength below the half-width of the interommatidial angle (Lawson & Srinivasan, 2020). We found that for walking behaviour on the trackball, this was indeed the case, with flies showing no significant response to moving gratings below 5.2°. However, when we tracked the head-movements of the same flies, it appears that they do turn in the direction of the grating motion, showing they are able to pick up on these patterns. Moreover, we saw that flies slowed down in response to gratings at 5.2° , when they showed no obvious optomotor response.

This may help to explain why some have not been able to find this so-called hyperacute behaviour in fly walking behaviour (Fenk et al., 2022), whilst it has been found with flying behaviour (Juusola et al., 2017; Kemppainen et al., 2022). Although it should be noted that in the walking paper, the flies' heads were fixed in place, which we have found to degrade performance (Fenk et al., 2021). This result shows that the measuring the head-movements might provide a more sensitive, and even simpler measure of testing optomotor behaviour, since it can even be tracked in free-walking flies (Geurten et al., 2014).

Finally, despite finding no overall optomotor effect at 5.2°, we found flies actually had both an optomotor and anti-optomotor response when we aligned the behaviour around the head-saccades of flies. This could suggest that low magnitude optomotor effects at very small gratings are obscured by being composed of both types of behaviour. The transiency of saccades is potentially one reason as to why the average head-movements are a much more concrete measure of optomotor ability, whereas the leg movements which are associated with head-saccades are longer lasting, leading to the anti-optomotor effect obscuring the optomotor effect for ball motion, but not for head-motion. Another reason could be that the bell-curve with respect to temporal frequency for head-movements is wider than it is for body movements. This makes sense with respect to the gain-control hypothesis for the bell-shaped tuning curve, as the head movement – optic flow feedback loop is limited by the fact that the head can only turn to a maximum eccentricity, limiting any runaway positive feedback and relinquishing the need for a gain-limiting system.

As well as looking at the optomotor response on the scale of the very small, we also looked at the response on the scale of the very fast. According to a large body of literature on the subject, both the response of the LPTCs and the optomotor performance is degraded at high temporal frequencies (Duistermars et al., 2012). We had seen some evidence that in bees this performance even turned negative at high temporal frequencies. We found that this was not the case for flies, and the performance simply degraded as the temporal frequency increased. We did find that the optomotor effects remained in place at higher velocities than the slowdown effects, giving further credence to the idea that these two behaviours possess different tuning mechanisms (Creamer et al., 2018). The lack of optomotor response at higher velocities does however contradict the finding that 6.6° gratings do not exhibit optomotor reversal at very high velocities (Kemppainen et al., 2022). Whether extra-stimulus effects such as air movement is the cause of those findings, or whether there is some break-

down in the temporal frequency tuning for very small gratings is unknown. We were unable to test such high speeds with such small gratings in our setup as the resolution of the screen, even running at 360Hz was not sufficient accurately present smooth grating motion.

1.5 Conclusions and Future Directions

Our investigation into sustained anti-optomotor behaviour provides supporting evidence that saccadic behaviour is in some way involved in the response. We suggest that given the previous finding that synaptic inhibition of HS cells is not sufficient to prevent the response, that an investigation into the electrical properties of these cells holds potential, particularly, the various effects of inhibiting the whole cell, the synaptic transmission, and the gap-junctions only. We would suggest that if the response we find is dependent on the electrical properties, then the resultant effects on the behaviour itself could lead to a number of secondary hypotheses about the ways gap junctions are modulated over temperature and age (Augustin et al., 2019). We also suspect that the afferent feedback is in some way involved in the anti-optomotor response, accordingly, blocking LALps-ANContra would be a first candidate for a neuron that may modulate the response (Fujiwara et al., 2022).

The finding of hyperacuity in the head-movement data provides evidence for the dynamic eye hypothesis, accordingly, the investigation of the role of eye-muscle movements on the head-optomotor response is likely to be fruitful since this now appears to be an experimentally modifiable component in active vision (Fenk et al., 2022).

2 Structural Evidence for Binocularity in *Drosophila*

2.1 Introduction

2.1.1 Evidence for Stereopsis in *Drosophila*

It has always been assumed that *Drosophila* cannot perform stereopsis because of immutable characteristics of their visual system. First, they should have only a small degree of binocular overlap, such that they would have to have fairly good optical resolution to take advantage of it. Secondly, they should have fairly bad visual resolution. Recent evidence suggests that neither of these assumptions may be true; the discovery of *Drosophila* microsaccadic active vision rebuts the static eye paradigm. If this is true, the best way to model the resolution of a fly eye is not in spatial coordinates (the acceptance angles and size of photoreceptors) but as a function of space and time (dynamically narrowing and widening acceptance angles as photoreceptors of different sizes are moving ultrafast photomechanically).

The first assumption also requires a reassessment in light of recent evidence. First discovered in *Drosophila* in 1991 (Franceschini et al., 1991), *Drosophila* eye muscles appear to displace the entire retina by vergence rotation, increasing the binocular range (Fenk et al., 2022; Franceschini et al., 1991). It has been argued that these vergence movements allow *Drosophila* to perform stereopsis, since they appear to occur more frequently when flies perform a gap-crossing task, which would require them to estimate how far away they are from a surface (Fenk et al., 2022); although it has been shown elsewhere that binocular occlusion has no effect on the performance of flies in this task (Pick & Strauss, 2005). The first assumption is also countered by evidence that microsaccadic contraction increases the binocular range of flies even further (Kemppainen et al., 2022), this time as an intrinsic part of the phototransduction pathway (Hardie & Franze, 2012). The second assumption, that fly

vision is necessarily low resolution, has also been countered evidence, both in the literature (Juusola et al., 2017; Kemppainen et al., 2022) and in chapter two of this thesis. Without these two assumptions, it appears that the *Drosophila* have the functional and anatomical capacity to perform stereopsis. Moreover, since both eye-muscles and photoreceptor microsaccades are components of active vision, it is likely that any stereopsis that is to be observed will arise from the correlating the positions of objects on each retina with the self-induced motion - from muscle movements and microsaccades - which could then be used to extract the depth information. In accordance with this view, flies have been shown to behave differently to an equal-diameter 3D pin, than a 2D dot (Kemppainen et al., 2022), and that this feature is abolished when one eye is occluded.

Suppose it is the case that insects such as *Drosophila* can use the binocular disparity between the two eyes to extract depth. In that case, we should expect to find evidence of neural integration between the left and right visual areas to allow binocular information to integrate and enable this computation to happen. This functionality should be integral to the brain's structure and observable in connectome datasets such as the Hemibrain Dataset (Scheffer et al., 2020). In order to reduce the search space for where in the brain this structural evidence might lie, we looked at the the only other insect in which binocular disparity has been demonstrated: the praying mantis. First demonstrated conclusively in 1983 (Rossel, 1983), mantids employ a binocular overlap of 70 ° (Rossel, 1983) to perform stereopsis.

2.1.2 Mantis Vs Fruit Fly: Differences in Visual Anatomy

Mantids are visual predators, and as such have extremely good vision. Compared to the fruit fly's roughly 800 ommatidia (Ready et al., 1976), mantids have 9000 (Rossel, 1979). Around the frontal region of the eye the interommatidial angle is less than 1 degree (Rossel, 1979). With such different visual anatomies, we might expect the visual systems to be

organised somewhat differently between the two animals. Indeed, the mantis optic lobes are considerably larger than the central brain (Rosner et al., 2017), an extreme ratio which is not shared by the fruit fly. In the early visual system, the anatomical organisation between the fruit fly and mantis is similar. Photoreceptors input to the lamina, which then passes input to the medulla. In the mantis, the lobula complex is segregated into 5 lobes: the outer 2 lobes, the anterior lobe, the dorsal lobe and the slope (Rosner et al., 2017), whereas in the fruit fly there is only the lobula and lobula plate (Shinomiya et al., 2019). It has been suggested that the outer lobes are similar to the lobula in the fruit fly, and that either the anterior or dorsal lobes in the mantis is homologous to the lobula plate (Rosner et al., 2017). For the slope there is no obvious fruit fly counterpart.

Therefore, at the broad anatomical level, there is no evidence to suggest that there are distinctions between *Drosophila* and Mantis that would prevent *Drosophila* from being able to perform stereopsis, and the regions of Mantis that are not homologous with *Drosophila* have not yet shown to be involved in stereopsis. To date, four classes of mantis neuron involved in computing stereopsis have been identified (Rosner et al., 2019). These are: the Tangential Optic Lobe Projection Neuron (TAOpro), the Columnar Comissural Neuron (CoCOM), the Tangential Centrifugal Neuron of the Anterior Lobe (TAcen), and the Tangential Centrifugal Neuron of the Medulla (TMEcen)

2.1.3 TAOpro

This neuron widely innervates both outer lobes unilaterally, as well as sending neurites to the distal portion of the anterior lobe (Rosner et al., 2019). Interestingly, it innervates regions of the lobe outside which have receptive fields outside the binocular range, so it is unlikely to solely be involved in stereopsis. (Rosner et al., 2019) show that it responds to monocular, ipsilateral cues, as well as binocular disparity. In the mantis, the disparity corresponds to

about 50 mm away from the animal (Rosner et al., 2019). For comparison, 25 mm is the ideal strike distance for a mantis (Nityananda et al., 2016). If there is a *Drosophila*-counterpart to this neuron, it would widely innervate the lobula or ventral part of the medulla, and terminate deep in the posterior slope (Rosner et al., 2019).

2.1.4 TAcen & TMEcen

These neurons provide feedback from the ipsilateral (TAcen) or both ipsi- and contralateral (TMEcen) central brain to the anterior lobe (TAcen) or medulla (TMEcen) (Rosner et al., 2019). Response properties of these neurons suggest their preferred disparity is around 100mm or more away, and so much further than the strike distance for a prey item. Since these neurons do not select for 3D distances within the striking range. It has been suggested they could be used to provide feedback about which parts of the visual field likely correspond to background based on their visual disparity (Rosner et al., 2019). Many neurons in the *Drosophila* brain transmit information from the medulla and lobula plate to the central brain.

2.1.5 CoCOM

The CoCOM neuron takes its namesake from the fact that it projects along the commissure and as such is the only neuron found in the mantis (Rosner et al., 2019) that directly transfers information between the optic lobes. Within the outer lobes, CoCOM expands dendritically along the anterior-posterior axis, but very narrowly along the dorsoventral. As such, it has been found to have very small receptive fields (Yamawaki, 2019).

The CoCOM neuron has an obvious counterpart in *Drosophila*: Lobula Columnar 14 (LC14) (Rosner et al., 2019). LC14 cells (also known as Dorsal Cluster Neurons or DCNs) were first discovered in 2002 (Morales et al., 2002). LC14s extend from one lobula to the contralateral lobula, and there is also a subset: LC14b, that has dendrites in the medulla (Morales et al.,

2002; Otsuna & Ito, 2006). Functionally, LC14s have been shown to respond to small moving objects (Fenk et al., 2022), potentially as a result of the receptive field size (Yamawaki, 2019). Most, but not all, of the CoCom neurons have binocular response characteristics (Rosner et al., 2019). Considering the available evidence, it is likely that CoCom neurons contribute to the integration of binocular information. While direct interhemispheric transfer is not essential for a stereoptic neuron, its presence is likely a revealing characteristic, as observed in the Mantis. Most neurons likely serve multiple functions within the brain, and the same is likely true for LC14 neurons. Among their potential roles, involvement in stereopsis is plausible. The anatomical positioning of CoCom within the Mantis visual system indicates a disparity between vertebrate and insect binocularity. In vertebrates, the optic chiasm ensures neural signals are binocular upon arrival at the occipital lobe. Conversely, in insects, the initial stages of visual processing seem to be monocular, progressively integrating towards more central areas. Whether this discrepancy arises due to anatomical circumstance or represents a general coding mechanism remains unknown.

Supporting this view, the LC14s have also been investigated for their role in performance on the Buridan assay. There is some degree of anatomical variability in the left-right asymmetry of the LC14s. It has been found that the number of LC14s on each side of the brain is variable between different individuals, although the wiring patterns are robust in the face of this variability (Langen et al., 2013). This variability arises from the number of LC14s that end up becoming LC14b cells, which is itself a result of the notch signalling (Langen et al., 2013). It has been observed that the variability in LC14 asymmetry is related to the behavioural variability in the Buridan assay (Linneweber et al., 2020). Flies normally exhibit some degree of variation in how closely they walk between the opposing stripes on this assay, with some flies walking almost exactly between the stripes, and others walking in a much more roundabout fashion. This variability appears to be intrinsic to each fly (Buchanan et al., 2015;

Linneweber et al., 2020), although non-heritable. (Linneweber et al., 2020) finds that the asymmetry of LC14b cells is inversely proportional to the variability of performance on the Buridan assay. Since tight performance on the Buridan assay will necessarily require the black bar to be maintained in the binocular region of the fly's field of view it lends credence to the idea that the LC14 neurons are tuned to processing binocular visual information.

Moreover, it has been found that inhibiting the LC14 cells increases the absolute deviation in behavioural response between flies, resulting in very poor performance on the Buridan assay (Linneweber et al., 2020). This effect is rescued by inhibiting the LC14s on only one side of the brain, monocular deprivation also rescued the effect. It further lends to the conclusion that asymmetry is baked into the system, since asymmetry is not a property of all neurons. In addition, there is a substantial variability in the amount of asymmetry observed between individuals (Linneweber et al., 2020). Variability, in itself, is another characteristic of fly behaviour and neural anatomy (Buchanan et al., 2015).

It is unknown how either variability, or asymmetry would support a role for LC14 stereopsis, but both findings should invite an abundance of caution for trying to extrapolate out results from an analysis of the Hemibrain. This is because the hemibrain contains only one side of the fly brain, and it is the connectome of only one fly. Taking this limitation in mind, we will now turn to investigating the anatomical structure and connections of the LC14 cells which may help to shed light on their role for fly stereopsis.

2.2 Methods & Results

The LC14 cells are likely to be important in insect stereopsis, as they are structurally suited to the transfer of binocular information that is needed to carry out that task. We investigated the structural and anatomical properties of the LC14 cells, and we believe this evidence gives more credence to the idea that they are involved in the task. The results of this analysis are shown below.

2.2.1 FlyLight Reconstruction

Binocular stereopsis is likely to involve the comparison between different parts of the binocular visual field at the same altitudinal visual receptive field, and at varying azimuthal receptive fields. The lobula is retinotopically organised (Shinomiya et al., 2019). If the LC14 cells carry out stereopsis, they are likely to need to project in a broadly retinotopic pattern, that is they need to project from one region of the lobula, to the same region on the contralateral side.

In order to assess the pattern of projection we selected Multi-Color Flip Out (MCFO) images from the flylight database (Jenett et al., 2012) that were identified as containing possible LC14 cells in the NeuronBridge tool (Clements et al., 2022). We manually filtered out out datasets with misexpression and collated the data images. The images in FlyLight are registered to the same brain volume and therefore allow for valid comparisons. These are shown in the figure below.

In the anterior-posterior axis, the LC14 cells project approximately retinotopically. Innervations that LC14s make on the anterior part of the lobula correspond to anterior innervations on the contralateral side and vice versa for the posterior section. On the ventral-dorsal axis, the neurons also do not appear undergo any significant retinotopic distortion as they travel across the hemispheres (figure 35a). Thus it is likely that the LC14s transmit information be-

tween the two lobulae in a roughly retinotopic pattern. Given the noise and low resolution of the expression data, the exact pattern of projection is not observable, and there may be fine-grade distortions present in the projection. In fact, some distortion on the azimuthal axis is expected, although that cannot be ascertained from this dataset. Approximate retinotopicity is a feature shared by the CoCOM neurons in the mantis (Rosner et al., 2019).

2.2.2 Hemibrain Analysis

As a model organism, the brain of the fruit fly provides a much easier basis to investigate stereopsis when compared to the mantis. One of the aspects of this is that we do not have to infer architecture from the activity of the neurons, since we have direct access to the connectome. The hemibrain connectome (Scheffer et al., 2020) is a reconstruction of the connectome of a single female fly, extending from just past the central brain, to most of the lobula. This means that it sheds light on the connectomics of the central areas like the mushroom body and ellipsoid body very well, but its extension into visual areas is less comprehensive. Nonetheless, it does contain large parts of the lobula, and as such contains a set of neurons identified as LC14 neurons, although obviously only on one side (the right side) of the brain.

Inputs and Outputs of the LC14 Cells Neurons identified in the Hemibrain as having inputs to the LC14 neurons are shown (figure 35b). By far the largest class of neuron to input to LC14 was that of the unknown class (figure 35c). Existence of unknown neuron types is common to find within the Hemibrain dataset, but is particularly a problem around the edges of the sectioned brain (Scheffer et al., 2020), where there are often only tiny fragments of neurons which are difficult to identify. Keeping this in mind, we can still gain insight from what is left over. Disregarding the connections for which the input type is unknown, each LC14 post-synapse was counted along with the neuron class innervating the cell, providing

the absolute amount of input to the LC14 cells for each class of neuron (Figure 35d).

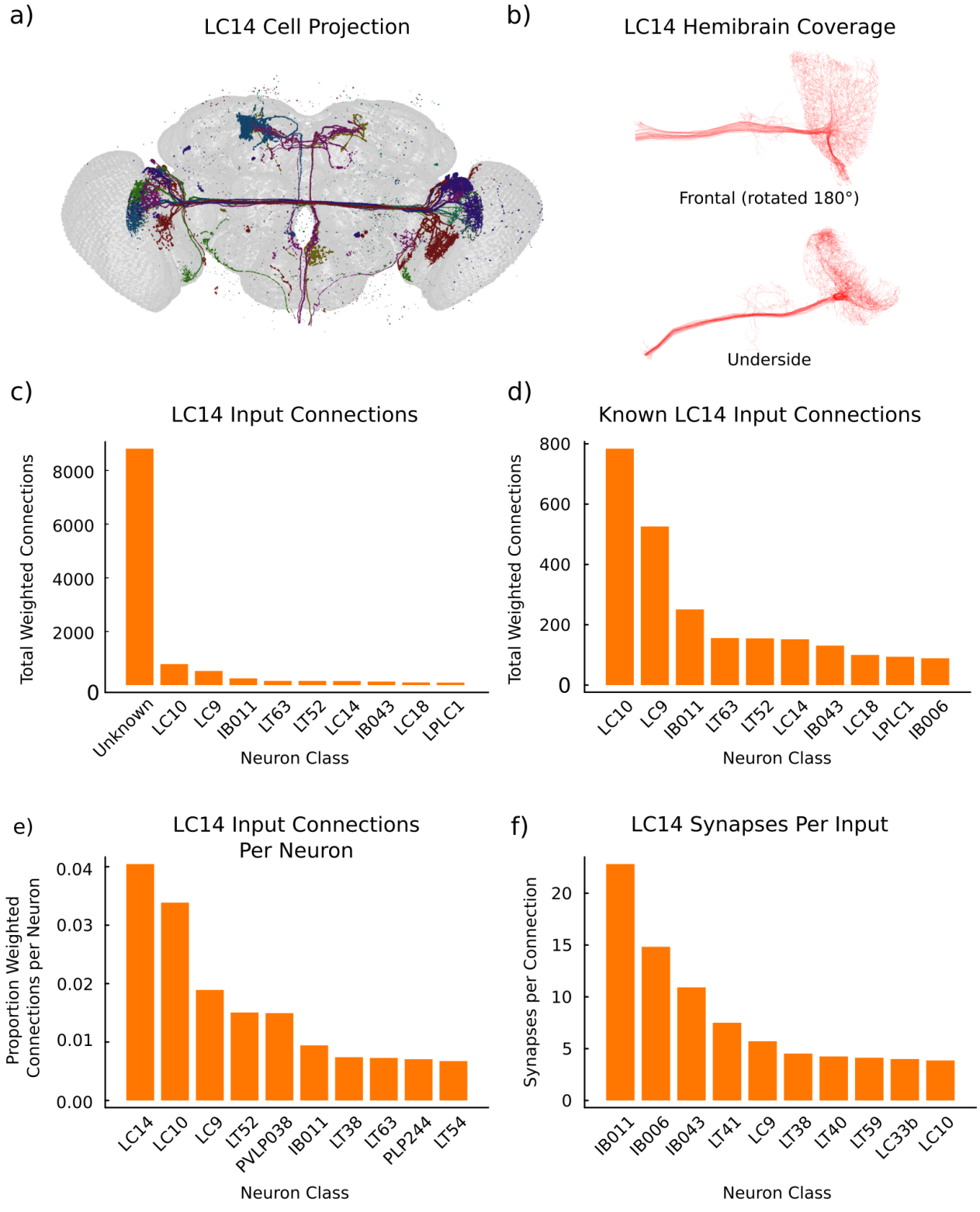

Figure 35: Input connections to LC14 cells.
(a) MCFO images collated showing individual LC14 projections.
(b) LC14 skeletons present within the Hemibrain dataset.
(c) Overall weighted inputs to LC14 cells by neuron class
(d) Overall weighted inputs to LC14 cells by neuron class, ignoring unknown neurons.
(e) The proportion of inputs per LC14 neuron by each neuron class.
(f) The number of synapses made per connection by neuron class.

The largest 3 input classes are LC10, LC9, and IB011. LC9 and LC10 are visual projection neurons like LC14, taking input from the lobula and projecting to visual glomeruli like AOTu (Wu et al., 2016). IB011 is a neuron that extends massively into the ipsi- and contra-lateral central brain. It is a major output of SMP156, another cross-hemispheric neuron, and itself an output of the sexually dimorphic ADN neuron (Nojima et al., 2021). Because all the inputs are pooled together over all of the LC14 cells, this method could give more weight to neuron classes that have very strong inputs to some LC14 neurons, but otherwise do not have strong inputs to others.

An alternative approach is to take each LC14 neuron, measure the proportion of input classes for the individual neurons and take the average over all the LC14 neurons. This method ranks LC14 inputs to LC14 neurons higher, suggesting there are many rather weak inputs between LC14 cells (figure 35e). The same method also ranks IB011 neurons lower, suggesting that there are a few large inputs from IB011 neurons, but these are not well distributed among the LC14 cells, indeed looking at the number of synapses pun connection, IB011 cells rank the highest (Figure 35f). LC10 and LC9 cells retain most of their same ranking, suggesting that their inputs are both well distributed and strong.

Turning to the outputs of LC14 cells, the vast majority of LC14 pre-synapses do not have an identifiable class of postsynaptic partner (figure 36a). The connections that are identifiable suggest strong outputs to PS103, DNp26, and PS132 (figure 36b). The PS neurons are situated in the posterior slope, whilst the DNp26 is a downstream neuron. These outputs suggest a more downstream role compared to other LC neurons, which primarily output in visual glomeruli.

This difference is almost certainly because the major output of LC14 neurons is in the contralateral lobula, not present in the Hemibrain dataset, although there are still likely to neurons in the current data that project from the contralateral side. Similar to the input neurons,

the existence of strong but not-well-distributed connections is likely to affect the rankings, since the synapses per output of the PS103 and DNp26 are the highest ranked among the output types (figure 36d). Indeed, looking again at average distribution of output classes, averaged over every individual neuron, LC14 outputs represent the strongest output class, followed by LC10 and LC6 neurons (figure 36a).

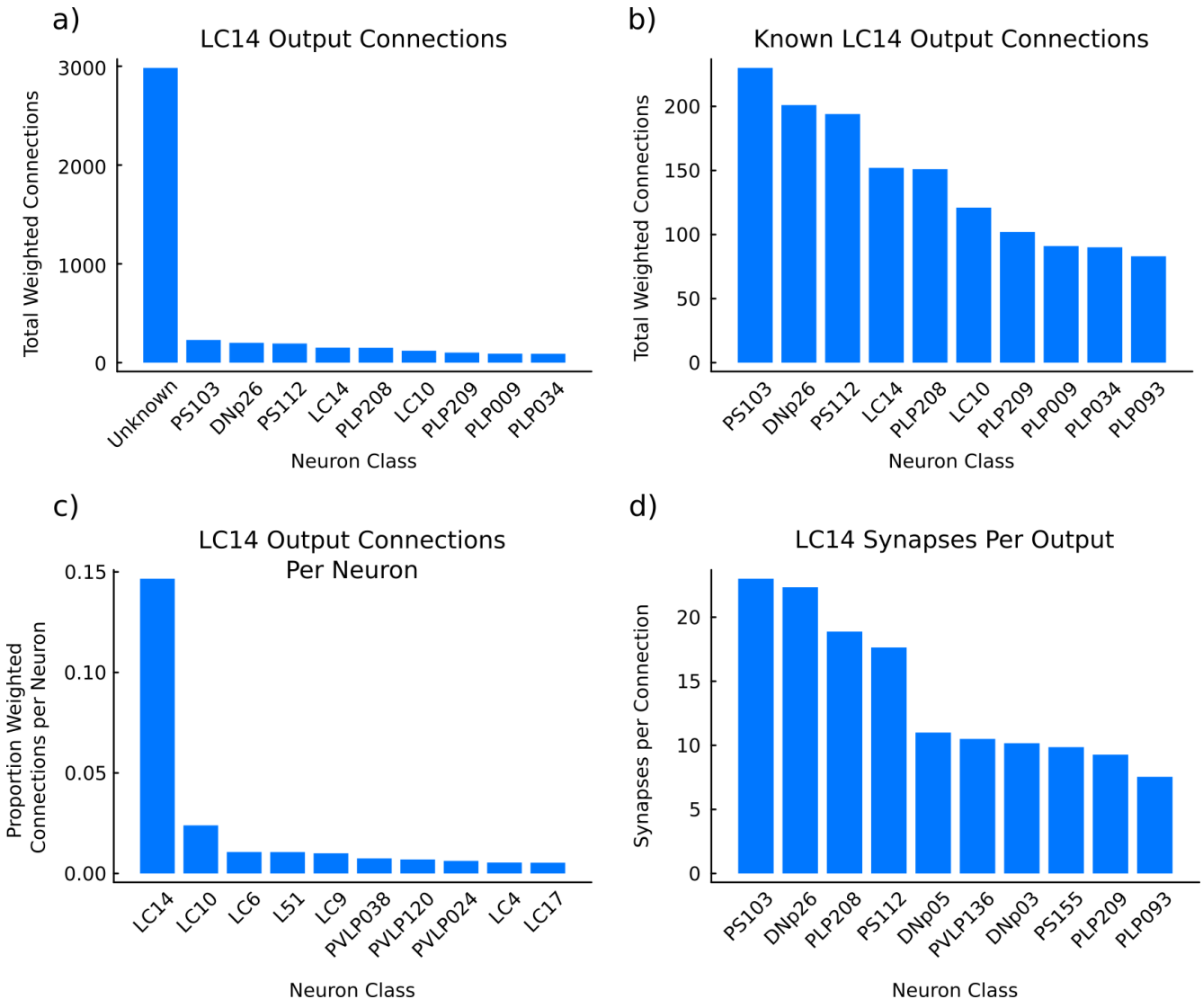

Figure 36: Outputs of LC14 cells.
(a) Overall weighted outputs to LC14 cells by neuron class
(b) Overall weighted outputs to LC14 cells by neuron class, ignoring unknown neurons.
(c) The proportion of outputs per LC14 neuron by each neuron class.
(d) The number of synapses made per output connection by neuron class.

There are Two Subclasses of LC14 Neuron We represented the input connections to LC14 cells, and LC14 cells themselves as a directed-weighted graph containing the input

connections to LC14 cells (figure 37a). Subjectively, the graph appears to diverge into to halves, both of which were highly connected within the half but sparsely connected in-between. Two quantify this subjective appearance, we ran a multi-level graph partitioning algorithm (Karypis & Kumar, 1998) on the graph of the connections of upstream cells. This approach successively coarsens the graph to partition until it is computationally viable to compute the partition. After this the simplified graph is projected back into its original state. The automatically partitioned graph recreates the qualitative impression for which nodes correspond to which group (figure 37b). To find out whether these subclasses represented an anatomical distinction, we looked at the properties of the LC14 cells within the partitioned groups.

The graph partition mirrors an anatomical distinction in the anterior-posterior direction. With one subclass of neuron innervating the medial lobula (LC14-m) and one innervating the more distal lobula (LC14-d) (figure 37c). This anatomical distinction is also manifested in the input types to the two different subgroups. We looked at the main inputs to LC14 neurons (LC10 and LC9), we found that the LC14-d cells were more highly connected to LC10, and LC14-m cells were more highly connected to LC9 cells (figure 37d). LPLC1, a neuron involved in collision avoidance (Tanaka & Clark, 2022) was the only other neuron that showed a large disparity between the group 1 and 2 connections. Since the two groups are anatomically distinct, one might question whether the connectivity distinction arises purely from this, or whether there are other developmental mechanisms to determine which neuron each subclass chose to partner with. Neither the LC10 nor LC9 neurons are anatomically segregated on the anterior-posterior axis, and so this is unlikely to be the cause of the distinction.

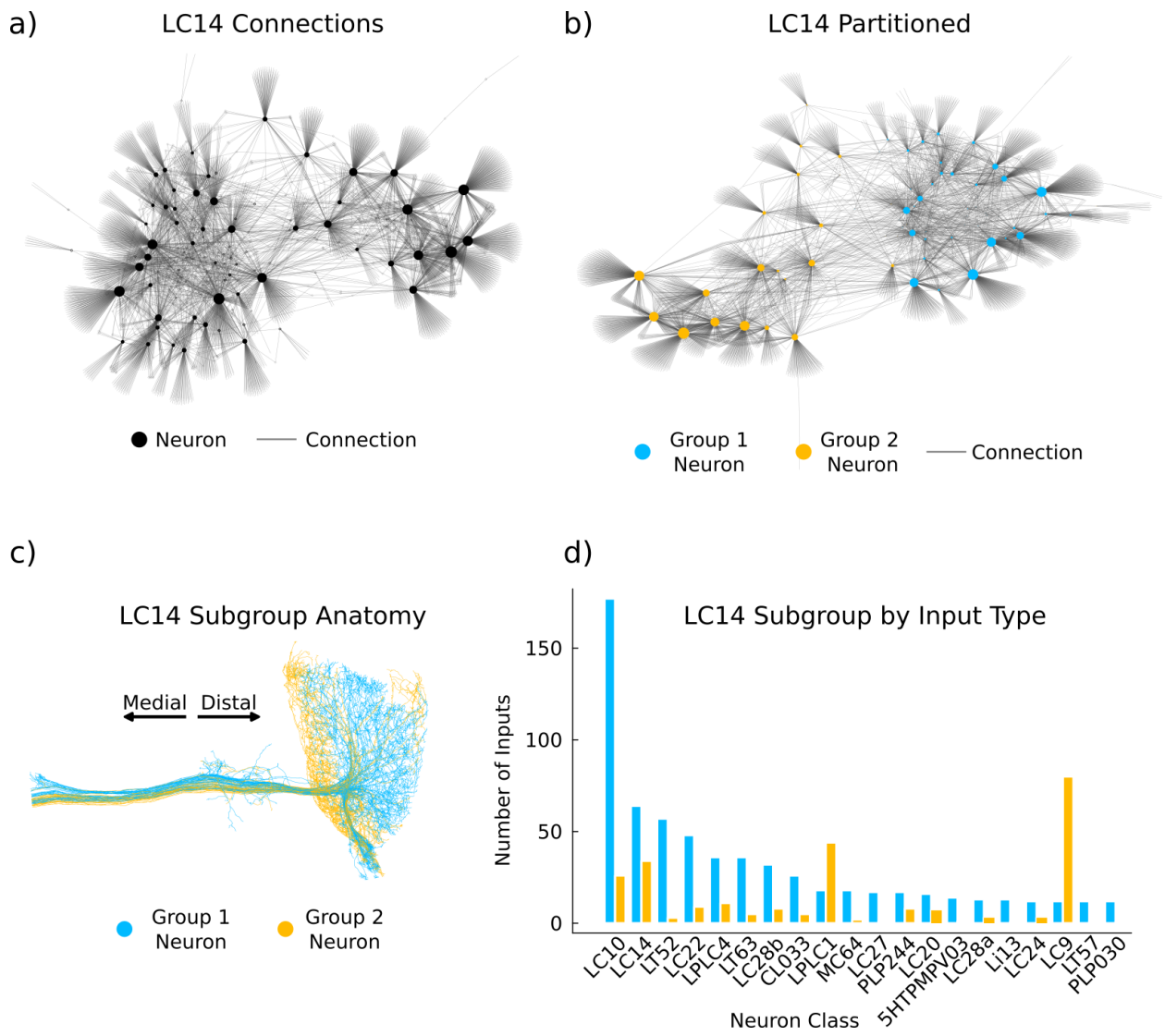

Figure 37: LC14 neurons, segregated using an automated method.
(a) The graph of LC14 neurons and their inputs. Cells shown in black, size proportionate to their input- degree.
(b) LC14 neurons and inputs, colours indicate the identified neuron group each cell belongs to. The overall appearance differs from a) because graphs are plotted using a semi-random method.
(c) Anatomy of the group 1 and 2 LC14 neurons. Group 1 is located more distally than group 2.
(d) The proportion of LC14 input by neuron class and identified LC14 subgroup. Group 1 neurons receive disproportionately more input from LC10, whilst group 2 neurons receive more from LC9 and LPLC1.

LC14 Self-Connections One of the key-connectivity motifs identified in the mantis was the lateral-inhibition of CoCOM neurons by CoCOM neurons projecting in the opposite direction (Rosner et al., 2019). If the LC14 cells are neural correlates of the CoCOM neurons, we would expect to see a similar motif appearing here. Particularly, we would expect to see high levels of connectivity between LC14 neurons, we would expect those connections to

come from the contralateral LC14 neurons, and we would expect those contralateral neurons to have receptive fields in areas surrounding the ipsilateral LC14 receptive field but on the contralateral side. LC14 self-connectivity is easily obtainable from the hemibrain connectome, whether the connections come from contralateral LC14s is more difficult, but still possible to obtain from the hemibrain, but the contralateral receptive field innervation is not available from hemibrain dataset.

LC14 neurons take input from the lobula (figure 38a), and they output information primarily to the lobula itself, but also to the posterior lateral protocerebrum and other central areas (Figure 38c). Within the lobula itself, output is transmitted to the superficial portions, but is seemingly concentrated at the upper anterior and lower posterior regions - not a property shared by the mantis CoCOM neurons (figure 38d).

The LC14 neurons do not appear to connect to each-other as strongly as they connect to some other LC neurons, however, these self-connections do still make up the fourth largest input to themselves. Moreover, while the strength of individual connections are not strong, they do appear to be fairly ubiquitous with most LC14 neurons connecting to at least one other LC14 neuron (figure 38e). We found that the primary output area of LC14-LC14 connections appears to be in the commissure itself, with virtually no LC14-LC14 output within the lobula itself (figure 38f). There are two explanations for this connectivity regime. The first could be that the commissure-connections arise from developmentally overactive synapse formation between cells when they are brought within close proximity in the commissure. LC14 self-wiring might therefore be coincidental to function they play within the brain. Alternatively, if the axons are retinotopically organised, this could be an anatomically-driven circuit mechanism to allow proximal LC14s to interact with each-other in-transit, either via the synapses, or even by some other extra-synaptic mechanism such as gap junctions (Ammer et al., 2022), or via ephaptic effect (Zhang et al., 2019). In order to answer this question, we

investigated whether LC14 cells retain their retinotopicity in transit to the contralateral lobula.

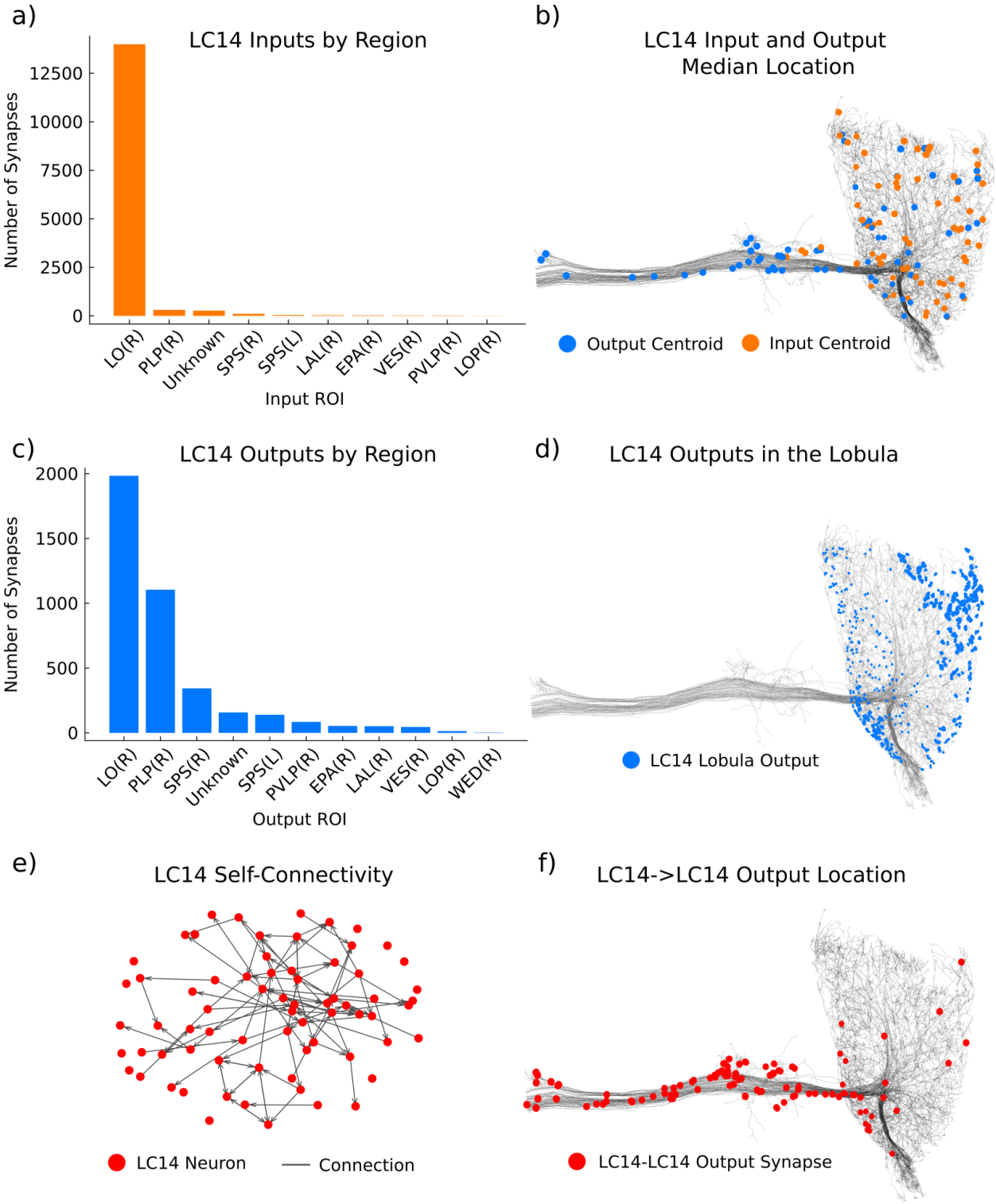

Figure 38: LC14 to LC14 connectivity motifs.
(a) LC14 inputs by region, most being from the lobula.
(b) Locations of the average inputs and outputs for each LC14 neuron.
(c) Output locations of LC14 neurons, most output to the lobula; but also to the PLP and SPS.
(d) Locations of output synapsis within the lobula, showing most occurring at the ventral-distal and dorsal- medial quadrants.
(e) LC14 self-connectivity graph. Most LC14s connect to at least one other LC14 neuron.
(f) Output locations of the LC14 synapses, most occurring within the commissure.

Retinotopic Consistency of the LC14 Cells Some lobula columnar neurons retain their topography along their projection neuropil, such as the LC9 and LC10 neurons (Wu et al., 2016). In order to ascertain whether this is the case for LC14 cells, we consulted the hemibrain connectome. For each LC14 neuron in the dataset, we defined the input centroid of that neuron as being the median 3D location of all the post-synaptic densities (i.e. inputs), regardless of whether the pre-synaptic cell types were known. This approach was chosen since the LC14 arborisations are fairly local within the lobula, and this definition places the centroids roughly in the centre of these arborisations. We then sectioned the LC14 cell skeletons into planes with the normal of each plane being the average vector along the the commissure (figure 39a). This approach allows us to see how the organisation of LC14 cells changes as they travel through the commissure. Where there were two or more segments of the skeleton within the plane being looked at, the segment closest to the centre of the median location of all the other segments was chosen to represent that cell. Finally, we sought a way to test whether the topology of the LC14 neurons is conserved within the commissure. We defined each LC14 neuron as having *n* neighbouring LC14 neurons, which were the set of emphn cells with the closest centroids or segments. We tested how the collection of these neighbourhoods changed as the neurons project along the commissure as a measure of retinotopicity.

We compared the neighbourhoods of centroids in the lobula, to the neighbourhoods of skeleton segments in the commissure, and observed how these neighbourhoods changed as we moved along the commissure (Figure 39b-c). This comparison shows that there is an initial drop in retinotopicity, which is most likely to do with the method, since these initial segments contain non-commissure components such as the cell bodies (figure 39b-c). After this drop, some retinotopicity is regained, with on average each neuron segment sharing about 13 neurons, from its original 30 neighbours, which is more than would be expected from an en-

tirely random distribution of axons, but well within the 95% confidence interval (which would be 16 shared neighbours).

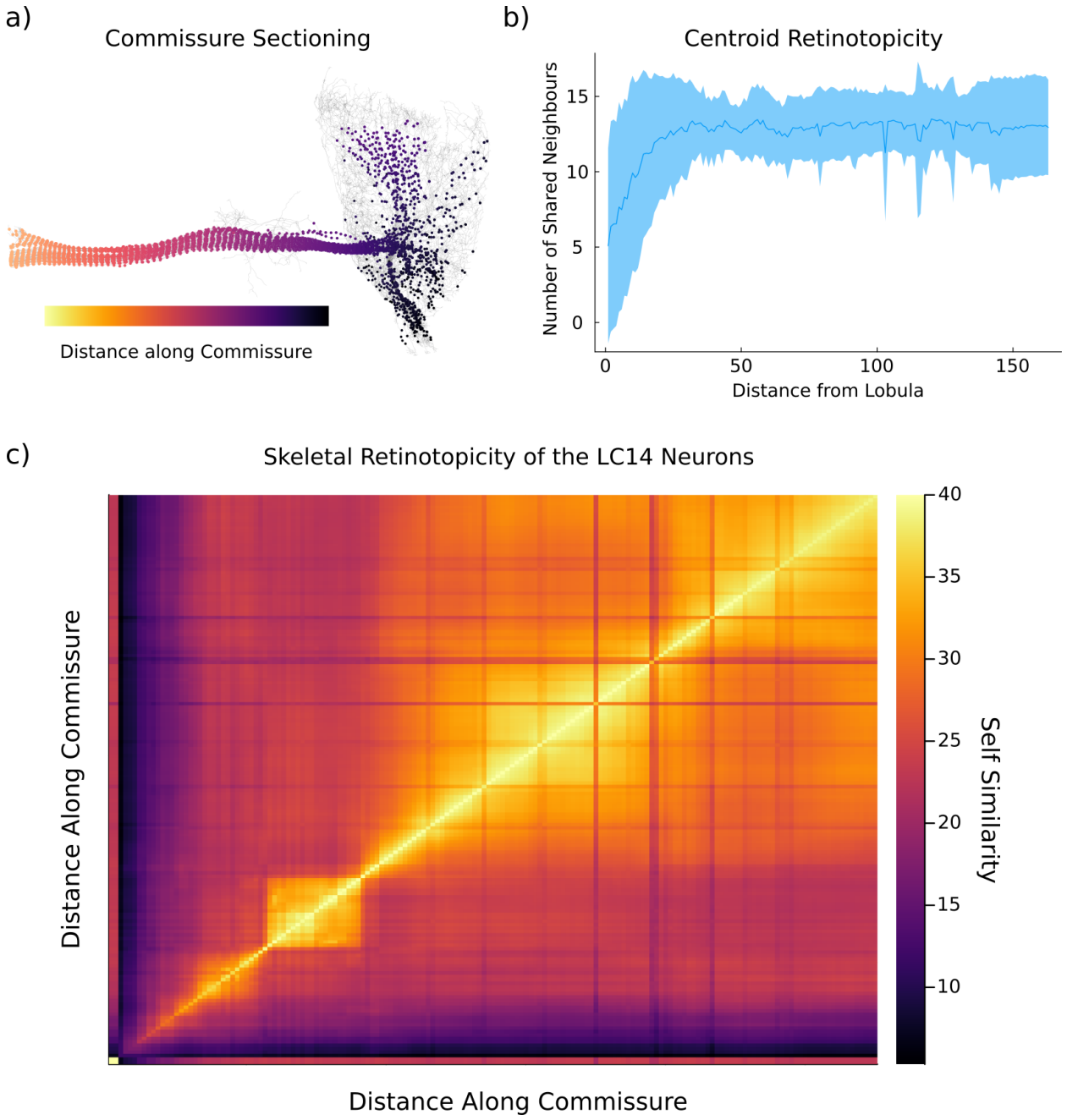

Figure 39: Retinotopicity of the LC14 Neurons.
(a) Schematic showing how sections along the commissure are sliced to determine the neighbourhood of closest neurons within that slice.
(b) Retinotopicity along the commissure, compared to the locations of input centroids of LC14 cells. Retinotopicity is initially low, likely because of interference of skeletons going towards the cell body.
(c) Retinotopicity between each commissure point, showing zones where the topology is conserved

2.3 Discussion

2.3.1 Inputs to LC14 Neurons

The known input to LC14 cells comes from LC10, LC9, and IB011. LC9 and LC10 are both known to be involved in courtship behaviour including mate pursuit (Bidaye et al., 2020), and correct wing extension orientation of males during the courtship process (Ribeiro et al., 2018). IB011, though not well studied, has been proposed to be important for female orientation in males (Nojima et al., 2021), and its second-order connection to a sexually dimorphic neuron again suggests a role in mating behaviour (Nojima et al., 2021). If many of the inputs to LC14 are found to be courtship-adjacent, does this suggest a role in courtship behaviour, or could this be a artefact of the reporting of neuron purpose within the literature. As a counter-example, we repeated the analysis for an LC neuron known not to be involved in the courtship pathway. Inputs to LC13 were analysed, and beside from the connections from classes than were unknown and self-self connections, the 3 most common neuron types were LC11, Li19, and LC20. LC11 has been implicated in object detection (Keleş & Frye, 2017), and the others have been otherwise uncharacterised. This suggests that finding neurons highly implicated in sexual behaviours is not the norm for the LC neurons in general.

How far can the Hemibrain dataset be trusted? Initial reports of the segmentation approach are likely to report accurate skeleton and connectivity data, with low levels of misidentification (Scheffer et al., 2020). However, this may degrade fairly quickly when extending towards the edges of the known map as we are in this case. Indeed, the large number of unknown neurons should be some cause for concern, particularly as these are likely to be biased in the direction of not including identities for neurons that project from more distal areas, since these are the neurons without full cell bodies identified within the connectome, this however has not prevented useful information from being extract from even these most distal regions

of hemibrain coverage (Tanaka & Clark, 2022). This being the case, it is also likely that the actual number of cells for which the cell class is unknown is vastly overestimated, since most of these cells are likely to come from partial segments of cells, meaning that many cells will be double-counted.

As such this data should likely be interpreted as a map of the connections between LC14 and the central brain, rather than a comprehensive map of all the connections to LC14. Indeed, the other major connectome dataset, FAFB (Zheng et al., 2018) does not show such a strong connection between LC10 and LC14 cells (G. A. Linneweber, personal communication). Putting aside the potentially peripheral location of the LC14 cells, in general the different datasets have their advantages and disadvantages. In cases where synapses might be identified along particularly tortuous dendrites the FAFB dataset probably skews more accurate, as it is constructed manually. Others have pointed out that the automated nature of the hemibrain construction allows particularly numerous or dense connectivity patterns to be more accurate in the hemibrain dataset. This general agreement in accuracy, however, is probably superseded however by the fact that the location of the LC14 cells is on the precipice of the hemibrain dataset, whereas the FAFB dataset contains fully-formed cells.

2.3.2 There are Two Subclasses of LC14 Neuron

We found that the connectivity of the LC14 neurons segregates the cells into posterior and an anterior subclasses. Furthermore, these subclasses are differentially innervated by LC9 and LC10 neurons, and are anatomically distinct. The striking differences between these cell types, which are sub-classed based only on their connectivity, demonstrates the general validity of this method for producing functional distinctions between cell-classes in an unbiased way, which could be furthermore be combined with transcriptional relationships (H. Li

et al., 2022) to partition neurons into subclasses with even greater accuracy.

What is the nature of the distinction between the two LC14 subclasses? The anatomical distinction suggests the LC14-d cells innervate the parts of the lobula more focussed on the anterior, binocular region of visual space, whilst the LC14-m cells are focussed on the posterior region of visual space (Shinomiya et al., 2019). This will probably interact with our finding that LC14-d receives primarily inputs from LC10, and LC14-m from LC9. The LC10 inputs suggest a role for these cells in courtship behaviour (Ribeiro et al., 2018) which might explain why they innervate the LC14 neurons in a region representing the frontal region of the visual field. Although, it may well be the case that the LC10 cells are in general disposed to track moving objects and their input to LC14 is for a role broader than courtship alone. The anatomical location of LC14-d is interesting, since it covers a posterior region of the visual field, it is unclear why this would require binocular integration.

One possibility is that these two subclasses of cells are actually the subclasses LC14 and LC14-b, which are not distinguished within the hemibrain connectome. It has been noted that the LC14-b cells (alternative M-DCNs) terminate only in the posterior medulla (Linneweber et al., 2020), which represents the anterior region of visual space (Shinomiya et al., 2019). Since the LC14-d cells innervate the lobula within this same region of the field of view, this would suggest that the LC14-d cells we have identified are actually the LC14b cells, and the LC14-m cells are the other LC14 cells or L-DCNs. The L-DCNs, have not been as well studied as the M-DCNs, and their role is essentially unknown.

2.3.3 LC14 Self-Connections

LC14-LC14 synapses were identified as very common for most of the LC14 cells studied, a property which would lend themselves well to the performance of stereopsis, as has been proposed in the mantis. Particularly striking was the fact that where these connections

occur, they almost always occur in the commissure itself. This observation lent itself to the hypothesis that if retinotopic consistency is maintained within the commissure as it is with some LC cells, then these commissural synapses could represent a mechanism by which LC14 neurons transfer information between similar receptive fields. For this reason, we decided to test whether this retinotopicity is maintained in transit.

2.3.4 Retinotopic Consistency of the LC14 Cells

We found that the retinotopicity of neurons is not fully conserved in transit through the brain in LC14 cells. Firstly, this raises the question of how, in the developing brain, the growth cones reform to project to roughly the same areas of the lobula as we found when we looked at the FlyLight reconstruction. Secondly, the lack of topographic consistency suggests that any mechanism where the LC14 self-self interaction relies on anatomical proximity, does not exist, or at least requires an explanation for why this interaction is not between cells with neighbouring receptive fields. This reasoning raises the possibility that the microcircuitry of the LC14 cells does not match that of the CoCOM neuron, bringing into question the hypothesis that the LC14 cells carry out the same role, or at least the same role via the same purported mechanism. However, as noted at the beginning, we currently only have access to one half of the LC14 neurons, and it is quite plausible that the majority of self-self connections are made between LC14 neurons at the contralateral lobula. If this is true, then this would suggest that the number of LC14-LC14 connections made in the commissure are insignificant in with respect to the neural mechanism.

2.4 Conclusions and Future Directions

We set out to conduct this analysis into the bilateral connections of the *Drosophila* optic lobes to determine the anatomical similarity to those depth-sensitive neurons of the mantis. The

LC14 cells, display some similarities in their overall anatomical arrangement, projecting to a roughly retinotopic area. However, we found inconclusive evidence to say that the self-self input could carry out a similar form of lateral inhibition in the mantis. Of course, the connectome for the mantis does not - yet - exist, and those circuit mechanisms set out (Rosner et al., 2019) are only a proposal of the circuit mechanisms to support binocular stereopsis. The lateral inhibition could just as easily come not directly between LC14 cells, but via a third-party as well. Our other findings suggest the evidence of two subclasses of LC14 cell, which may be the existence of LC14a and LC14b cells within the dataset. The anatomical and functional distinction between these cells does therefore require explanation, and possibly suggests that they transmit different kinds of information from the lobula.

3 Concluding Remarks

We present the independent discovery of the sustained anti-optomotor response. The response exhibits head movements that contain two components of behaviour that is not obvious from the locomotory behaviour, and demonstrates that fly behaviour is made up of multiple mechanisms stacked on top of each other. Particularly in the case of active vision, multiple mechanisms add up to both stabilise and modify vision to allow for the acquisition of maximum useful information, meaning that under different internal and external contexts, different components behave differently. This is clear in the case where we demonstrate visual hyperacuity, which is evident from the head motion but not from the locomotion. This fundamental result shows that all levels of the active visual apparatus must be taken into account when both investigating behaviour in an attempt to infer the information held in the underlying neural activity, but also when considering the ways in which flies naturally operate. This being the case, in our virtual reality experiments, we have also presented an entirely unnatural environment for the fly, and with it appeared the existence of an unnatural behaviour, the anti-optomotor response. The results of our investigation suggest that the behaviour co-occurs with the saccadic behaviour of the fly, and we believe that investigating the ways in which afferent or efferent mechanisms, which are characteristic of active vision might contribute to the behaviour is a promising avenue for future work. Finally, we present an investigation into the neural circuitry that might allow active visual mechanisms to extract depth information from the environment. Without a full visual intact connectome, the conclusions we have drawn are only preliminary, however the techniques of applying graph segregation to functionally characterise neurons, as well as to calculate how the arrangement of the retinotopic information is transmitted can be broadly applied, and are easily applicable once this becomes available.

References

1. Agi, E. *et al.* The Evolution and Development of Neural Superposition. *Journal of Neurogenetics* **28,** 216–232. ISSN: 0167-7063 (Dec. 2014).
2. Aimon, S., Cheng, K. Y., Gjorgjieva, J. & Kadow, I. C. G. Complex Patterns of Neuronal Activity Underpin a Global Change in Brain State during Walk in Drosophila, 2022.01.17.476660 (July 2022).
3. Ammer, G., Vieira, R. M., Fendl, S. & Borst, A. Anatomical Distribution and Functional Roles of Electrical Synapses in Drosophila. *Current Biology* **32,** 2022–2036.e4. ISSN: 0960-9822 (May 2022).
4. Apostolopoulou, A. A. & Lin, A. C. Mechanisms Underlying Homeostatic Plasticity in the Drosophila Mushroom Body in Vivo. *Proceedings of the National Academy of Sciences* **117,** 16606–16615 (July 2020).
5. Arenz, A., Drews, M. S., Richter, F. G., Ammer, G. & Borst, A. The Temporal Tuning of the Drosophila Motion Detectors Is Determined by the Dynamics of Their Input Elements. *Current biology: CB* **27,** 929–944. ISSN: 1879-0445 (Apr. 2017).
6. Augustin, H., Zylbertal, A. & Partridge, L. A Computational Model of the Escape Response Latency in the Giant Fiber System of Drosophila Melanogaster. *eNeuro* **6,** ENEURO.0423–18.2019. ISSN: 2373-2822 (Apr. 2019).
7. Bahl, A., Serbe, E., Meier, M., Ammer, G. & Borst, A. Neural Mechanisms for Drosophila Contrast Vision. *Neuron* **88,** 1240–1252. ISSN: 0896-6273. (2023) (Dec. 2015).
8. Bajcsy, R., Aloimonos, Y. & Tsotsos, J. K. Revisiting Active Perception. *Autonomous Robots* **42,** 177–196. ISSN: 1573-7527 (Feb. 2018).
9. Beetz, M. J. *et al.* Flight-Induced Compass Representation in the Monarch Butterfly Heading Network. *Current Biology* **32,** 338–349.e5. ISSN: 0960-9822. (2023) (Jan. 2022).

10. Behnia, R., Clark, D. A., Carter, A. G., Clandinin, T. R. & Desplan, C. Processing Properties of ON and OFF Pathways for Drosophila Motion Detection. *Nature* **512,** 427–430. ISSN: 0028-0836. (2023) (Aug. 2014).

11. Bender, J. A. & Dickinson, M. H. Visual Stimulation of Saccades in Magnetically Tethered Drosophila. *Journal of Experimental Biology* **209,** 3170–3182. ISSN: 0022-0949 (Aug. 2006).

12. Bezanson, J., Edelman, A., Karpinski, S. & Shah, V. B. Julia: A Fresh Approach to Numerical Computing. *SIAM Review* **59,** 65–98. ISSN: 0036-1445. (2023) (Jan. 2017).

13. Bidaye, S. S. *et al.* Two Brain Pathways Initiate Distinct Forward Walking Programs in Drosophila. *Neuron* **108,** 469–485.e8. ISSN: 0896-6273 (Nov. 2020).

14. Blaj, G. & van Hateren, J. H. Saccadic Head and Thorax Movements in Freely Walking Blowflies. *Journal of Comparative Physiology. A, Neuroethology, Sensory, Neural, and Behavioral Physiology* **190,** 861–868. ISSN: 0340-7594 (Nov. 2004).

15. Blondeau, J. & Heisenberg, M. The Three-Dimensional Optomotor Torque System ofDrosophila Melanogaster. *Journal of comparative physiology* **145,** 321–329. ISSN: 1432-1351 (Sept. 1982).

16. Bloomquist, B. T. *et al.* Isolation of a Putative Phospholipase c Gene of Drosophila, norpA, and Its Role in Phototransduction. *Cell* **54,** 723–733. ISSN: 0092-8674 (Aug. 1988).

17. Borst, A & Egelhaaf, M. In Vivo Imaging of Calcium Accumulation in Fly Interneurons as Elicited by Visual Motion Stimulation. *Proceedings of the National Academy of Sciences of the United States of America* **89,** 4139–4143. ISSN: 0027-8424 (May 1992).

18. Borst, A., Haag, J. & Mauss, A. S. How Fly Neurons Compute the Direction of Visual Motion. *Journal of Comparative Physiology A* **206,** 109–124. ISSN: 1432-1351 (Mar. 2020).

19. Bradski, G. The OpenCV Library. *Dr. Dobb's Journal of Software Tools* (2000).

20. Brainard, D. H. & Vision, S. The Psychophysics Toolbox. *Spatial vision* **10,** 433–436 (1997).

21. Brezovec, L. E., Berger, A. B., Druckmann, S. & Clandinin, T. R. *Mapping the Neural Dynamics of Locomotion across the Drosophila Brain* Mar. 2022. (2023).

22. Buchanan, S. M., Kain, J. S. & de Bivort, B. L. Neuronal Control of Locomotor Handedness in Drosophila. *Proceedings of the National Academy of Sciences of the United States of America* **112,** 6700–6705. ISSN: 0027-8424. (2023) (May 2015).

23. Bush, N. E., Solla, S. A. & Hartmann, M. J. Whisking Mechanics and Active Sensing. *Current Opinion in Neurobiology. Systems Neuroscience* **40,** 178–188. ISSN: 0959-4388 (Oct. 2016).

24. Cellini, B. & Mongeau, J.-M. Active Vision Shapes and Coordinates Flight Motor Responses in Flies. *Proceedings of the National Academy of Sciences* **117,** 23085–23095 (Sept. 2020).

25. Cellini, B. & Mongeau, J.-M. Nested Mechanosensory Feedback Actively Damps Visually Guided Head Movements in Drosophila. *eLife* **11** (eds Palmer, S. E. & Calabrese, R. L.) e80880. ISSN: 2050-084X (Oct. 2022).

26. Cellini, B., Salem, W. & Mongeau, J.-M. Mechanisms of Punctuated Vision in Fly Flight. *Current Biology* **31,** 4009–4024.e3. ISSN: 0960-9822 (Sept. 2021).

27. Censi, A., Straw, A. D., Sayaman, R. W., Murray, R. M. & Dickinson, M. H. Discriminating External and Internal Causes for Heading Changes in Freely Flying Drosophila. *PLOS Computational Biology* **9,** e1002891. ISSN: 1553-7358 (Feb. 2013).

28. Chiappe, M. E. & Jayaraman, V. in *Genetically Encoded Functional Indicators* (ed Martin, J.-R.) 83–101 (Humana Press, Totowa, NJ, 2012). ISBN: 978-1-62703-014-4.

29. Chiappe, M. E., Seelig, J. D., Reiser, M. B. & Jayaraman, V. Walking Modulates Speed Sensitivity in Drosophila Motion Vision. *Current Biology* **20,** 1470–1475. ISSN: 0960-9822 (Aug. 2010).

30. Clark, D. A., Bursztyn, L., Horowitz, M. A., Schnitzer, M. J. & Clandinin, T. R. Defining the Computational Structure of the Motion Detector in Drosophila. *Neuron* **70,** 1165–1177. ISSN: 0896-6273 (June 2011).

31. Clements, J. *et al.* NeuronBridge: An Intuitive Web Application for Neuronal Morphology Search across Large Data Sets, 2022.07.20.500311 (July 2022).

32. Creamer, M. S., Mano, O. & Clark, D. A. Visual Control of Walking Speed in Drosophila. *Neuron* **100,** 1460–1473.e6. ISSN: 0896-6273 (Dec. 2018).

33. Cruz, T. L., Pérez, S. M. & Chiappe, M. E. Fast Tuning of Posture Control by Visual Feedback Underlies Gaze Stabilization in Walking Drosophila. *Current Biology* **31,** 4596–4607.e5. ISSN: 0960-9822 (Oct. 2021).

34. Cuntz, H., Haag, J., Forstner, F., Segev, I. & Borst, A. Robust Coding of Flow-Field Parameters by Axo-Axonal Gap Junctions between Fly Visual Interneurons. *Proceedings of the National Academy of Sciences* **104,** 10229–10233 (June 2007).

35. De Palma, A. & Pareti, G. The Ways of Metaphor in Neuroscience, or Being on the Right or Wrong Track. *Nuncius* **22,** 97–124. ISSN: 0394-7394 (2007).

36. Dill, M., Wolf, R. & Heisenberg, M. Behavioral Analysis of Drosophila Landmark Learning in the Flight Simulator. *Learning & Memory* **2,** 152–160. ISSN: 1072-0502, 1549-5485 (Jan. 1995).

37. Donner, K. & Hemilä, S. Modelling the Effect of Microsaccades on Retinal Responses to Stationary Contrast Patterns. *Vision Research* **47,** 1166–1177. ISSN: 0042-6989 (Apr. 2007).

38. Dror, R. O., O'Carroll, D. C. & Laughlin, S. B. Accuracy of Velocity Estimation by Reichardt Correlators. *Journal of the Optical Society of America A* **18,** 241. ISSN: 1084-7529, 1520-8532 (Feb. 2001).

39. Du, P., Kibbe, W. A. & Lin, S. M. Improved Peak Detection in Mass Spectrum by Incorporating Continuous Wavelet Transform-Based Pattern Matching. *Bioinformatics (Oxford, England)* **22,** 2059–2065. ISSN: 1367-4811 (Sept. 2006).

40. Duistermars, Care, R. & Frye, M. Binocular Interactions Underlying the Classic Optomotor Responses of Flying Flies. *Frontiers in Behavioral Neuroscience* **6.** ISSN: 1662-5153 (2012).

41. Duistermars, B. J., Chow, D. M., Condro, M. & Frye, M. A. The Spatial, Temporal and Contrast Properties of Expansion and Rotation Flight Optomotor Responses in Drosophila. *The Journal of Experimental Biology* **210,** 3218–3227. ISSN: 0022-0949 (Sept. 2007).

42. Fenk, L. M. *et al.* Muscles That Move the Retina Augment Compound Eye Vision in Drosophila. *Nature* **612,** 116–122. ISSN: 1476-4687 (Dec. 2022).

43. Fenk, L. M., Kim, A. J. & Maimon, G. Suppression of Motion Vision during Course-Changing, but Not Course-Stabilizing, Navigational Turns. *Current biology: CB* **31,** 4608–4619.e3. ISSN: 1879-0445 (Oct. 2021).

44. Fischbach, K. F. & Dittrich, A. P. M. The Optic Lobe of Drosophila Melanogaster. I. A Golgi Analysis of Wild-Type Structure. *Cell and Tissue Research* **258,** 441–475. ISSN: 1432-0878 (Dec. 1989).

45. Fischer, P. J. & Schnell, B. Multiple Mechanisms Mediate the Suppression of Motion Vision during Escape Maneuvers in Flying Drosophila. *iScience* **25,** 105143. ISSN: 2589-0042 (Oct. 2022).

46. Fite, K. V. Two Types of Optomotor Response in the Domestic Pigeon. *Journal of Comparative and Physiological Psychology* **66,** 308–314. ISSN: 0021-9940 (1968).

47. Fitzgerald, J. E. & Clark, D. A. Nonlinear Circuits for Naturalistic Visual Motion Estimation. *eLife* **4** (ed Carandini, M.) e09123. ISSN: 2050-084X (Oct. 2015).

48. Fox, J. L. & Frye, M. A. Figure–Ground Discrimination Behavior in Drosophila. II. Visual Influences on Head Movement Behavior. *Journal of Experimental Biology* **217,** 570–579. ISSN: 0022-0949 (Feb. 2014).

49. Franceschini, N, Chagneux, R, Kirschfeld, K & Mucke, A. *Vergence Eye Movements in Flies* in *Synapse-Transmission-Modulation: Proceedings of the 19th Göttingen Neurobiology Conference* (1991), 275.

50. Fujiwara, T., Brotas, M. & Chiappe, M. E. Walking Strides Direct Rapid and Flexible Recruitment of Visual Circuits for Course Control in Drosophila. *Neuron* **110,** 2124–2138.e8. ISSN: 0896-6273 (July 2022).

51. Fujiwara, T., Cruz, T. L., Bohnslav, J. P. & Chiappe, M. E. A Faithful Internal Representation of Walking Movements in the Drosophila Visual System. *Nature Neuroscience* **20,** 72–81. ISSN: 1546-1726 (Jan. 2017).

52. Geurten, B. R. H., Jähde, P., Corthals, K. & Göpfert, M. C. Saccadic Body Turns in Walking Drosophila. *Frontiers in Behavioral Neuroscience* **8.** ISSN: 1662-5153 (2014).

53. Gidon, A. *et al.* Dendritic Action Potentials and Computation in Human Layer 2/3 Cortical Neurons. *Science (New York, N.Y.)* **367,** 83–87 (Jan. 2020).

54. Gonzalez-Bellido, P. T., Wardill, T. J., Kostyleva, R., Meinertzhagen, I. A. & Juusola, M. Overexpressing Temperature-Sensitive Dynamin Decelerates Phototransduction and

Bundles Microtubules in Drosophila Photoreceptors. *The Journal of Neuroscience* **29,** 14199–14210. ISSN: 0270-6474. (2023) (Nov. 2009).

55. Götz, K. G. Course-Control, Metabolism and Wing Interference during Ultralong Tethered Flight in Drosophila Melanogaster. *Journal of Experimental Biology* **128,** 35–46. ISSN: 0022-0949 (Mar. 1987).

56. Götz, K. G. & Wenking, H. Visual Control of Locomotion in the Walking fruitflyDrosophila. *Journal of comparative physiology* **85,** 235–266. ISSN: 1432-1351 (Sept. 1973).

57. Green, W. E. & Oh, P. Y. Optic-Flow-Based Collision Avoidance. *IEEE Robotics & Automation Magazine* **15,** 96–103. ISSN: 1558-223X (Mar. 2008).

58. Groschner, L. N., Malis, J. G., Zuidinga, B. & Borst, A. A Biophysical Account of Multiplication by a Single Neuron. *Nature* **603,** 119–123. ISSN: 1476-4687. (2023) (Mar. 2022).

59. Gruntman, E., Reimers, P., Romani, S. & Reiser, M. B. Non-Preferred Contrast Responses in the Drosophila Motion Pathways Reveal a Receptive Field Structure That Explains a Common Visual Illusion. *Current Biology* **31,** 5286–5298.e7. ISSN: 0960-9822 (Dec. 2021).

60. Haag, J. & Borst, A. Dye-Coupling Visualizes Networks of Large-Field Motion-Sensitive Neurons in the Fly. *Journal of Comparative Physiology A* **191,** 445–454. ISSN: 1432-1351 (May 2005).

61. Haikala, V., Joesch, M., Borst, A. & Mauss, A. S. Optogenetic Control of Fly Optomotor Responses. *The Journal of Neuroscience: The Official Journal of the Society for Neuroscience* **33,** 13927–13934. ISSN: 1529-2401 (Aug. 2013).

62. Hardie, R. C. & Franze, K. Photomechanical Responses in Drosophila Photoreceptors. *Science (New York, N.Y.)* **338,** 260–263 (Oct. 2012).

63. Hardie, R. C. & Minke, B. The Trp Gene Is Essential for a Light-Activated Ca2+ Channel in Drosophila Photoreceptors. *Neuron* **8,** 643–651. ISSN: 0896-6273 (Apr. 1992).

64. Hateren, J. H. V. & Schilstra, C. Blowfly Flight and Optic Flow: II. Head Movements during Flight. *Journal of Experimental Biology* **202,** 1491–1500. ISSN: 0022-0949 (June 1999).

65. Heisenberg, M. & Wolf, R. On the Fine Structure of Yaw Torque in Visual Flight Orientation ofDrosophila Melanogaster. *Journal of comparative physiology* **130,** 113–130. ISSN: 1432-1351 (June 1979).

66. Heisenberg, M. & Wolf, R. Reafferent Control of Optomotor Yaw Torque inDrosophila Melanogaster. *Journal of Comparative Physiology A* **163,** 373–388. ISSN: 1432-1351 (May 1988).

67. Heisenberg, M., Wonneberger, R. & Wolf, R. Optomotor-blindH31—aDrosophila Mutant of the Lobula Plate Giant Neurons. *Journal of comparative physiology* **124,** 287–296. ISSN: 1432-1351 (Dec. 1978).

68. Hengstenberg, R. Spike Responses of 'Non-Spiking' Visual Interneurone. *Nature* **270,** 338–340. ISSN: 1476-4687 (Nov. 1977).

69. Henning, M., Ramos-Traslosheros, G., Gür, B. & Silies, M. Populations of Local Direction–Selective Cells Encode Global Motion Patterns Generated by Self-Motion. *Science Advances* **8,** eabi7112 (Jan. 2022).

70. Hindmarsh Sten, T., Li, R., Otopalik, A. & Ruta, V. Sexual Arousal Gates Visual Processing during Drosophila Courtship. *Nature* **595,** 549–553. ISSN: 0028-0836. (2023) (July 2021).

71. Horridge, A. *What Does the Honeybee See? And How Do We Know?: A Critique of Scientific Reason* ISBN: 978-1-921536-99-1 (ANU Press, 2009).

72. How, M. J. & Zanker, J. M. Motion Camouflage Induced by Zebra Stripes. *Zoology* **117,** 163–170. ISSN: 0944-2006 (June 2014).

73. Jenett, A. *et al.* A GAL4-driver Line Resource for Drosophila Neurobiology. *Cell Reports* **2,** 991–1001. ISSN: 2211-1247 (Oct. 2012).

74. Joesch, M., Schnell, B., Raghu, S. V., Reiff, D. F. & Borst, A. ON and OFF Pathways in Drosophila Motion Vision. *Nature* **468,** 300–304. ISSN: 1476-4687 (Nov. 2010).

75. Jun, J. J. *et al.* Fully Integrated Silicon Probes for High-Density Recording of Neural Activity. *Nature* **551,** 232–236. ISSN: 0028-0836. (2023) (Nov. 2017).

76. Juusola, M. *et al.* Microsaccadic Sampling of Moving Image Information Provides Drosophila Hyperacute Vision. *eLife* **6** (ed Rieke, F.) e26117. ISSN: 2050-084X. (2023) (Sept. 2017).

77. Karypis, G. & Kumar, V. A Fast and High Quality Multilevel Scheme for Partitioning Irregular Graphs. *SIAM Journal on Scientific Computing* **20,** 359–392. ISSN: 1064-8275 (Jan. 1998).

78. Katz, B. & Minke, B. Drosophila Photoreceptors and Signaling Mechanisms. *Frontiers in Cellular Neuroscience* **3.** ISSN: 1662-5102 (2009).

79. Keleş, M. F. & Frye, M. A. Object-Detecting Neurons in Drosophila. *Current Biology* **27,** 680–687. ISSN: 0960-9822 (Mar. 2017).

80. Kemppainen, J. *et al.* Binocular Mirror-Symmetric Microsaccadic Sampling Enables Drosophila Hyperacute 3D Vision. *Proceedings of the National Academy of Sciences of the United States of America* **119,** e2109717119. ISSN: 1091-6490 (Mar. 2022).

81. Ketkar, M. D. *et al.* First-Order Visual Interneurons Distribute Distinct Contrast and Luminance Information across ON and OFF Pathways to Achieve Stable Behavior. *eLife* **11** (eds Clark, D. A., Desplan, C. & Ache, J.) e74937. ISSN: 2050-084X (Mar. 2022).

82. Ketkar, M. D. *et al.* Luminance Information Is Required for the Accurate Estimation of Contrast in Rapidly Changing Visual Contexts. *Current biology: CB* **30,** 657–669.e4. ISSN: 1879-0445 (Feb. 2020).

83. Kim, A. J., Fenk, L. M., Lyu, C. & Maimon, G. Quantitative Predictions Orchestrate Visual Signaling in Drosophila. *Cell* **168,** 280–294.e12. ISSN: 0092-8674 (Jan. 2017).

84. Kim, A. J., Fitzgerald, J. K. & Maimon, G. Cellular Evidence for Efference Copy in Drosophila Visuomotor Processing. *Nature Neuroscience* **18,** 1247–1255. ISSN: 1546-1726 (Sept. 2015).

85. Kiral, F. R. *et al.* Brain Connectivity Inversely Scales with Developmental Temperature in Drosophila. *Cell Reports* **37,** 110145. ISSN: 2211-1247 (Dec. 2021).

86. Klapoetke, N. C. *et al.* A Functionally Ordered Visual Feature Map in the Drosophila Brain. *Neuron* **110,** 1700–1711.e6. ISSN: 1097-4199 (May 2022).

87. Kunze, P. Untersuchung des Bewegungssehens fixiert fliegender Bienen. *Zeitschrift für vergleichende Physiologie* **44,** 656–684. ISSN: 1432-1351 (Nov. 1961).

88. Land, M. F. Motion and Vision: Why Animals Move Their Eyes. *Journal of Comparative Physiology A* **185,** 341–352. ISSN: 1432-1351 (Oct. 1999).

89. Langen, M. *et al.* Mutual Inhibition among Postmitotic Neurons Regulates Robustness of Brain Wiring in Drosophila. *eLife* **2,** e00337. ISSN: 2050-084X (Mar. 2013).

90. Lawson, K. K. K. & Srinivasan, M. V. Contrast Sensitivity and Visual Acuity of Queensland Fruit Flies (Bactrocera Tryoni). *Journal of Comparative Physiology A* **206,** 419–428. ISSN: 1432-1351 (May 2020).

91. Li, F. *et al.* The Connectome of the Adult Drosophila Mushroom Body Provides Insights into Function. *eLife* **9,** e62576. ISSN: 2050-084X (Dec. 2020).

92. Longden, K. D., Schützenberger, A., Hardcastle, B. J. & Krapp, H. G. Impact of Walking Speed and Motion Adaptation on Optokinetic Nystagmus-like Head Movements in the Blowfly Calliphora. *Scientific Reports* **12,** 11540. ISSN: 2045-2322 (July 2022).

93. Lukežič, A., Vojíř, T., Čehovin, L., Matas, J. & Kristan, M. Discriminative Correlation Filter with Channel and Spatial Reliability. *International Journal of Computer Vision* **126,** 671–688. ISSN: 0920-5691, 1573-1405. arXiv: 1611.08461 [cs]. (2023) (July 2018).

94. Lyu, C., Abbott, L. F. & Maimon, G. Building an Allocentric Travelling Direction Signal via Vector Computation. *Nature* **601,** 92–97. ISSN: 1476-4687 (Jan. 2022).

95. Maccormac, E. R. in *Philosophy and Technology II: Information Technology and Computers in Theory and Practice* (eds Mitcham, C. & Huning, A.) 157–170 (Springer Netherlands, Dordrecht, 1986). ISBN: 978-94-009-4512-8.

96. Maimon, G., Straw, A. D. & Dickinson, M. H. Active Flight Increases the Gain of Visual Motion Processing in Drosophila. *Nature Neuroscience* **13,** 393–399. ISSN: 1546-1726 (Mar. 2010).

97. Maisak, M. S. *et al.* A Directional Tuning Map of Drosophila Elementary Motion Detectors. *Nature* **500,** 212–216. ISSN: 1476-4687 (Aug. 2013).

98. Mano, O. *et al.* Long Timescale Anti-Directional Rotation in Drosophila Optomotor Behavior, 2023.01.06.523055 (Jan. 2023).

99. Mauss, A. S. *et al.* Neural Circuit to Integrate Opposing Motions in the Visual Field. *Cell* **162,** 351–362. ISSN: 0092-8674 (July 2015).

100. Maye, A., Hsieh, C.-h., Sugihara, G. & Brembs, B. Order in Spontaneous Behavior. *PLOS ONE* **2,** e443. ISSN: 1932-6203 (May 2007).

101. Meier, M. *et al.* Neural Circuit Components of the Drosophila OFF Motion Vision Pathway. *Current biology: CB* **24,** 385–392. ISSN: 1879-0445 (Feb. 2014).

102. Mendes, C. S., Bartos, I., Akay, T., Márka, S. & Mann, R. S. Quantification of Gait Parameters in Freely Walking Wild Type and Sensory Deprived Drosophila Melanogaster. *eLife* **2,** e00231. ISSN: 2050-084X. (2023) (Jan. 2013).

103. Mitchiner, J. C., Pinto, L. H. & Vanable, J. W. Visually Evoked Eye Movements in the Mouse (Mus Musculus). *Vision Research* **16,** 1169–IN7. ISSN: 0042-6989 (Jan. 1976).

104. Moore, P. W. B., Hall, R. W., Friedl, W. A. & Nachtigall, P. E. The Critical Interval in Dolphin Echolocation: What Is It? *The Journal of the Acoustical Society of America* **76,** 314–317. ISSN: 0001-4966 (July 1984).

105. Morales, J. *et al.* Drosophila Fragile X Protein, DFXR, Regulates Neuronal Morphology and Function in the Brain. *Neuron* **34,** 961–972. ISSN: 0896-6273 (June 2002).

106. Morante, J. & Desplan, C. Photoreceptor Axons Play Hide and Seek. *Nature Neuroscience* **8,** 401–402. ISSN: 1546-1726 (Apr. 2005).

107. Muijres, F. T., Elzinga, M. J., Iwasaki, N. A. & Dickinson, M. H. Body Saccades of Drosophila Consist of Stereotyped Banked Turns. *The Journal of Experimental Biology* **218,** 864–875. ISSN: 1477-9145 (Mar. 2015).

108. Neuhauss, S. C. F. *et al.* Genetic Disorders of Vision Revealed by a Behavioral Screen of 400 Essential Loci in Zebrafish. *Journal of Neuroscience* **19,** 8603–8615. ISSN: 0270-6474, 1529-2401 (Oct. 1999).

109. Nityananda, V., Bissianna, G., Tarawneh, G. & Read, J. Small or Far Away? Size and Distance Perception in the Praying Mantis. *Philosophical Transactions of the Royal Society B: Biological Sciences* **371,** 20150262 (June 2016).

110. Nojima, T. *et al.* A Sex-Specific Switch between Visual and Olfactory Inputs Underlies Adaptive Sex Differences in Behavior. *Current Biology* **31,** 1175–1191.e6. ISSN: 0960-9822 (Mar. 2021).

111. Otsuna, H. & Ito, K. Systematic Analysis of the Visual Projection Neurons of Drosophila Melanogaster. I. Lobula-specific Pathways. *Journal of Comparative Neurology* **497,** 928–958. ISSN: 1096-9861 (2006).

112. Pacheco, D. A., Thiberge, S. Y., Pnevmatikakis, E. & Murthy, M. Auditory Activity Is Diverse and Widespread throughout the Central Brain of Drosophila. *Nature Neuroscience* **24,** 93–104. ISSN: 1546-1726 (Jan. 2021).

113. Pick, S. & Strauss, R. Goal-Driven Behavioral Adaptations in Gap-Climbing Drosophila. *Current biology: CB* **15,** 1473–1478. ISSN: 0960-9822 (Aug. 2005).

114. Popper, K. R. *Of Clouds and Clocks: An Approach to the Problem of Rationality and the Freedom of Man* (St. Louis, Washington University, 1966).

115. Ranganathan, R., Malicki, D. M. & Zuker, C. S. Signal Transduction in Drosophila Photoreceptors. *Annual review of neuroscience* **18,** 283–317. ISSN: 1545-4126 (Jan. 1995).

116. Ready, D. F., Hanson, T. E. & Benzer, S. Development of the Drosophila Retina, a Neurocrystalline Lattice. *Developmental Biology* **53,** 217–240. ISSN: 0012-1606 (Oct. 1976).

117. Reichardt, W. & Wenking, H. Optical Detection and Fixation of Objects by Fixed Flying Flies. *Die Naturwissenschaften* **56,** 424–425. ISSN: 0028-1042 (Aug. 1969).

118. Reiser, M. B. & Dickinson, M. H. Visual Motion Speed Determines a Behavioral Switch from Forward Flight to Expansion Avoidance in Drosophila. *Journal of Experimental Biology* **216,** 719–732. ISSN: 0022-0949 (Feb. 2013).

119. Ribeiro, I. M. A. *et al.* Visual Projection Neurons Mediating Directed Courtship in Drosophila. *Cell* **174,** 607–621.e18. ISSN: 0092-8674 (July 2018).

120. Rister, J. *et al.* Dissection of the Peripheral Motion Channel in the Visual System of Drosophila Melanogaster. *Neuron* **56,** 155–170. ISSN: 0896-6273 (Oct. 2007).

121. Rivera-Alba, M. *et al.* Wiring Economy and Volume Exclusion Determine Neuronal Placement in the Drosophila Brain. *Current Biology* **21,** 2000–2005. ISSN: 0960-9822. (2023) (Dec. 2011).

122. Robie, A. A., Straw, A. D. & Dickinson, M. H. Object Preference by Walking Fruit Flies, Drosophila Melanogaster, Is Mediated by Vision and Graviperception. *The Journal of Experimental Biology* **213,** 2494–2506. ISSN: 0022-0949. (2023) (July 2010).

123. Rossel, S. Regional Differences in Photoreceptor Performance in the Eye of the Praying Mantis. *Journal of comparative physiology* **131,** 95–112. ISSN: 1432-1351 (June 1979).

124. Rossel, S. Binocular Stereopsis in an Insect. *Nature* **302,** 821–822. ISSN: 1476-4687 (Apr. 1983).

125. Scheffer, L. K. *et al.* A Connectome and Analysis of the Adult Drosophila Central Brain. *eLife* **9,** e57443. ISSN: 2050-084X (Sept. 2020).

126. Schnell, B. *et al.* Processing of Horizontal Optic Flow in Three Visual Interneurons of the Drosophila Brain. *Journal of Neurophysiology* **103,** 1646–1657. ISSN: 1522-1598 (Mar. 2010).

127. Schnell, B., Raghu, S. V., Nern, A. & Borst, A. Columnar Cells Necessary for Motion Responses of Wide-Field Visual Interneurons in Drosophila. *Journal of Comparative Physiology. A, Neuroethology, Sensory, Neural, and Behavioral Physiology* **198,** 389–395. ISSN: 1432-1351 (May 2012).

128. Sen, R. *et al.* Moonwalker Descending Neurons Mediate Visually Evoked Retreat in Drosophila. *Current biology: CB* **27,** 766–771. ISSN: 1879-0445 (Mar. 2017).

129. Shaw, S. R. Early Visual Processing in Insects. *Journal of Experimental Biology* **112,** 225–282. ISSN: 0022-0949 (Sept. 1984).

130. Shaw, S. R., Fröhlich, A. & Meinertzhagen, I. A. Direct Connections between the R7/8 and R1–6 Photoreceptor Subsystems in the Dipteran Visual System. *Cell and Tissue Research* **257,** 295–302. ISSN: 1432-0878 (Jan. 1989).

131. Shinomiya, K. *et al.* The Organization of the Second Optic Chiasm of the Drosophila Optic Lobe. *Frontiers in Neural Circuits* **13.** ISSN: 1662-5110 (2019).

132. Shinomiya, K., Nern, A., Meinertzhagen, I. A., Plaza, S. M. & Reiser, M. B. Neuronal Circuits Integrating Visual Motion Information in Drosophila Melanogaster. *Current Biology* **32,** 3529–3544.e2. ISSN: 0960-9822 (Aug. 2022).

133. Shinomiya, K. *et al.* Candidate Neural Substrates for Off-Edge Motion Detection in Drosophila. *Current biology: CB* **24,** 1062–1070. ISSN: 1879-0445 (May 2014).

134. Shiraiwa, T. & Carlson, J. R. Proboscis Extension Response (PER) Assay in Drosophila. *Journal of Visualized Experiments : JoVE,* 193. ISSN: 1940-087X (Apr. 2007).

135. Shyu, W.-H. *et al.* Electrical Synapses between Mushroom Body Neurons Are Critical for Consolidated Memory Retrieval in Drosophila. *PLOS Genetics* **15,** e1008153. ISSN: 1553-7404 (May 2019).

136. Silies, M. *et al.* Modular Use of Peripheral Input Channels Tunes Motion-Detecting Circuitry. *Neuron* **79,** 111–127. ISSN: 1097-4199 (July 2013).

137. Srinivasan, M. V., Lehrer, M., Kirchner, W. H. & Zhang, S. W. Range Perception through Apparent Image Speed in Freely Flying Honeybees. *Visual Neuroscience* **6,** 519–535. ISSN: 1469-8714, 0952-5238 (May 1991).

138. Srinivasan, M. V., Poteser, M. & Kral, K. Motion Detection in Insect Orientation and Navigation. *Vision Research* **39,** 2749–2766. ISSN: 0042-6989 (Aug. 1999).

139. Srinivasan, M. V. *et al.* Robot Navigation Inspired by Principles of Insect Vision. *Robotics and Autonomous Systems. Field and Service Robotics* **26,** 203–216. ISSN: 0921-8890. (2023) (Feb. 1999).

140. Stewart, F. J., Baker, D. A. & Webb, B. A Model of Visual–Olfactory Integration for Odour Localisation in Free-Flying Fruit Flies. *Journal of Experimental Biology* **213,** 1886–1900. ISSN: 0022-0949 (June 2010).

141. Stringer, C. *et al.* Spontaneous Behaviors Drive Multidimensional, Brainwide Activity. *Science (New York, N.Y.)* **364,** eaav7893 (Apr. 2019).

142. Strother, J. A. *et al.* The Emergence of Directional Selectivity in the Visual Motion Pathway of Drosophila. *Neuron* **94,** 168–182.e10. ISSN: 1097-4199 (Apr. 2017).

143. Sy, T. *et al.* Cholinergic Circuits Integrate Neighboring Visual Signals in a Drosophila Motion Detection Pathway. *Current biology : CB* **21.** ISSN: 1879-0445. (2023) (Dec. 2011).

144. Takemura, S.-y. *et al.* The Comprehensive Connectome of a Neural Substrate for 'ON' Motion Detection in Drosophila. *eLife* **6** (ed Borst, A.) e24394. ISSN: 2050-084X. (2023) (Apr. 2017).

145. Takemura, S.-y. *et al.* A Visual Motion Detection Circuit Suggested by Drosophila Connectomics. *Nature* **500,** 175–181. ISSN: 1476-4687. (2023) (Aug. 2013).

146. Tammero, L. F., Frye, M. A. & Dickinson, M. H. Spatial Organization of Visuomotor Reflexes in Drosophila. *Journal of Experimental Biology* **207,** 113–122. ISSN: 0022-0949 (Jan. 2004).

147. Tanaka, R. & Clark, D. A. Neural Mechanisms to Exploit Positional Geometry for Collision Avoidance. *Current biology: CB* **32,** 2357–2374.e6. ISSN: 1879-0445 (June 2022).

148. Theobald, J. C., Duistermars, B. J., Ringach, D. L. & Frye, M. A. Flies See Second-Order Motion. *Current Biology* **18,** R464–R465. ISSN: 0960-9822 (June 2008).

149. Tuthill, J. C., Chiappe, M. E. & Reiser, M. B. Neural Correlates of Illusory Motion Perception in Drosophila. *Proceedings of the National Academy of Sciences* **108,** 9685–9690 (June 2011).

150. Tuthill, J. C., Nern, A., Holtz, S. L., Rubin, G. M. & Reiser, M. B. Contributions of the 12 Neuron Classes in the Fly Lamina to Motion Vision. *Neuron* **79,** 128–140. ISSN: 0896-6273 (July 2013).

151. Vallat, R. Pingouin: Statistics in Python. *Journal of Open Source Software* **3,** 1026. ISSN: 2475-9066. (2023) (Nov. 2018).

152. Virtanen, P. *et al.* SciPy 1.0: Fundamental Algorithms for Scientific Computing in Python. *Nature Methods* **17,** 261–272. ISSN: 1548-7105 (Mar. 2020).

153. Vogt, N. & Desplan, C. The First Steps in Drosophila Motion Detection. *Neuron* **56,** 5–7. ISSN: 0896-6273 (Oct. 2007).

154. Wardill, T. J. *et al.* Multiple Spectral Inputs Improve Motion Discrimination in the Drosophila Visual System. *Science (New York, N.Y.)* **336,** 925–931. ISSN: 1095-9203 (May 2012).

155. Warren, W. H., Kay, B. A., Zosh, W. D., Duchon, A. P. & Sahuc, S. Optic Flow Is Used to Control Human Walking. *Nature Neuroscience* **4,** 213–216. ISSN: 1097-6256 (Feb. 2001).

156. Warzecha, A.-k. & Egelhaaf, M. Intrinsic Properties of Biological Motion Detectors Prevent the Optomotor Control System from Getting Unstable. *Philosophical Transactions of the Royal Society of London. Series B: Biological Sciences* **351,** 1579–1591 (Nov. 1996).

157. Wertz, A., Borst, A. & Haag, J. Nonlinear Integration of Binocular Optic Flow by DNOVS2, A Descending Neuron of the Fly. *The Journal of Neuroscience* **28,** 3131–3140. ISSN: 0270-6474 (Mar. 2008).

158. Wertz, A., Haag, J. & Borst, A. Integration of Binocular Optic Flow in Cervical Neck Motor Neurons of the Fly. *Journal of Comparative Physiology. A, Neuroethology, Sensory, Neural, and Behavioral Physiology* **198,** 655–668. ISSN: 1432-1351 (Sept. 2012).

159. Whittington, J. C. R. & Bogacz, R. Theories of Error Back-Propagation in the Brain. *Trends in Cognitive Sciences* **23,** 235–250. ISSN: 1364-6613, 1879-307X (Mar. 2019).

160. Williamson, W. R., Peek, M. Y., Breads, P., Coop, B. & Card, G. M. Tools for Rapid High-Resolution Behavioral Phenotyping of Automatically Isolated Drosophila. *Cell Reports* **25,** 1636–1649.e5. ISSN: 2211-1247 (Nov. 2018).

161. Wolf, R. & Heisenberg, M. Visual Control of Straight Flight in Drosophila Melanogaster. *Journal of Comparative Physiology A* **167,** 269–283. ISSN: 1432-1351 (July 1990).

162. Woo, M., Neider, J., Davis, T. & Shreiner, D. *OpenGL Programming Guide: The Official Guide to Learning OpenGL, Version 1.2* (Addison-Wesley Longman Publishing Co., Inc., 1999).

163. Wu, M. *et al.* Visual Projection Neurons in the Drosophila Lobula Link Feature Detection to Distinct Behavioral Programs. *eLife* **5** (ed Scott, K.) e21022. ISSN: 2050-084X (Dec. 2016).

164. Wu, M. *et al.* Visual Projection Neurons in the Drosophila Lobula Link Feature Detection to Distinct Behavioral Programs. *eLife* **5,** e21022. ISSN: 2050-084X. (2023).

165. Yamawaki, Y. Unraveling the Functional Organization of Lobula Complex in the Mantis Brain by Identification of Visual Interneurons. *Journal of Comparative Neurology* **527,** 1161–1178. ISSN: 1096-9861 (2019).

166. Yang, H. H. & Clandinin, T. R. Elementary Motion Detection in Drosophila: Algorithms and Mechanisms. *Annual Review of Vision Science* **4,** 143–163. ISSN: 2374-4650 (Sept. 2018).

167. Zhang, Y. *et al.* Asymmetric Ephaptic Inhibition between Compartmentalized Olfactory Receptor Neurons. *Nature Communications* **10,** 1560. ISSN: 2041-1723 (Apr. 2019).

168. Zheng, Z. *et al.* A Complete Electron Microscopy Volume of the Brain of Adult Drosophila Melanogaster. *Cell* **174,** 730–743.e22. ISSN: 1097-4172 (July 2018).

169. Zweifel, N. O. & Hartmann, M. J. Z. Defining "Active Sensing" through an Analysis of Sensing Energetics: Homeoactive and Alloactive Sensing. *Journal of Neurophysiology* **124,** 40–48. ISSN: 0022-3077 (July 2020).